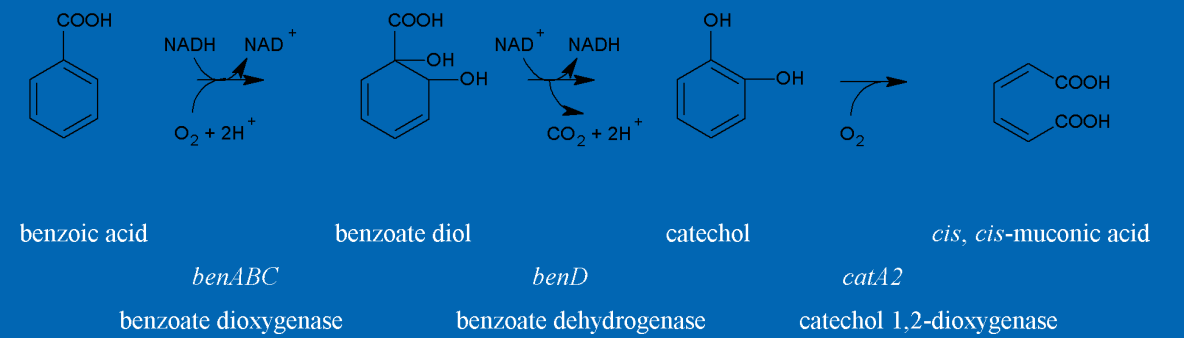


## Optimization of *Pseudomonas putida* KT2440 as host for the production of *cis, cis*-muconate from benzoate



Optimization of *Pseudomonas putida* KT2440 as host for the  
production of *cis, cis*-muconate from benzoate

Jozef B.J.H. van Duuren

**Thesis committee****Thesis supervisors**

Prof. dr. G. Eggink  
Professor of Industrial Biotechnology, Wageningen University

Prof. dr. ir. V.A.P. Martins dos Santos  
Professor of Systems and Synthetic Biology, Wageningen University

**Thesis co-supervisor**

Dr. A.E. Mars  
Scientist at Food & Biobased Research, Wageningen UR

**Other members**

Prof. dr. J.P.M. Sanders	Wageningen University
Dr. S.W.M. Kengen	Wageningen University
Prof. dr. J.H. de Winde	Delft University of Technology
Dr. ir. J. Wery	Dyadic, Wageningen

This research was conducted under the auspices of the Graduate School VLAG

Optimization of *Pseudomonas putida* KT2440 as host for the  
production of *cis, cis*-muconate from benzoate

Jozef B.J.H. van Duuren

**Thesis**

Submitted in fulfillment of the requirements for the degree of doctor  
at Wageningen University  
by the authority of the Rector Magnificus  
Prof. dr. M.J. Kropff,  
in the presence of the  
Thesis Committee appointed by the Academic Board  
to be defended in public  
on Monday 12 September 2011  
at 4:00 p.m. in the Aula

Optimization of *Pseudomonas putida* KT2440 as host for the production of *cis, cis*-muconate from benzoate

J.B.J.H. van Duuren

PhD thesis, Wageningen University, The Netherlands (2011)

With propositions in English and Dutch and a summary in English, Dutch and German

ISBN: 978-90-8585-990-1





# Contents

Chapter 1	Introduction	9
Chapter 2	Generation of a <i>catR</i> deficient mutant of <i>P. putida</i> KT2440 that produces <i>cis, cis</i> -muconate from benzoate at high rate and yield	25
Chapter 3	pH-stat fed-batch process to enhance the production of <i>cis, cis</i> -muconate from benzoate by <i>Pseudomonas putida</i> KT2440-JD1	45
Chapter 4	Modeling carbon-limited growth of <i>Pseudomonas putida</i> KT2440 on glucose	61
Chapter 5	A limited LCA of bio-adipic acid: manufacturing the nylon-6,6 precursor adipic acid using the benzoic acid degradation pathway from different feedstocks	87
Chapter 6	Discussion and outlook	101
Summary		115
Samenvatting		117
Zusammenfassung		121
Acknowledgements		125
Curriculum Vitae		127
Publications		129
Training Activities		131



# Chapter 1

## Introduction

## Industrial biotechnology

Industrial biotechnology (white biotechnology) is a rapidly growing area in which enzymatic or microbial processes are used for the production of fine and bulk chemicals. Examples of fine chemicals produced by white biotechnology are antibiotics, amino acids, vitamins and enzymes. Typical bulk products produced by means of fermentation include organic acids like citric acid, lactic acid, and succinic acid, and biofuels. 99% of the biofuels that are currently being produced in the USA consist of bioethanol, but biomethane and biohydrogen are considered to be interesting alternative options<sup>1</sup>.

Supportive trends for industrial biotechnology are the increasing prices of fossil fuels and climate change awareness, as well as the need for novel bioproducts and processes. Compared to the traditional petrochemical processes, biotechnological procedures have the potential to reduce the environmental impact through green chemistry<sup>2</sup>, by using new feedstocks and by reducing waste streams including greenhouse gas emissions. By choosing feedstocks with a relatively low energetic value and process burden, energy, and thus fossil fuel, can be saved for the production process. In this regard waste streams such as aromatic waste products from the petrochemical industry and organic waste from e.g. agroindustry are especially interesting because of their low commercial value and process burden. Furthermore, with organic waste as resource, a green production process can be developed, which is independent of the petrochemical industry<sup>3</sup>, and does not compete with the food supply. Aromatic compounds derived from the natural degradation of lignin from plant materials may also be a promising source for green biotechnological processes as they provide interesting chemical structures, and do not compete with the food supply either.

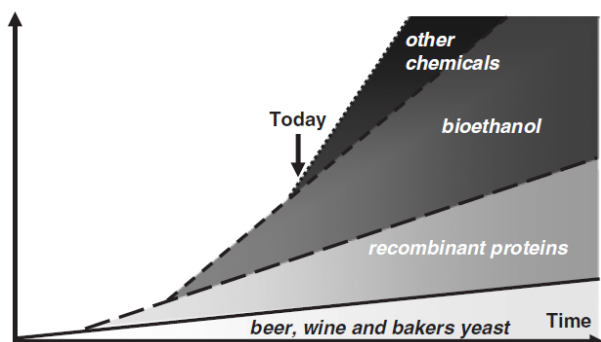


**Figure 1.** Illustration of development of the market value over time concerning fermentation products produced with *Saccharomyces cerevisiae*<sup>4</sup>.

Innovation offers new products of white biotechnology. According to McKinsey (2008), new processes are currently being developed for large-scale production of biobased monomers as ethylene, lactic acid, succinic acid, and 1,3-propanediol. Also, existing chemically produced polymers can be synthesized via biological means e.g. polyurethane, unsaturated polyester resins, nylon 6, acrylonitrile-butadiene-styrene resins, polyacrylamide, polybutadiene, acrylic fibers, and

nylon 6,6. In particular, the market value of fermentation products derived with *S. cerevisiae* is expected to grow much above the general market growth (fig. 1)<sup>4</sup>.

## Biocatalysis

In the last decades, many new and improved biocatalysts have been developed with the help of advanced molecular technologies, which are now being applied to a broad array of industrial processes. Bioprocesses are engineered for best performance at the enzyme, host, and process level<sup>5</sup>. In biocatalytic processes enzymes or whole cells are used to perform chemical transformations of substrates into the desired compounds. Because of regio- and stereo-selectivity of enzymes, biotechnological products usually accumulate in a pure form. Consequently, pure chiral building blocks are produced, which is an important feature for natural products with biological activity, namely pharmaceutical compounds and bioactive ingredients. Since 1955, hundreds of enzymes have been identified. Thirty percent of the characterized enzymes are oxygenases, which can oxidize thousands of environmental chemicals showing the large variety of possible bioconversions. These enzymes are catalogued in the University of Minnesota Biocatalysis/Biodegradation Database<sup>6,7</sup>.

Isolated enzymes as biocatalyst are typically used for hydrolytic or isomerization reactions. Examples of such enzymes are: lipases to produce amides or alcohols, nitrilases to produce acids, as industrially performed by BASF (Germany)<sup>5</sup>. Furthermore, amidases, aspartases, and thermolysin are used to produce amino acids and acylase is used to produce penicillin, as industrially performed by DSM (The Netherlands). Other examples of companies involved in developing and applying biocatalysis for large scale manufacture processes are Bayer, DOW, Evonik, and Lonza. Enzymes are produced with a large number of heterologous micro-organisms such as *Pseudomonas putida* (*P. putida*), *Escherichia coli* (*E. coli*), *Bacillus subtilis*, *Pichia pastoris*, etc.

Whole cells are especially used for biocatalytic reactions involving oxygenase enzymes or cofactors. The cellular environment provides the optimal conditions for the function and stability of enzymes and the regeneration of involved cofactors<sup>8</sup>. Also, the use of whole cells is attractive when biotransformation becomes more complex, because of the involvement of a cascade of enzymes.

**Table 1.** Industrial oxygenase processes with *P. putida* or *E. coli* involved as a whole cell biocatalyst.

Product	Substrate	Organism	volume/ yield	Applicability	Source
2-quinolinecarboxylic acid	2-methylquinoline	<i>P. putida</i> ATCC 33015 <sup>9</sup>	10 g L <sup>-1</sup> / 86%	Biologically active compound	Pfizer (USA)
Indigo	Glucose	<i>E. coli</i> <sup>10</sup>	18 g L <sup>-1</sup>	Pigment	Genencor International (USA) Kyowa Hakko Kogyo Co (Japan)
Trans-4-hydroxy-L-proline	Glucose	<i>E. coli</i> <sup>11</sup>	25 g L <sup>-1</sup>	Pharmaceutical	
4-[6-Hydroxypyridin-3-yl]-4-oxobutyrate	(S)-Nicotine	<i>Pseudomonas</i> DSM 8653 <sup>5,12</sup>	<i>sp.</i> 15 g L <sup>-1</sup>	Pharmaceutical	Lonza (Switzerland)
5-methylpyrazine-2-carboxylic acid	2,5-dimethylpyrazine	<i>P. putida</i> ATCC 33015 <sup>13</sup>	24 g L <sup>-1</sup> / 99%	Pharmaceutical	Lonza (Switzerland)

For industry, oxidative biotransformations are especially interesting due to the potential to produce new chemical products. Oxygenases are able to incorporate one or two oxygen atoms from molar oxygen in substrates, leading to regio-specific and/or enantio-specific hydroxylation of non-activated carbons<sup>8</sup>. Molar oxygen is a much cheaper and more environmentally friendly oxidant than chemical oxidants<sup>14</sup>. Table 1 gives an overview of industrial biocatalytic processes with oxygenases expressed in *P. putida* or *E. coli*.

## Solvent tolerance

Hydrophobic substrates and/or products can be toxic to microorganisms, thereby decreasing their value for biotechnological applications. Because of their hydrophobic character, solvents accumulate in the hydrophobic cell membrane causing loss of ions, metabolites, lipids, proteins, and the dissipation of pH and electric potential<sup>15</sup>. Above a certain threshold, the disorganization of the cell membrane even leads to cell lysis and death. The dissipation of pH and electrical potential causes reduction of ATP synthesis, which is reflected by the downregulation of the expression of the genes for the proton-consuming ATP synthase<sup>16</sup>. The electrical and pH potential are generated by the excretion of protons over the cell membrane, which is driven by the oxidation of NADH and other redox carriers via the electron transport chain. The accumulation of solvents causes a defect in the electron transfer, resulting in the production of superoxide anions, causing oxidative stress<sup>15</sup>.

The lipopolysaccharides in combination with divalent cations and proteins required for the maintenance of cell envelope are a defense barrier<sup>15,16,17</sup>. The addition of Mg<sup>2+</sup> to the medium does have a positive influence on the solvent tolerance of *Pseudomonas*<sup>18</sup>.

The toxicity of a hydrophobic solvent is related to the logarithm of its partition coefficient in n-octanol and water (log P<sub>ow</sub>). Solvent with a log P<sub>ow</sub> value between 1.5-4.0 are generally highly toxic to microorganisms<sup>15</sup>. For the solvents catechol, toluene, and phenol, which are discussed in this thesis, the partition coefficients are 1.3, 2.5, and 1.2, respectively<sup>19</sup>.

In the presence of solvents, gram-negative bacteria like *P. putida* respond by changing the *cis*-to-*trans* isomerization of unsaturated membrane fatty acids (short-term response). Furthermore, the phospholipid head groups compositions are changed, and the saturated fatty acids content is increased (long-term response), resulting in a decrease of membrane fluidity through denser packaging of the cell membrane<sup>15</sup>.

Some strains of *P. putida* have shown to be extremely tolerant to organic solvents. Such solvent-tolerant *P. putida* strains contain energy-dependent efflux pumps, which actively export toxic organic solvents to the external medium<sup>15,20</sup>. These efflux pumps belong to the resistance-nodulation-cell division (RND) family. For the solvent-tolerant strains *P. putida* S12, and *P. putida* DOT-T1E, the genes encoding for efflux pumps *srpABC*, and *ttgABC/ttgDEF/ttgGHI*, respectively, have been characterized and described<sup>21,22</sup>. The ability to convert toluene is not necessary for toluene tolerance. The solvent tolerant *P. putida* DOT-T1 can use toluene via the toluene dioxygenase pathway as sole carbon source in a concentration of up to 90% (vol/vol) toluene<sup>23</sup>. The solvent tolerant strain *P. putida* S12 does not convert toluene and was described to be able to grow

in the presence of 2% (vol/vol) toluene<sup>24</sup>. The RND efflux pumps are related to high ATP costs generated by the proton motive force, which is also reflected in increased energy generation<sup>16,25,26</sup>. The solvent tolerant strains *P. putida* DOT-T1E and *P. putida* S12 increase the NADH regeneration to increase the proton excretion. Besides the efflux pumps, the phospholipid concentration was higher in the solvent-tolerant strains after exposure to solvents, suggesting a greater ability to repair damaged membranes through efficient turnover and increased phospholipid biosynthesis<sup>15</sup>. Additionally, in the presence of toluene, the periplasmic space of *P. putida* DOT-T1 increases and evaginations by membrane vesicles were observed<sup>23</sup>. Also, it has been shown for *P. putida* S12 and DOT-T1 that elements of the solvent tolerance parasitize the flagellar transport system for excretion of solvents<sup>15</sup>.

During biotechnological processes hydrophobic products can be extracted from the broth with solvents in order to recycle biomass and medium as well as to prevent high concentrations. Such processes are called two-phase *in situ* extraction systems. Solvent-tolerant strains are able to resist these harsh conditions and are therefore considered to be very useful as a biocatalyst in two-phase fermentors<sup>20</sup>.

### ***P. putida* KT2440**

The research described in this thesis focuses on the development of *P. putida* KT2440 as a whole-cell biocatalyst for the cofactor-dependent oxidative transformation of benzoate to *cis*, *cis*-muconate. The strain, which contains 18 dioxygenases and 15 monooxygenases, of which some have been characterized and others are still putative<sup>27</sup>, is a soil bacterium that is well known for its metabolic versatility, including the ability to convert several aromatic compounds. By metabolizing these compounds, *P. putida* KT2440 contributes to the recycling of bio-waste compounds.

*P. putida* KT2440 is a plasmid-free variant of the toluene-degrading *P. putida* mt-2<sup>3,6,28,29</sup>. The genome of *P. putida* KT2440 has been sequenced<sup>28</sup>. Its single circular chromosome consists of 6,181,863 bp with an average G+C content of 61%. In total, 5516 genes are characterized, of which 5350 are protein coding<sup>30,31</sup>. The renowned stress-resistance by some of the strains, amenability for genetic manipulation, and suitability as a host for the expression of heterologous genes have rendered *P. putida* an attractive subject of research for biotechnological applications<sup>15,32</sup>, while the underlying molecular base for its metabolism contributes greatly to its development as an industrial strain<sup>3,6</sup>. Specifically described potential applications of the strain are: the production of biopesticides and plant growth promoters, bioremediation, biocatalysis, and production of bioplastics<sup>28</sup>. Also, *P. putida* KT2440 was the first Gram-negative soil bacterium which is certified as a safety strain by the Recombinant DNA Advisory Committee<sup>33</sup>.

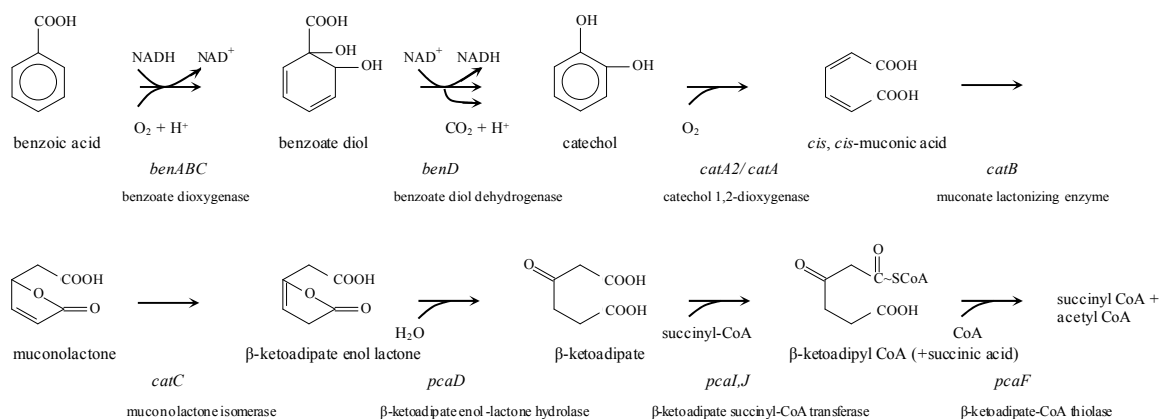


**Figure 2.** Metabolic pathway of benzoate in *P. putida* KT2440<sup>3</sup>.

Although *P. putida* KT2440 is not specifically described as solvent tolerant, it contains the genes *ttgABC*, *ttg2A*, and *tolC* related to solvent tolerance and it can survive in a concentration of up to 0.11% (vol/vol) toluene<sup>34</sup>. The stress response of *P. putida* KT2440 upon the presence of aromatic solvents like toluene was comparable, but more intensive, to the stress from the acidic hydrophilic aromatic compound 3-methylbenzoate. Genes for outer membrane proteins, including efflux pumps were upregulated, and genes responsible for membrane functions and energy transduction were down regulated in the presence of aromatics in *P. putida* KT2440. The down regulated membrane activities concern the synthesis of porins, peptidoglycan and flagella for motility. Based on this stress reaction it can be concluded that in contrast to solvent tolerant *P. putida*, *P. putida* KT2440 reacts to the hostile environment by minimizing its energy expenditure. Moreover, the presence of 3-methylbenzoate triggered an oxidative stress and heat shock responses in *P. putida* KT2440<sup>34</sup>. The heat shock response was reported under different environmental stresses<sup>35</sup>. The oxidative stress response was more severe than the heat shock response, probably because of the formation of chemically active intermediates as catechol in the presence of 3-methylbenzoate.

### **Biotransformation of aromatic compounds by *P. putida* KT2440**

*P. putida* KT2440, like any other *P. putida* strain, is able to use benzoate as carbon source. Benzoate is degraded by the products of the *ben* operon to the central metabolite catechol, which is further converted to H<sub>2</sub>O and CO<sub>2</sub> via the *ortho*-cleavage pathway and the TCA-cycle (fig. 2)<sup>36,37</sup>. Since various aromatic compounds are converted to catechol, *Pseudomonas* sp. can also degrade other aromatics via the *ortho*-cleavage pathway (fig. 3)<sup>38,39,40</sup>. However, the conversion of catechol is known to be slow. This is most likely caused by the cleavage of the benzene ring, which has an energetically stable chemical structure as a consequence of the resonance hybrid structure. This slow conversion can result in the accumulation of catechol, which causes oxidative stress<sup>41,42,43</sup> as catechol forms reactive oxygen species and spontaneously yields colored polymers<sup>44</sup>. *P. putida* KT2440 contains two different genes that code for catechol 1,2-dioxygenase for the conversion of catechol to *cis, cis*-muconate, namely gene *PP\_3166* (*catA2*) on the *ben* operon and gene *catA* on

the *cat* operon. The expression and physiologic role of *catA2* remain to be confirmed<sup>3</sup>. Furthermore, its appearance has not been seen in any other *ben* operon<sup>3</sup>. *P. putida* KT2440 probably contains these two isozymes to enhance the substrate range specificity for catechol analogues and/or to increase the capacity to prevent the accumulation of catechol<sup>45,46</sup>.

### Generation of a biocatalyst for the conversion of benzoate to *cis, cis*-muconate

During the research performed for this thesis a mutant of *P. putida* KT2440 was generated that converts benzoate to *cis, cis*-muconate (Fig. 2). The compound *cis, cis*-muconate contains a dicarboxylic acid structure with conjugated double bonds, which can be hydrogenated to adipic acid, which is a raw material for nylon-6,6. Benzoate dioxygenase and catechol 1,2-dioxygenase are involved in this conversion, of which the first dioxygenase is cofactor-dependent. However, there is no net consumption of the cofactor inside the cell upon conversion of benzoate to *cis, cis*-muconate, because the cofactor is regenerated by the benzoate diol dehydrogenase.

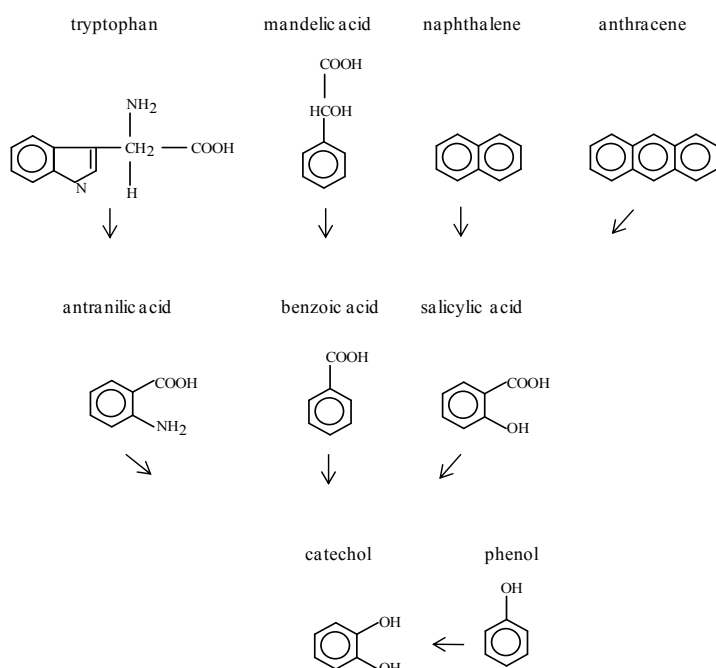


**Figure 3.** Catechol as a central metabolite in the conversion of aromatic compounds by *Pseudomonas fluorescens*<sup>37</sup>.

In the cytoplasm of the bacterium *cis, cis*-muconate is a dissociated dicarboxylic acid. Metabolic compounds can be exported by primary transport, which is directly related to the free-energy of ATP, or by secondary transport, which is dependent on the concentration gradient, electrical potential and pH-gradient<sup>47</sup>. The genes related to the export of carboxylic acids in *P. putida* are not well defined yet. The highest final concentration can be reached based on ATP-driven export<sup>47</sup>. Uniport of undissociated weak acids or symport of dissociated weak acids in combination with proton pumping that enforces the proton motive force are energetically similar under process

conditions. Consequently, the final product concentration that can be reached probably dependent on the availability of free energy and the export machinery that is available in the cell<sup>47,48</sup>. The efficiency of an industrial process for the production of *cis*, *cis*-muconic acid increases significantly at high product concentrations and reduced pH. However both characteristics will lead to the use of extra physiological energy in the form of ATP, which should be taken into account. The regeneration of NADH for ATP synthase by the central metabolism is dependent on the uptake rate of glucose, the excretion of by products, and biomass formation. *P. putida* is able to compensate for high energy demands by increasing the energy metabolism<sup>25</sup>. This capacity is even larger than needed under maximal growth conditions, which makes *P. putida* a very suitable whole-cell biocatalyst.

### **“Omics” and systems biology**

The sheer advances in high-throughput technologies based on the availability of a genome sequence in the last decade, have provided us with an invaluable toolbox for understanding and engineering cell behaviour<sup>49</sup>. The most commonly used “omic” techniques study the expressions of genes (transcriptome) and proteins (proteome), and the presence of metabolites (metabolome) at whole-cell level (fig. 4). One of the major challenges is to integrate transcriptomic, proteomic, and metabolomic information to give a more complete picture from the physiology of living organisms<sup>50</sup>. Transcriptomics and proteomics are especially used to identify regulated genes and proteins, respectively<sup>51,52</sup>. Metabolomics represent the end products of cellular processes<sup>53</sup>. Metabolomic, transcriptomic, and proteomic measurements reflect each a different level of regulation that may not correspond with each other. The gene and protein expression are regulated by the presence of metabolites and environmental conditions. Furthermore, there may be a pool of roaming RNA polymerase available in a cell, which activates sets of genes dependent on the presence of alternative  $\delta$  factors, DNA supercoiling, the presence of glutamate, and specific promoter strength<sup>34</sup>. Levels of mRNA, representing the gene expression, are not directly proportional to the induction or the expression of the proteins they code for. Post-transcriptional regulatory systems influence translation efficiency as well as stability of the protein<sup>51,52,54</sup>. In addition to post-transcriptional regulatory systems, post-translational modifications occur, which are bound to have an important role in regulating the protein activity. These regulatory systems are induced by heat-shock and other environmental conditions. Protein expression and adjustments can be visualized by 2D-gel electrophoresis and further analyzed with MALDI-MS. The presence and the structural analyses of metabolic compounds can be measured by HPLC and NMR, respectively.

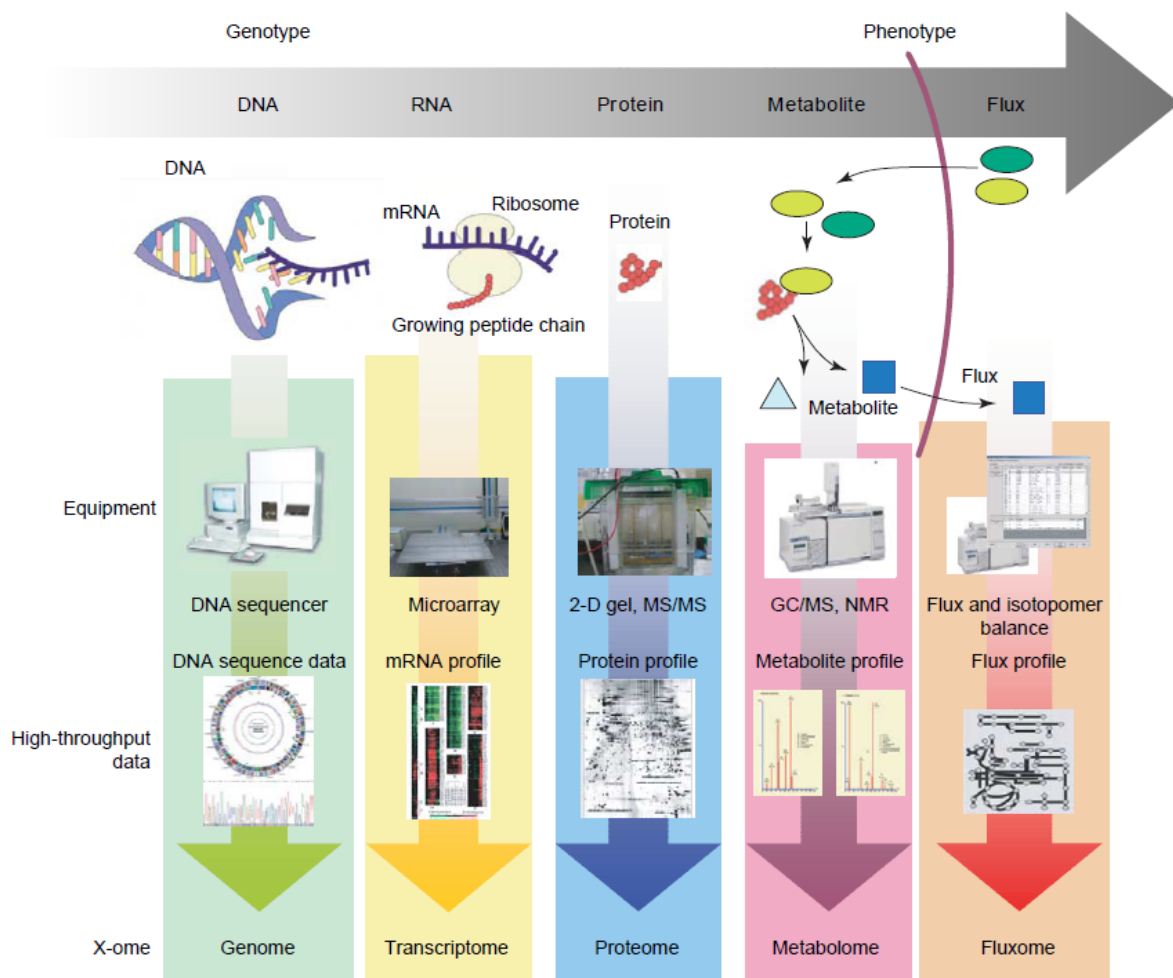


**Figure 4.** Overview of the most common “omics” techniques, of which some are used in combination of a constraint based model for systems biology<sup>49</sup>.

### Genome-scale, constraint-based modeling of metabolism

To reconstruct the complex cellular system, simply cataloguing and assigning gene functions do not allow for predicting the relationships between genotype and phenotype. To understand the functioning microbial cells, the high level of complexity requires approaches that can address the various interacting subcellular networks (metabolic, regulatory, signaling). Thus far, the most developed such approach deals with genome-scale reconstruction and modeling of the organism’s metabolic and transport network (Fig. 5). A reconstruction of the metabolic network is currently the best way to model an organism’s metabolism at genome-scale<sup>4,55</sup>. A genome-wide metabolic constraint-based model consists of a linear programmed stoichiometric reconstruction, gene-protein-reaction relationships defining the network structural properties, and flux distribution potential. A major advantage of this approach is that no knowledge regarding the kinetics or regulation of the reactions is required for building of the model. The availability of the genome sequence of *P. putida* KT2440 as well a solid body of experimental research has made it possible to reconstruct the genome-scale metabolic and transport network as reported by Puchalka *et al.*<sup>56</sup>, Nogales *et al.*<sup>57</sup>, and Sohn *et al.*<sup>58</sup>. A genome-scale model can be used to perform *in silico*

gene deletion studies as well as to predict growth yields, product formation, and, to a certain extent, the outcome of adaptive evolution or engineering<sup>49</sup>. Maximization of growth or ATP synthesis, minimization of substrate utilization or respiration, or increased production rate of a particular product can be defined as the objective function<sup>59,60</sup>. Methods such as Flux balance analysis (FBA) and Flux variability analysis (FVA) are used to study possible flux distributions and navigate the metabolic space of the organism, respectively, thereby generating testable hypotheses (Fig. 5)<sup>59,61,62</sup>. The measurement of the macro-molecular composition of biomass, as well as of growth related parameters, and the experimental flux distributions by means of isotopic labeling (fluxomics) are very valuable for experimental validation of the models<sup>63-67</sup>. Various “omics” datasets can be used to further reduce the space of solutions and generate more accurate predictions of phenotype data<sup>4,60</sup>.

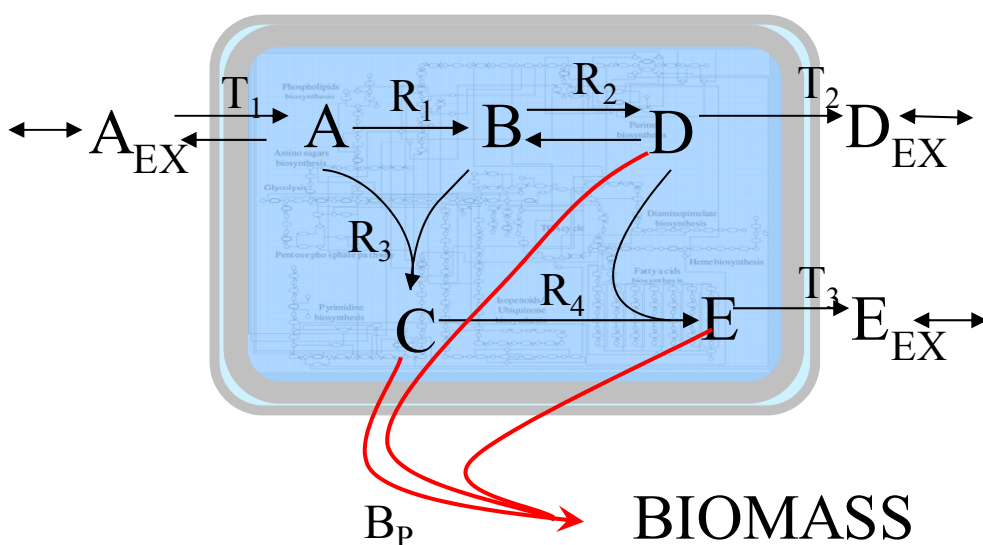


**Figure 5.** Schematic representation of a constrained based model of metabolism.

To optimize industrial microorganisms and fermentation processes, experimental biology techniques applied for system biology can also be used for metabolic engineering. Systems metabolic engineering integrates regulatory, metabolic, and other cellular networks<sup>68</sup>. The next step will be the development of kinetic models that will be able to predict dynamic time-dependent metabolic fluxes. Important hereby is to integrate the regulation<sup>4</sup>. Recognition of regulation patterns will allow for reverse engineering resulting in higher accuracy of predictions<sup>68</sup>.

### Life cycle assessment

As compared to petrochemical processes, those based on biotechnology have the potential to decrease the environmental impact. Consequently, part of the chemical industry is shifting from the petrochemistry to bio-based production. The main focus so far, largely due to governmental subsidies, has been on the bio-fuel market (fig 1). However, available renewable feedstocks and

alternative technologies have also been introduced in the chemical industry<sup>2,5</sup>. Processes related to production, product use, and product fate can be modeled by life cycle assessment (LCA). LCA supports the business and R&D strategy concerning process design based on criteria, such as usage of renewable feedstock, selectivity of the catalyst, solvent use, yield, risk, waste generation, and energy demand. Based on (laboratorial) processes and literature data, industrial processes can be simulated. One of the important parts of LCA analysis is determining the most costly portion of the life cycle. As a result, the criteria can be effectively reduced by focusing on this particular phase. For an LCA, it is essential to formulate a goal and scope concerning social safety, health, and environmental benefits. In this research, a limited LCA was carried out to compare the petrochemical and combined biotechnological and chemical production of adipic acid. The biotechnological conversion includes the conversion of several substrates to *cis, cis*-muconate. After acidification, *cis, cis*-muconate can be hydrogenated and acidified to adipic acid that can be used as raw material for nylon-6,6<sup>69</sup>. This homopolymer is for example used in carpets and the auto industry, because of its long lasting and strong features. The goal of this LCA was to establish a lower environmental impact. Categories that were taken into account are energy demand and global warming (greenhouse gas emission). In order to compare different production processes equally, a cradle-to-factory gate LCA (limited LCA) must be developed with the scope confined to the process from raw materials until the end of the production process. As a result, the LCA represents the sum of a cascade of technological applications responsible for supplies for the product<sup>70</sup>. In general, the choice of feedstock as well as final product concentration in the fermentation broth often turn out to be important parameters for the process design LCA<sup>2,5</sup>.

## Research aim and outline

The aim of this research project was to develop *P. putida* KT2440 as a whole-cell factory for biocatalysis of benzoate to a valuable metabolic intermediate by “omics”-driven research and validation.

In chapter 2 is described how mutant *P. putida* KT2440-JD1 was derived from the wild type strain *P. putida* KT2440. The aim was to convert benzoate to a metabolic intermediate of the benzoate pathway. By NTG-mutagenesis and enrichment, a mutant strain of *P. putida* KT2440 was obtained able to convert benzoate to *cis, cis*-muconate while grown on glucose. The maximum specific production rate was determined through batch and wash-out experiments. Transcriptomics and proteomics experiments were carried out during continuous fermentations to characterize *P. putida* KT2440-JD1 in more detail.

In chapter 3, the aim was to develop a process for the accumulation of *cis, cis*-muconate. The substrate and product toxicities were determined, and it was shown that catechol accumulated during the conversion of benzoate to *cis, cis*-muconate. Due to the accumulation of catechol a pH-stat fed-batch process was developed in order to maintain the concentration catechol at a constant low level.

In chapter 4, the constraint-based model iJP815 was further restricted to allow more accurate predictions. The maintenance and yield values as well as the macro-molecular composition of the

biomass of *P. putida* KT2440 when grown on glucose were determined by performing continuous fermentations at various dilution rates. FBA was (indirectly) assessed by transcriptomics, and the FVA by the obtained growth-related parameters, the macro-molecular composition and already published <sup>13</sup>C measurements.

In chapter 5, a limited LCA of the combined biotechnological and chemical production process was performed based on data from chapter 3 and literature. The aim was to determine leads for reducing the use of energy and emissions of greenhouse gases in a combined biotechnological and chemical process for the production of adipic acid from benzoate. The data were compared to the petrochemical process. Besides benzoate, various aromatic compounds with a lower energetic value were considered in the LCA. Also, the impacts of improvement of the bioprocess e.g. increase of the final concentration of *cis*, *cis*-muconate in the fermentation process, was modeled.

Chapter 2: Generation of a *catR* deficient mutant of *P. putida* KT2440 that produces *cis*, *cis*-muconate from benzoate at high rate and yield

Chapter 3: pH-stat fed-batch process to enhance the production of *cis*, *cis*-muconate from benzoate by *P. putida* KT2440-JD1

Chapter 4: Modeling carbon-limited growth of *Pseudomonas putida* KT2440 on glucose

Chapter 5: Limited LCA of bio-adipic acid manufacturing the nylon-6,6 precursor adipic acid using the benzoic acid degradation pathway from different feedstocks

## References

1. Kumar R, Singh S, Singh OV. 2008. Bioconversion of lignocellulosic biomass: biochemical and molecular perspectives. *J Ind Microbiol Biotechnol* 35:377-391.
2. Hatti-Kaul R, Törnvall U, Gustafsson L, Börjesson P. 2007. Industrial biotechnology for the production of bio-based chemicals--a cradle-to-grave perspective. *Trends Biotechnol* 25:119-124.
3. Jiménez JI, Miñambres B, García E, Díaz JL. 2002. Genomic analysis of the aromatic catabolic pathways from *Pseudomonas putida* KT2440. *Environ Microbiol* 4:824-841.
4. Nielsen J, Jewett MC. 2008. Impact of systems biology on metabolic engineering of *Saccharomyces cerevisiae*. *FEMS Yeast Res* 8:122-131.
5. Schmid A, Dordick JS, Hauer B, Kiener A, Wubbolts M, Witholt B. 2001. Industrial biocatalysis today and tomorrow. *Nature* 409:258-268.
6. Wackett LP. 2003. *P. putida* - a versatile biocatalyst. *Nat Biotechnol* 21:136-138.
7. University of Minnesota Biocatalysis/Biodegradation Database, <http://umbbd.msi.umn.edu/>.
8. Duetz WA, van Beilen JB, Witholt B. 2001. Using proteins in their natural environment: potential and limitations of microbial whole-cell hydroxylations in applied biocatalysis. *Curr Opin Biotechnol* 12:419-425.
9. Wong JW, Watson Jr. HA, Bouressa JF, Burns MP, Cawley JJ, Doro AE, Guzek DB, Hintz MA, McCormick EL, Scully DA, Siderewicz JM, Taylor WJ, Truesdell SJ, Wax RG. 2002. Biocatalytic Oxidation of 2-Methylquinoxaline to 2-Quinoxalinecarboxylic Acid. *Org Proc Res Dev* 6:477-481.
10. Berry A, Dodge TC, Pepsin M, Weyler W. 2002. Application of metabolic engineering to improve both the production and use of biotech indigo. *J Ind Microbiol Biotechnol* 28:127-133.
11. Shibasaki T, Hashimoto S, Mori H, Ozaki A. 2000. Construction of a novel hydroxyproline-producing recombinant *Escherichia coli* by introducing a proline 4-hydroxylase gene. *J Biosci Bioeng* 90:522-525.
12. Schmid R, Urlacher BU, Schmid R. 2007. Modern biooxidation: enzymes, reactions and applications. Wiley-VCH.
13. Kiener A. 1992. Enzymatic Oxidation of Methyl Groups on Aromatic Heterocycles: A Versatile Method for the Preparation of Heteroaromatic Carboxylic Acids. *Angew Chem Int Ed* 6:774-775.
14. Li Z, van Beilen JB, Duetz WA, Schmid A, de Raadt A, Griengl H, Witholt B. 2002. Oxidative biotransformations using oxygenases. *Curr Opin Chem Biol* 6:136-144.
15. Ramos JL, Duque E, Gallegos MT, Godoy P, Ramos-Gonzalez MI, Rojas A, Teran W, Segura A. 2002. Mechanisms of solvent tolerance in gram-negative bacteria. *Annu Rev Microbiol* 56:743-768.
16. Volkers RJ, de Jong AL, Hulst AG, van Baar BL, de Bont JA, Wery J. 2006. Chemostat-based proteomic analysis of toluene-affected *Pseudomonas putida* S12. *Environ Microbiol* 8:1674-1679.
17. Ramos JL, Duque E, Rodríguez-Herva JJ, Godoy P, Haïdour A, Reyes F, Fernández-Barrero A. 1997. Mechanisms for solvent tolerance in bacteria. *J Biol Chem* 272:3887-3890.
18. Macfarlane EL, Kwasnicka A, Ochs MM, Hancock RE. 1999. PhoP-PhoQ homologues in *Pseudomonas aeruginosa* regulate expression of the outer-membrane protein OprH and polymyxin B resistance. *Mol Microbiol* 34:305-316.
19. Smith JT, Vinjamoori DV. 1995. Rapid determination of logarithmic partition coefficients between n-octanol and water using micellar electrokinetic capillary chromatography. *J Chromatogr B Biomed Appl* 669:59-66.
20. de Bont JAM. 1998. Solvent-tolerant bacteria in biocatalysis. *Tibtech* 16:493-499.
21. Kieboom J, Dennis JJ, Zylstra GJ, de Bont JA. 1998. Active efflux of organic solvents by *Pseudomonas putida* S12 is induced by solvents. *J Bacteriol* 180:6769-6772.
22. Rojas A, Duque E, Mosqueda G, Golden G, Hurtado A, Ramos JL, Segura A. 2001. Three efflux pumps are required to provide efficient tolerance to toluene in *Pseudomonas putida* DOT-T1E. *J Bacteriol* 183:3967-3973.
23. Ramos JL, Duque E, Huertas MJ, Haïdour A. 1995. Isolation and expansion of the catabolic potential of a *Pseudomonas putida* strain able to grow in the presence of high concentrations of aromatic hydrocarbons. *J Bacteriol* 177:3911-3916.
24. Kieboom J, Bruinenberg R, Keizer-Gunnink I, de Bont JA. 2001. Transposon mutations in the flagella biosynthetic pathway of the solvent-tolerant *Pseudomonas putida* S12 result in a decreased expression of solvent efflux genes. *FEMS Microbiol Lett*. 198:117-122.
25. Blank LM, Ionidis G, Ebert BE, Bühler B, Schmid A. 2008. Metabolic response of *Pseudomonas putida* during redox biocatalysis in the presence of a second octanol phase. *FEBS J* 275:5173-5190.

26. Volkers RJ, Ballerstedt H, Ruijssenaars H, de Bont JA, de Winde JH, Wery J. 2009. TrgI, toluene repressed gene I, a novel gene involved in toluene-tolerance in *Pseudomonas putida* S12. *Extremophiles* 13:283-297.
27. Dos Santos VA, Heim S, Moore ER, Strätz M, Timmis KN. 2004. Insights into the genomic basis of niche specificity of *Pseudomonas putida* KT2440. *Environ Microbiol* 6:1264-1286.
28. Nelson KE, Weinel C, Paulsen IT, Dodson RJ, Hilbert H, Martins dos Santos VAP, Fouts DE, Gill SR, Pop M, Holmes M, Brinkac L, Beanan M, DeBoy RT, Daugherty S, Kolonay J, Madupu R, Nelson W, White O, Peterson J, Khouri H, Hance I, Chris Lee P, Holtzapple E, Scanlan D, Tran K, Moazzez A, Utterback T, Rizzo M, Lee K, Kosack D, Moestl D, Wedler H, Lauber J, Stjepandic D, Hoheisel J, Straetz M, Heim S, Kiewitz C, Eisen JA, Timmis KN, Dusterhöft A, Tümmeler B, Fraser CM. 2002. Complete genome sequence and comparative analysis of the metabolically versatile *Pseudomonas putida* KT2440. *Environ Microbiol* 4:799-808.
29. Williams PA, Murray K. 1974. Metabolism of benzoate and the methylbenzoates by *Pseudomonas putida* (*arvilla*) mt-2: evidence for the existence of a TOL plasmid. *J Bacteriol* 120:416-423.
30. NCBI, <http://www.ncbi.nlm.nih.gov/sites/entrez?Db=genome&Cmd=ShowDetailView&TermToSearch=266>
31. Frank S, Klockgether J, Hagendorf P, Geffers R, Schöck U, Pohl T, Davenport CF, Tümmeler B. 2011. *Pseudomonas putida* KT2440 genome update by cDNA sequencing and microarray transcriptomics. *Environ Microbiol* 13:1309-1326.
32. Ramos JL, Wasserfallen A, Rose K, Timmis KN. 1987. Redesigning metabolic routes: manipulation of TOL plasmid pathway for catabolism of alkylbenzoates. *Science* 235:593-596.
33. Federal register. 1982. Certified host-vector systems, 17197.
34. Domínguez-Cuevas P, González-Pastor JE, Marqués S, Ramos JL, de Lorenzo V. 2006. Transcriptional tradeoff between metabolic and stress-response programs in *Pseudomonas putida* KT2440 cells exposed to toluene. *J Biol Chem* 281:11981-11991.
35. Cao B, Loh KC. Catabolic pathways and cellular responses of *Pseudomonas putida* P8 during growth on benzoate with a proteomics approach. 2008. *Biotechnol Bioeng* 101:1297-1312.
36. Assinder SJ, Williams PA. 1990. The TOL plasmids: determinants of the catabolism of toluene and the xylenes. *Adv Microb Physiol* 31:1-69.
37. Feist CF, Hegeman GD. 1969. Phenol and benzoate metabolism by *Pseudomonas putida*: regulation of tangential pathways. *J Bacteriol* 100:869-877.
38. Haigler BE, Pettigrew CA, Spain JC. 1992. Biodegradation of mixtures of substituted benzenes by *Pseudomonas* sp. strain JS150. *Appl Environ Microbiol* 58:2237-2244.
39. Panke S, Sánchez-Romero JM, de Lorenzo V. 1998. Engineering of quasi-natural *Pseudomonas putida* strains for toluene metabolism through an *ortho*-cleavage degradation pathway. *Appl Environ Microbiol* 64:748-751.
40. Tao Y, Fishman A, Bentley WE, Wood TK. 2004. Oxidation of benzene to phenol, catechol, and 1,2,3-trihydroxybenzene by toluene 4-monooxygenase of *Pseudomonas mendocina* KR1 and toluene 3-monooxygenase of *Ralstonia pickettii* PKO1. *Appl Environ Microbiol* 70:3814-3820.
41. Benndorf D, Loffhagen N, Babel W. 2001. Protein synthesis patterns in *Acinetobacter calcoaceticus* induced by phenol and catechol show specificities of responses to chemostress. *FEMS Microbiol Lett* 200:247-252.
42. Schmidt E, Knackmuss HJ. 1984. Production of *cis*, *cis*-muconate from benzoate and 2-fluoro-*cis*, *cis*-muconate from 3-fluorobenzoate by 3-chlorobenzoate degrading bacteria. *Appl Microbiol Biotechnol* 20:351-355.
43. Schreiber A, Hellwig M, Dorn E, Reineke W, Knackmuss HJ. 1980. Critical reactions in fluorobenzoic acid degradation by *Pseudomonas* sp. B13. *Appl Environ Microbiol* 39:58-67.
44. Benndorf D, Thiersch M, Loffhagen N, Kunath C, Harms H. 2006. *Pseudomonas putida* KT2440 responds specifically to chlorophenoxy herbicides and their initial metabolites. *Proteomics* 6:3319-3329.
45. Kim BJ, Choi WJ, Lee EY, Cho CY. 1988. Enhancement of *cis*, *cis*-muconate productivity by overexpressing of catechol 1,2-dioxygenase in *Pseudomonas putida* BCM114. *Biotechnol Bioprocess Eng* 3:112-114.
46. Nakai C, Uyeyama H, Kagamiyama H, Nakazawa T, Inouye S, Kishi F, Nakazawa A, Nozaki M. 1995. Cloning, DNA sequencing, and amino acid sequencing of catechol 1,2-dioxygenases (pyrocatechase) from *Pseudomonas putida* mt-2 and *Pseudomonas arvilla* C-1. *Arch Biochem Biophys* 321:353-362.
47. van Maris AJ, Konings WN, van Dijken JP, Pronk JT. 2004. Microbial export of lactic and 3-hydroxypropanoic acid: implications for industrial fermentation processes. *Metab Eng* 6:245-255.
48. Abbott DA, Zelle RM, Pronk JT, van Maris AJA. 2009. Metabolic engineering of *Saccharomyces cerevisiae* for production of carboxylic acids: current status and challenges. *FEMS Yeast Res* 9:1123-1136.

49. Lee SY, Lee DY, Kim TY. 2005. Systems biology for strain improvement. *Trends biotechnol* 23:349-358.
50. Sauer U, Heinemann M, Zamboni N. Genetics. 2007. Getting closer to the whole picture. *Science* 316:550-551.
51. de Groot MJL, Daran-Lapujade P, van Breukelen B, Knijnenburg TA, de Hulster EAF, Reinders MJT, Pronk JT, Heck AJR, Slijper M. 2007. Quantitative proteomics and transcriptomics of anaerobic and aerobic yeast cultures reveals post-transcriptional regulation of key cellular processes. *Microbiology* 153:3864-3878.
52. Kolkman A, Daran-Lapujade P, Fullaondo A, Olsthoorn MM, Pronk JT, Slijper M, Heck AJ. 2006. Proteome analysis of yeast response to various nutrient limitations. *Mol Syst Biol* 2006:0026.
53. Kayser A, Weber J, Hecht V, Rinas U. 2005. Metabolic flux analysis of *Escherichia coli* in glucose-limited continuous culture. I. Growth-rate-dependent metabolic efficiency at steady state. *Microbiology* 151:693-706.
54. Rosen R, Ron EZ. 2002. Proteome analysis in the study of the bacterial heat-shock response. *Mass Spectrom Rev* 21:244-265.
55. Price ND, Reed JL, Palsson BØ. 2004. Genome-scale models of microbial cells: evaluating the consequences of constraints. *Nat Rev Microbiol* 2:886-897.
56. Puchalka J, Oberhardt MA, Godinho M, Bielecka A, Regenhardt D, Timmis KN, Papin JA, Martins dos Santos VA. 2008. Genome-scale reconstruction and analysis of the *Pseudomonas putida* KT2440 metabolic network facilitates applications in biotechnology. *PLoS Comput Biol* 4(10).
57. Nogales J, Palsson BØ, Thiele I. 2008. A genome-scale metabolic reconstruction of *Pseudomonas putida* KT2440: iJN746 as a cell factory. *BMC Syst Biol* 2:79.
58. Sohn SB, Kim TY, Park JM, Lee SY. 2010. *In silico* genome-scale metabolic analysis of *Pseudomonas putida* KT2440 for polyhydroxyalkanoate synthesis, degradation of aromatics and anaerobic survival. *Biotechnol J* 5:739-750.
59. Kauffman KJ, Prakash P, Edwards JS. 2003. Advances in flux balance analysis. *Curr Opin Biotechnol* 14:491-496.
60. Reed JL, Vo TD, Schilling CH, Palsson BO. 2003. An expanded genome-scale model of *Escherichia coli* K-12. *Genome Biol* 4:R54.
61. Mahadevan R, Schilling CH. 2003. The effects of alternate optimal solutions in constraint-based genome-scale metabolic models. *Metab Eng* 5:264-276.
62. Teusink B, Wiersma A, Molenaar D, Francke C, de Vos WM, Siezen RJ, Smid EJ. 2006. Analysis of growth of *Lactobacillus plantarum* WCFS1 on a complex medium using a genome-scale metabolic model. *J Biol Chem* 281:40041-40048.
63. Hanegraaf PP, Muller EB. 2001. The dynamics of the macromolecular composition of biomass. *J Theor Biol* 212:237-251.
64. Lange HC, Heijnen JJ. 2001. Statistical reconciliation of the elemental and molecular biomass composition of *Saccharomyces cerevisiae*. *Biotechnol Bioeng* 75:334-344.
65. Reed JL, Palsson BØ. 2003. Thirteen years of building constraint-based *in silico* models of *Escherichia coli*. *J Bacteriol* 185: 2692-2699.
66. del Castillo T, Ramos JL, Rodríguez-Herva JJ, Fuhrer T, Sauer U, Duque E. 2007. Convergent peripheral pathways catalyze initial glucose catabolism in *Pseudomonas putida*: genomic and flux analysis. *J Bacteriol* 189:5142-5152.
67. Fuhrer T, Fischer E, Sauer U. 2005. Experimental identification and quantification of glucose metabolism in seven bacterial species. *J Bacteriol* 187:1581-1590.
68. Park JH, Lee SY, Kim TY, Kim HU. 2008. Application of systems biology for bioprocess development. *Trends Biotechnol* 26:404-412.
69. Draths KM, Frost JW. 1993. Environmentally Compatible Synthesis of Adipic Acid from & Glucose. *J Am Chem Soc* 116: 399-400.
70. International Organization for Standardization. 2006. Life cycle assessment. ISO 14040:2006.



# Chapter 2

## Generation of a *catR* deficient mutant of *P. putida* KT2440 that produces *cis, cis*-muconate from benzoate at high rate and yield

**Abstract:** *P. putida* KT2440-JD1 was derived from *P. putida* KT2440 after N-methyl-N'-nitro-N-nitrosoguanidine (NTG)-mutagenesis and exposure to 3-fluorobenzoate (3-FB). The mutant was no longer able to grow using benzoate as a sole carbon source, but co-metabolized benzoate to *cis, cis*-muconate during growth on glucose, which accumulated in the growth medium. The specific production rate ( $q_{pm}$ ) was  $0.18 \pm 0.03$  g *cis, cis*-muconate/ (g<sub>DCW</sub> × h) in continuous cultures, and increased to 1.4 g *cis, cis*-muconate/ (g<sub>DCW</sub> × h) during wash-out cultivation. Transcriptome analysis showed that the *cat* operon was not induced in *P. putida* KT2440-JD1 in the presence of 5 mM benzoate, due to a point mutation in the highly conserved DNA binding domain of the transcriptional regulator (*catR*) of the *cat* operon. The *ben* operon was highly expressed in the presence of benzoate in the mutant and its parental strain. This operon contains PP\_3166 (*catA2*), which was shown to be a second catechol 1,2-dioxygenase besides CatA. *P. putida* KT2440-JD1 is the first *cis, cis*-muconate-accumulating mutant that was characterized at the genetic level. The specific production rate achieved is at least eight times higher than those reported for other *cis, cis*-muconate-producing strains.

**Keywords:** benzoate, catechol 1,2-dioxygenase, *cis, cis*-muconate, 3-fluorobenzoate, NTG mutagenesis, *P. putida* KT2440

Accepted for publication in Journal of Biotechnology. Co-Authors: Wijte D, Leprince A, Karge B, Puchałka J, Wery J, Martins dos Santos VAP, Eggink G, Mars AE.

## Introduction

*Pseudomonas putida* KT2440 is a metabolically versatile soil bacterium with significant potential for biotechnological applications, particularly in the areas of bioremediation and biotransformation<sup>1,2</sup>. The genome of *P. putida* KT2440 has been sequenced and annotated, which facilitates further development of the strain as a biocatalyst<sup>3</sup>. Furthermore, *P. putida* KT2440 can be used for the expression of cloned genes and it is the first Gram-negative soil bacterium that has been certified as a safety strain by the Recombinant DNA Advisory Committee<sup>4,5</sup>.

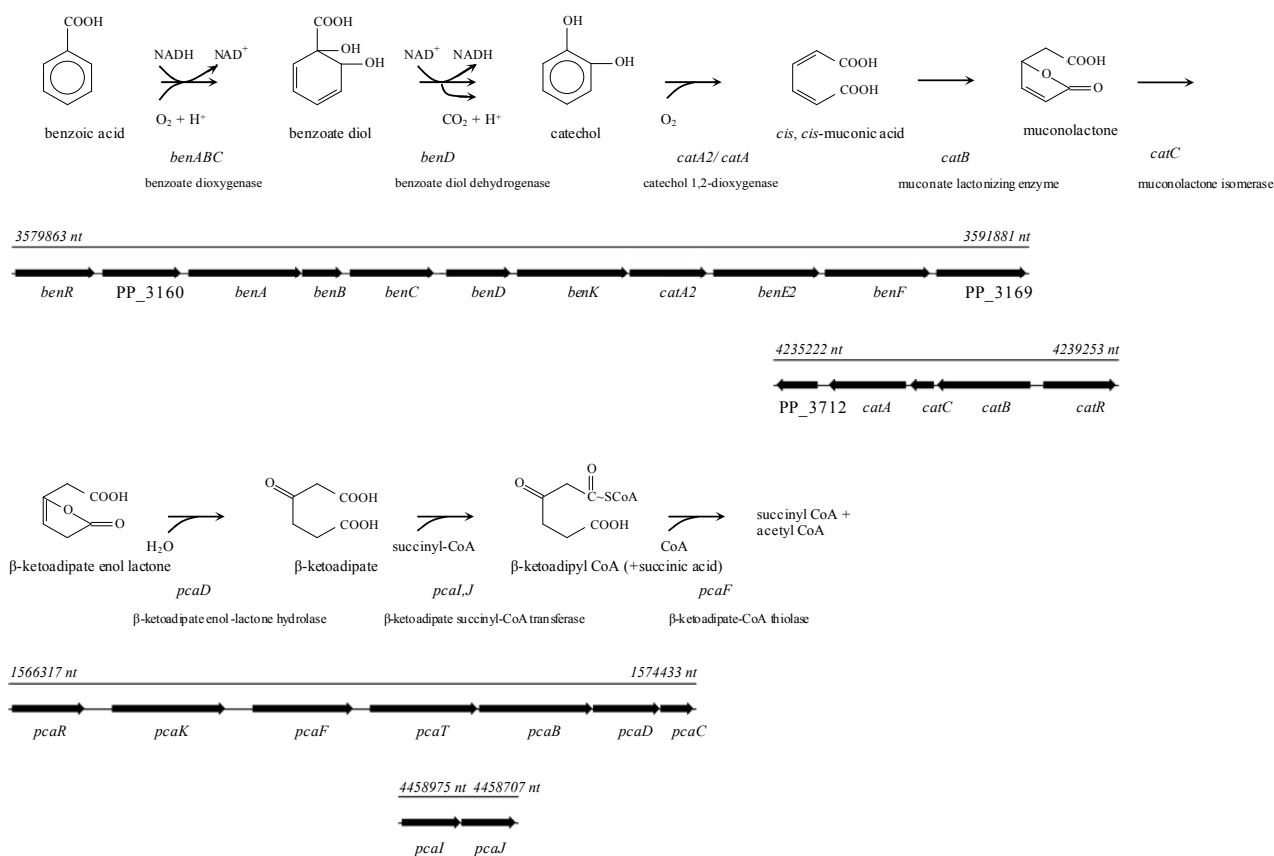


**Figure 1.** Metabolic pathway of benzoate and the genetic organization of the *ben*, *cat* and *pca* operons on the genome of *P. putida* KT2440<sup>6,7,8</sup>.

Like other *P. putida* strains, *P. putida* KT2440 grows with benzoate as a single carbon source<sup>6,9</sup>. Benzoate is converted to a diol by a co-factor dependent dioxygenase (Fig. 1). The resulting diol is further dehydrogenated to catechol, which regenerates the co-factor. Catechol is degraded to H<sub>2</sub>O and CO<sub>2</sub> via the so-called *ortho*-cleavage pathway and the Krebs cycle. The ring cleavage of catechol is carried out by a cofactor-independent catechol 1,2-dioxygenase, which converts catechol to *cis, cis*-muconate. The benzoate pathway is encoded by genes that belong to the *ben*, *cat* and *pca* operons (Fig. 1). *P. putida* KT2440 may have a functional overlap at the level of catechol 1,2-dioxygenase, since the genes PP\_3166 (*catA2*) on the *ben* operon and *catA* on the *cat* operon have a

76 % identity in the amino acid sequence. The extra *catA* gene has not been found in other *ben* operons of *Pseudomonas* species<sup>6</sup>. The expression and physiological function of the *catA2* gene has yet to be confirmed. Ring cleavage of catechol has been described as a rate limiting step in the degradation of aromatic compounds<sup>10,11,12,13</sup>. The extra gene for a catechol 1,2-dioxygenase may increase the ring-cleavage capacity of *P. putida* KT2440.

Intermediates of the benzoate pathway, such as benzoate diol and *cis, cis*-muconate, contain functional groups and may be of interest to the chemical industry<sup>14,15</sup>. Benzoate diol can be highly functionalized by oxidative and rearrangement reactions and *cis, cis*-muconate contains a dicarboxylic acid structure with conjugated double bonds, which can be hydrogenated to form adipic acid, a raw material for nylon-6,6. Due to the complexity of the conversion process and the involvement of a cofactor-dependent dioxygenase, whole cell biocatalysis is likely to be more suitable to produce compounds of industrial interest from benzoate than *in vitro* biocatalysis with purified enzymes. Furthermore, oxygenases are generally more stable *in vivo*<sup>16</sup>. The aim of this research is to obtain efficient whole-cell biocatalysts that co-metabolize benzoate to valuable intermediates using *P. putida* KT2440 as a parent strain. In order to obtain such biocatalysts, *P. putida* KT2440 was treated with NTG and exposed to 3-FB, which yielded solely mutants that converted benzoate to *cis, cis*-muconate. One of these mutants was further characterized.

## Material and methods

**Strain and cultivation conditions.** *P. putida* KT2440 (DSM6125) and its derivatives were grown in E-2 mineral medium (MM)<sup>17</sup> at 30°C and pH 7. Batch cultivations were done in Erlenmeyer flasks that were shaken at 200 rpm. Continuous cultivations were done in 2 L pH-controlled bioreactors with a working volume of 0.75 L (Applikon, The Netherlands). The oxygen saturation was kept above 50 % by stirring at 550 rpm and sparging with air at 0.75 L/min. Antifoam 204 (Sigma-Aldrich, USA) was added at a concentration of 0.02 %. Samples were taken during steady state, which was assumed to be reached after 5 volume changes. Three independent cultivations were done for each growth condition. After one steady state of the mutant strain *P. putida* KT2440-JD1, which converts benzoate to *cis, cis*-muconate, the dilution rate ( $D$ ) was increased to 1.3 h<sup>-1</sup> to cause a wash-out of the biomass. Five samples were taken within 3.5 hours to measure the concentration of biomass ( $C_x$ ), benzoate ( $C_b$ ) and *cis, cis*-muconate ( $C_m$ ), from which the maximum

growth rate ( $\mu_{max}$ ) and  $q_{pm}$  were calculated using the formulas  $C_{x_t} = C_{x_0} e^{(\mu-D)t}$  and  $\frac{dC_{m_t}}{dt} = q_{pm}C_{x_t} - DC_{m_t}$ . To calculate the  $q_{pm}$  this formula was rewritten to:  $\frac{C_{m_t}}{C_{x_t}} = \frac{q_{pm}}{\mu} (1 - e^{-\mu t}) + \frac{C_{m_0}}{C_{x_0}} e^{-\mu t}$ . During the steady states and the wash-out experiment the biomass yield ( $Y_{(X/S)}$ ) (g<sub>DCW</sub>/ g glucose) and the  $Y_{(P/S)}$  (mol benzoate/ mol *cis, cis*-muconate) were determined.

The intracellular concentrations of benzoate, catechol and *cis, cis*-muconate were measured in *P. putida* KT2440-JD1, that was grown in an Erlenmeyer shake flask on 35 mL MM with 5 mM

benzoate and 10 mM glucose. When benzoate was depleted, the cells were harvested, washed three times with cooled PBS buffer containing 136.9 mM NaCl, 2.68 mM KCl, 4.27 mM Na<sub>2</sub>HPO<sub>4</sub>·2H<sub>2</sub>O, 1.47 mM KH<sub>2</sub>PO<sub>4</sub> (pH 7.13), and frozen at -20°C. After this, the cells were resuspended and lysed in 1 mL buffer containing 10 mM Tris-HCL and 1 mM EDTA (pH 8) with 1 mg/ml lysozyme at room temperature for 25 min while shaking, after which the concentrations of benzoate, catechol and *cis, cis*-muconate were measured by HPLC.

**Analytical methods.**  $C_x$  was determined during steady state by measuring the OD<sub>600</sub> on a Ultrospec 2000 spectrophotometer (Pharmacia Biotech, Sweden). The relation between OD<sub>600</sub> and  $C_x$  was determined to be  $C_x = 0.41 \times \text{OD}_{600} + 0.11$  by measuring the OD<sub>600</sub> of steady state continuous cultures and by weighing the amount of cells in 10 mL culture samples. The latter was done in triplicate by filtering the culture samples through a pre-dried and weighed 0.2 µm cellulose-acetate filter (Whatmann, USA), after which the cells were washed with 5 mL phosphate buffer (3.9 g/L K<sub>2</sub>HPO<sub>4</sub> and 1.6 g/L NaH<sub>2</sub>PO<sub>4</sub>).

Benzoate and *cis, cis*-muconate were determined in the culture supernatant by HPLC using a Varian Microsorb<sup>tm</sup>-MVHPLC column (length, 250 nm; inside diameter, 4.6 mm; particle size, 5 µm) (Varian, USA) with a mobile phase: 130 mL/L methanol, 130 mL/L acetonitrile, 740 mL/L demineralized water, 26 µL/L TFA and 67.5 µL/L H<sub>3</sub>PO<sub>4</sub> (85 %) (1.25 mL/min) and a Waters 2487 UV detector (Waters, USA)<sup>18</sup>. Benzoate was measured at 207 nm and *cis, cis*-muconate at 260 nm. The supernatants were filtered (pore size of 0.2 µm) prior to analysis to remove solids and precipitated proteins.

Glucose in the culture supernatant was determined by HPLC using an Altech IOA-1000 Organic Acids Column (Altech, USA) at 90°C with 3 mM H<sub>2</sub>SO<sub>4</sub> as the mobile phase (0.4 mL/min) followed by detection using a Waters 2414 differential refractometer (Waters, USA). Prior to analysis, the supernatant was diluted 1:1 with 1 M H<sub>2</sub>SO<sub>4</sub> and filtered (pore size of 0.2 µm) to remove solids and precipitated proteins.

**NTG-mutagenesis and high throughput screening.** Mutants of *P. putida* KT2440 were generated by exposure to NTG. For this, *P. putida* KT2440 was grown in a batch culture on 4 g/L glucose for two days. The cells were harvested by centrifugation (3,250 × *g*, room temperature, 25 min) and washed with citrate-phosphate (CPI) buffer: 22.6 g/L Na<sub>2</sub>HPO<sub>4</sub>·2H<sub>2</sub>O, 7.6 g/L C<sub>6</sub>H<sub>8</sub>O<sub>7</sub>·H<sub>2</sub>O. The pH was adjusted to 6.0 with H<sub>3</sub>PO<sub>4</sub>. After washing, the cells were centrifuged and re-suspended in CPI buffer to an OD<sub>600</sub> of 5 and split in 3 batches of 25 mL. The optimal concentration was determined similar to Adelberg *et al.*<sup>19</sup> by adding 0, 60 and 100 µg/mL NTG to the batches. The cells were incubated for 30 min at 30°C, after which the supernatant was discarded by centrifugation. The cells were re-suspended in 25 mL Luria Broth (LB) and incubated for another 30 min at 30°C, after which the cultures were mixed with 12.5 mL 60 % glycerol and frozen at -80°C. The survival rate of the NTG treatment was determined by counting the number of colony forming units (CFU) on 1.5 % agar plates containing MM with 10 mM succinate. Compared to the culture that was not exposed to NTG, the culture that was exposed to 60 µg/ml NTG had a survival rate of 22 %, while the culture that was exposed to 100 µg/ml NTG had a survival rate of 4 %. *P. putida* KT2440 exposed to 60 µg/mL NTG was chosen to continue the research.

**Isolation of mutants that accumulate metabolic intermediates of the benzoate pathway.** The LB cell suspension with the NTG-treated *P. putida* KT2440 was inoculated into 25 mL MM with 20 mM 3-fluorobenzoate (3-FB), 10 mM succinate and 1 mM benzoate to an OD<sub>600</sub> of 0.1 and grown for 10 hours, after which it was transferred to two flasks with the same medium. One of the cultures was grown for 14 hours and the other for 24 hours. The LB cell suspension and the two cultures were plated on 1.5 % agar plates containing 20 mM 3-FB in MM with 10 mM succinate and 1 mM benzoate. The colonies were selected and inoculated onto 384-well plates containing MM with 10 mM succinate and 1 mM benzoate by using a Versarray® colony arrayer and picker (Bio-Rad, USA). Mutants were screened by testing their ability to grow in MM with either 10 mM benzoate or 10 mM succinate as their only source of carbon and energy. Mutants that grew with succinate, but no longer with benzoate, were frozen at -80°C in 15 % glycerol.

**Production of *cis*, *cis*-muconate during batch cultivations.** *P. putida* KT2440-JD1 was grown in batch cultures in MM with 1 mM benzoate and 10 mM of either succinate, citrate or glucose for 25 hours, after which 2 % of the cultures were transferred to the same medium to determine the  $\mu_{max}$  and  $q_{pm}$ . The  $\mu_{max}$  was determined from the slope of the natural logarithm of  $C_x$  over time during the exponential growth phase. The maximal  $q_{pm}$  in the batch cultures was calculated by using the

following formula: 
$$q_{pm} = \frac{dC_{m_t}}{(C_{x_t} \times dt)}$$

**Transcriptomics.** The transcriptome of each of the *P. putida* strains (KT2440 and KT2440-JD1) were analyzed for two of the three independent steady states that were obtained during continuous cultivation. Samples of 1 mL were taken from the cultures and immediately cooled by adding 1 mL of very cold methanol (-80 °C). The samples were quickly centrifuged at  $16,873 \times g$  at 4°C for 50 s, after which the supernatant was discarded. 1 mL RNAlater® (Ambion, USA) was added to stabilize and protect the RNA in the cells. The tubes were vortexed for 1 second and incubated at 4°C for 1-2 h, after which the cells were harvested by centrifugation ( $16,873 \times g$ , 4°C, 1 min). The cell pellet was dried for 5 min, frozen in liquid nitrogen, and stored at -80 °C.

Total RNA was isolated from the cell pellet using the Qiagen® RNeasy Mini Purification Kit and QIAGEN® RNase-Free DNase Set (Qiagen, The Netherlands). The concentration of RNA was determined at 260 nm using a ND-1000 spectrophotometer (NanoDrop, USA). Ten micrograms of total RNA were used to purify 1.2 to 2.2 µg of mRNA using the Ambion® MICROExpress Bacterial mRNA Purification kit (Ambion, USA). The purity of the isolated RNA was determined using the Bio-Rad Experion System (Bio-Rad, USA). cDNA was generated from mRNA using the Affymetrix Poly-A RNA control kit and random priming (Affymetrix, USA). The concentration of cDNA was determined at 260 nm using a ND-1000 spectrophotometer. 0.8-1.2 µg cDNA was fragmented with 0.1 U DNaseI (Pharmacia Biotech, Sweden) per µg DNA at 37°C for 10 min. The fragments were labeled with biotinylated GeneChip® DNA labeling reagent (Affymetrix, USA). The labeled and fragmented cDNA was hybridized to high-density oligonucleotide microarrays of Nimble Express™ arrays (Roche, Switzerland) and scanned by ServiceXS Leiden (Leiden, The Netherlands) according to Ballerstedt *et al.*<sup>20</sup>. The arrays were constructed according to the Affymetrix specifications of *P. putida* A530009N, which was based on the annotated genome of *P. putida* KT2440 (AE015451.1).

The data were analysed using the Bioconductor microarray analysis suite<sup>21</sup>. Raw data were normalized and the expression values computed with the GC-RMA algorithm using default parameters<sup>22</sup>. The Rank products algorithm was used to identify differentially expressed genes in pairwise comparisons between two conditions<sup>23</sup>. This algorithm identifies such genes by comparing the products of ranks of a particular gene in replicated measurements between the two conditions. It allows for the control of the false discovery rate (FDR – expected fraction of false positives among genes identified as differentially expressed) by providing gene a parameter termed percentage of false positives (PFP – an estimate of FDR) for each gene and thus addresses the multiple testing problem associated with identification of differences in microarray experiments (simultaneous testing of thousands of genes)<sup>24</sup>. Genes that had a PFP parameter of 0.05 or lower (i.e. 5% or less probability of being false positive) and a fold change above 2 or below 0.5 were considered as differentially expressed.

**Proteomics.** The proteome of each of the three independent steady states of *P. putida* KT2440 and *P. putida* KT2440-JD1 with or without benzoate was analyzed. The culture samples were identical to those used for transcriptomics. Per steady state, seven of these samples were pooled. Proteins were extracted from the pooled samples by using an SDS extraction protocol for *E. coli* and analyzed by 2-dimensional (2D) gel electrophoresis<sup>25,26</sup>. Additionally, a master 2D gel was prepared that contained equal amounts of protein from the four different conditions. For the first dimension electrophoresis, 150 µg protein was loaded on a 13 cm immobilized pH gradient (IPG) strip pH 4-7 in 250 µL rehydration buffer (9.5 M urea, 4 % (w/v) 3-[(3-cholamidopropyl)dimethylammonio]-1-propansulfonat, 1 % Destreak (GE Healthcare, USA), pH 8.5). Rehydration and isoelectric focusing was carried out using an IPGphor (GE Healthcare, USA) at 20 °C for a total of 30-57 kVh with the current set to 50 µA per strip. Prior to the second dimension, the IPG strips were incubated for 15 min in equilibration buffer (50 mM Tris-HCl, pH 8.8, 6 M urea, 30 % (v/v) glycerol, 2 % (w/v) SDS) containing 1 % (w/v) dithiothreitol (DTT)), followed by 15 min incubation in equilibration buffer containing 2.5 % (w/v) iodoacetamide instead of DTT. The second dimension electrophoresis was performed on lab-cast 12.5 % polyacrylamide gels in a Hoeffer SE600 electrophoresis unit (Hoeffer, USA). The IPG strips were placed on the top of 12.5 % polyacrylamide gels and sealed with a solution of 1 % (w/v) agarose with a trace of bromophenol blue. Gels were run at 15 mA per gel for 15 min, followed by 35 mA per gel until the bromophenol blue had migrated to the bottom of the gel. Proteins were visualized using Sypro Ruby (SR) (Bio-Rad, USA)<sup>27</sup>. Next, the SR stained gels were scanned using a Molecular Imager FX (Bio-Rad, USA) (100 µm resolution, middle sensitivity, 532 nm laser) and converted with Quantity-One 4.4.0 software (Bio-Rad, USA) to tiff-file format. Post-staining of the SR stained gels was done with ProteomIQ (Proteome Systems, USA)<sup>26</sup>.

Image analysis was performed using PDQuest software version 7.1.0 (Bio-Rad, USA). Normalization of spot volumes in a gel was performed using the ‘total density in valid spots’ option. The normalized intensity of spots on three replicate 2D gels was averaged. The relative change in protein abundance for *P. putida* strain KT2440 and *P. putida* KT2440-JD1 with or without benzoate was calculated by dividing the averaged normalized spot quantities of the different conditions. Proteins were significantly differentially expressed when the fold change was above 1.5 or below 0.7 and the *p* value was less than or equal to 0.05. Spots of all differently

expressed proteins were excised and digested in-gel with trypsin and analyzed with MALDI-MS according to Havlis *et al.*<sup>28</sup>. Peptides were analyzed by the Ultraflex TOF/ TOF Mass Spectrometer (Bruker Daltonics, USA), using delayed extraction and reflectron mode with positive ion detection. The mass scale was calibrated with the trypsin autodigestion product of known  $[M+H]^+$  mass, 2211.1 Da and the keratin 9 fragment  $[M+H]^+$ , 2705.2 Da. Proteins were identified using an in house-licensed Mascot search engine (version 2.1.0, Matrix Science, U.K.). The *P. putida* KT2440 database was searched using the MALDI TOF-MS data with carbamidomethyl cysteine as a fixed modification and oxidized methionine as a variable modification. Trypsin was specified as the proteolytic enzyme and up to two missed cleavages were allowed. The quality of peptide mass fingerprints and the certainty of protein identification were evaluated by MOWSE scores.

**DNA sequencing and analysis.** The 3,420 bp *cat* operon of *P. putida* KT2440-JD1 was amplified by a series of five overlapping PCR products covering a region of 4,031 bp. The following fragments: {*catA*} - {*catA/catC/catB*} - {*catB*} - {*catB/catR*} and {*catR*} were obtained using six sets of primers: *cat1fw/catA2Fw* (5'-AGTCGGAGGACTCGTAGCAA / 5'-ATCGAGCACTTCCTCGACCT), *catA1Rv/catCRv* (5'-GGTGCCGAGATGAAGAAGTG / 5'-AGCTCACCTGGGGTACAGAG), *catBFw/catBRv* (5'-GCCGCTTCTTCTACGAACAG / 5'-GATATTGGACGGTCGTCAGG), *cat3fw/catRRv* (5'-ATGTTGGCCTTGATCCCTTC / 5'-AGGTGGTCATTCGTTTCAGG), and *catRFw/cat3rv* (5'-GCCGCTTCTTCTACGAACAG / 5'-GCACGGTTTATCGACTGGTT), respectively. Besides, *catA2* was amplified by PCR using the primer set PP\_3166 fw1/PP\_3166 rv1 (5'-TGCCACTGCAACTCAATTTC / 5'-ACGACTGCACAGGCTTCAC). After purification using the Qiaquick PCR purification kit (Qiagen, The Netherlands), the PCR products were sent to BaseClear BV, The Netherlands, for sequencing with each of the described primers. Nucleotide sequences were blasted with the blastn program against the genome of *P. putida* KT2440 available in the GenBank database (accession no. AE015451.1) at the server of the National Centre for Biotechnology Information<sup>11</sup> in order to find any mutation appearing in the *P. putida* KT2440-JD1 mutant.

**Complementation of *P. putida* KT2440-JD1 with *catR*.** Complementation of *P. putida* KT2440-JD1 with the wildtype *catR* was carried out by cloning the gene into the replicative vector pBBR1MCS-5<sup>29</sup>. The wildtype *catR* was amplified from the genomic DNA of strain KT2440 by PCR with the following primers PP\_3716 fw/PP\_3716 rv (5'-CGACCGTCCAATATCAAATG / 5'-GGTGTGTTTCATATGGCCTGT). The PCR fragment was purified and cloned into an intermediate vector (pCR<sup>®</sup>2.1-TOPO<sup>®</sup>, Invitrogen) generating the plasmid pTOPO-3716. Restriction with *Apa*I and *Bam*HI enzymes of both pTOPO-3716 and pBBR1MCS-5 allowed the ligation of *catR* gene into pBBR1MCS-5, generating pBBR1MCS-5\_3716 that was then introduced into *P. putida* KT2440-JD1 by electroporation according to Holtwick *et al.*<sup>30</sup>. Transformants were selected on LB medium supplemented with gentamicin (30 µg/mL). The complemented mutant was grown in batch cultures on MM with 5 mM benzoate and gentamicin (30 µg/mL).

**Protein sequence and structure analysis of catechol 1,2-dioxygenases.** Protein sequences of CatA2 (Q88I35), CatA (Q88GK8) and catechol-1,2-dioxygenase from *P. arvilla* C1 (Q51433) were downloaded from Uniprot and aligned using ClustalW<sup>31,32</sup>. Structural models of the three proteins were downloaded from the SWISS-MODEL Repository<sup>33,34</sup>. The structures of CatA and CatA2 are based on the known structure of catechol-1,2-dioxygenase from *P. arvilla* C1 (PDB\_Id:2AZQ)<sup>35,36</sup>.

The structural models were visualized compared using the molecular graphics program Coot the structural models were visually compared<sup>37</sup>.

**Expressing and purification of *catA2*.** Gene *catA2* was amplified from the genome of *P. putida* KT2440 by PCR using the forward primer 5'-AAAAACATATGACCGTGAACATTTCCCATACTG-3' and the reverse primer 5'-TTTTTCTCGAGTCAGGCCTCCTGCAAAGCTC-3' containing a *NdeI* and *XhoI* site, respectively. The PCR fragment was ligated into the pET-28a(+) expression vector (Novagen, USA). The *catA2* insert was controlled by sequencing after amplification with the T7 and T7 term primer set (Eurofins MWG GmbH, Germany).

pET-28a(+) with and without the *catA2* insert were electro transformed into *E. coli* BLN21 and plated on LB with kanamycin (50 µg/mL). Transformants containing the plasmid with and without *catA2* were grown overnight in 25 mL LB with kanamycin (50 µg/mL) at 37°C with shaking. 5 mL of these cultures were used to inoculate 200 mL cultures with the same medium, to which 1 mM isopropyl b-d-thio-galactoside was added at the logarithmic phase. The cells were harvested by centrifugation at  $13,680 \times g$  at 4 °C for 30 min and frozen at -20°C. The frozen cells were resuspended in 15 mL 20 mM Tris buffer (pH 7.5), and lysed by adding a small amount of lysozyme from chicken egg (Fluka, USA) and sonicating. The crude cell extract was centrifuged at  $9,047 \times g$  at 4 °C for 10 min. *catA2* was purified from the crude extract by ÄKTA fast protein liquid chromatography (GE health care, USA) using a 5 mL NI-NTA column (Qiagen, The Netherlands). The proteins were eluted with 20 mM Tris-HCl (pH 8) with a 0-500 mM imidazol gradient at a flow rate of 5 mL/min for 20 minutes. The purification of CatA2 was monitored with SDS-PAGE and Westernblotting using His-Tag antibodies (Abcam, U. K.).

The activity of *catA2* was assayed by measuring the increase in *cis*, *cis*-muconate concentration from catechol in a buffer containing 20 mM Tris-HCl, 0.125 M imidazole (pH 7.8) at  $A_{256}$  using an UV mc2<sup>®</sup> spectrophotometer (SAFAS, Monaco). In order to determine the  $k_m$  value of the enzyme, the conversion rate of catechol to *cis*, *cis*-muconate was measured at 10 different concentrations of catechol ranging between from 0.0001 to 0.05 mM. The half maximum inhibitory concentration ( $IC_{50}$ ) was determined from the conversion of 0.05 mM catechol in the presence of 16 different concentrations of *cis*, *cis*-muconate ranging from 0 to 0.2 mM. The protein concentration was determined using the Coomassie plus<sup>™</sup> (Bradford) protein assay reagent (Thermo Fischer Scientific, USA). The values for  $K_m$ ,  $IC_{50}$ , and  $V_{max}$  were calculated by Graphpad Prism (Graphpad Software, Inc., USA).

## Results and discussion

**Isolation of *P. putida* KT2440 mutants that accumulate metabolic intermediates of the benzoate pathway.** *P. putida* KT2440 was exposed to NTG to generate mutants that accumulate benzoate intermediates. To enhance the amount of cells that were mutated in the benzoate pathway, the NTG-treated culture was exposed to 3-FB or 3-chlorobenzoate (3-ClB). Both compounds are substrate analogues of benzoate and 3-FB is known to become toxic when converted by the

benzoate pathway<sup>12,13,39</sup>. In this way, mutants that do not generate these toxic intermediates will have a selective advantage.

To determine the optimal concentrations of the substrate analogues, *P. putida* KT2440 was grown in MM with 10 mM succinate and 1 mM benzoate in the presence of increasing concentrations of 3-FB or 3-CIB. The accumulation of fluorocatechol derivatives is known to result in a violet coloration of the medium<sup>13</sup>. When *P. putida* KT2440 was exposed to 3-FB or 3-CIB a violet coloration of the medium was observed. Growth of *P. putida* KT2440 was more inhibited (Fig. 2) and the violet coloration was more intense and rapid when the cells were exposed to 3-FB as compared to 3-CIB. Therefore, two independent batch cultures of NTG-treated *P. putida* KT2440 cells were cultivated in the presence of 20 mM 3-FB. Batch culture 1 was grown for 14 hours and batch culture 2 for 24 hours, after which the cultures were plated. Individual colonies were screened for their ability to grow with benzoate as the sole source of carbon and energy. Three mutants that could no longer grow using benzoate were isolated from batch 1 and 84 mutants were isolated from batch 2, which represented 0.1 % and 4.4 %, respectively, of the total amount of colonies that were screened. No mutants were found when the NTG-treated *P. putida* KT2440 cells were not exposed to 3-FB. All mutants accumulated *cis*, *cis*-muconate in the medium when grown with succinate in the presence of benzoate. Therefore, the disability of the further conversion of 2-fluoro-*cis*, *cis*-muconate by the muconate lactonizing enzyme seems to have caused the selective advantage. 2-Fluoro-*cis*, *cis*-muconate has been observed as a dead-end metabolite<sup>12,13</sup>. One mutant *P. putida* KT2440-JD1 was selected for further study because of its relatively high  $Y_{(P/S)}$  in batch culture (data not shown) and because it was isolated from batch 1, which had the shortest period of exposure to 3-FB.

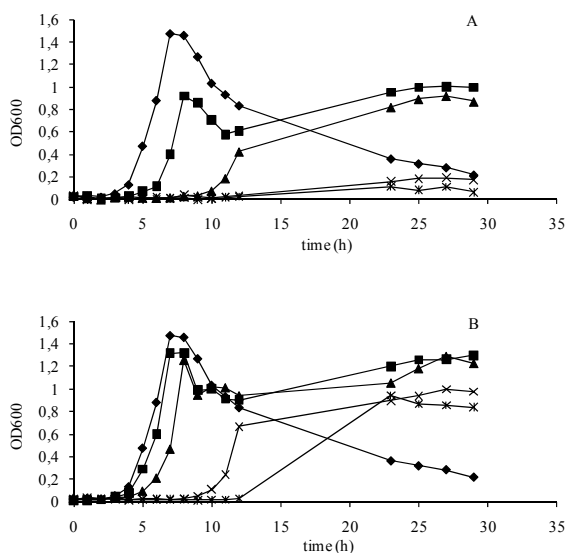


**Figure 2.** Growth of *P. putida* KT2440 during batch cultivations in MM with 10 mM succinate, 1 mM benzoate and 0 (♦), 5 (■), 10 (▲), 15 (×), or 20 mM (\*) 3-FB (3A) or 3-CIB (3B).

**Conversion of benzoate with different growth substrates.** To determine which carbon and energy sources are suitable for the production of *cis, cis*-muconate from benzoate by *P. putida* KT2440-JD1, the strain was grown in MM with 10 mM of either succinate, citrate, or glucose in combination with 1 mM benzoate. *P. putida* KT2440-JD1 was able to grow well with succinate, citrate or glucose (Fig. 3). The  $q_{pm}$  and  $Y_{(X/S)}$  were higher with glucose, while the  $Y_{(P/S)}$  was higher with citrate (Table 1). Since glucose is an inexpensive substrate and the  $Y_{(P/S)}$  with glucose was still high, this substrate was chosen for further studies.

**Table 1.** Growth and production of *cis, cis*-muconate by *P. putida* KT2440-JD1 in batch cultures with 10 mM of various substrates and 1 mM benzoate. The pre-cultures were grown on the same medium.

growth substrate	maximum $q_{pm}$ g/(gDCW*h)	$\mu_{max}$ h <sup>-1</sup>	Y(P/S) mol <i>cis, cis</i> -muconate/ mol benzoate	Y(X/S) gDCW/ g growth substrate
Succinate	0.5	1.0	0.68	0.29
Citrate	1.3	0.7	0.95	0.18
Glucose	2.0	0.7	0.89	0.30

**Continuous cultivations of *P. putida* KT2440 and KT2440-JD1 in the presence and absence of benzoate.** *P. putida* KT2440 and KT2440-JD1 were grown in triplicate in continuous cultures with 10 mM glucose in the presence and absence of 5 mM benzoate at a dilution rate of 0.2 h<sup>-1</sup>. In the absence of benzoate, the  $Y_{(X/S)}$  of *P. putida* KT2440 and KT2440-JD1 were 0.37 ± 0.02 and 0.36 ± 0.01 gDCW/g glucose, respectively. When 5 mM benzoate was present in the feed of *P. putida* KT2440, the  $Y_{(X/S)}$  in steady state cultures increased to 0.58 ± 0.04 gDCW/g glucose, due to the use of benzoate as additional growth substrate. With *P. putida* KT2440-JD1, the  $Y_{(X/S)}$  (0.40 ± 0.06 gDCW/g glucose) showed no significant change in the presence of benzoate. Benzoate was co-metabolized to *cis, cis*-muconate with an average  $Y_{(P/S)}$  of 0.89 ± 0.02 mol *cis, cis*-muconate/ mol benzoate and a  $q_{pm}$  of 0.18 ± 0.03 g *cis, cis*-muconate/ (gDCW\* h). The  $Y_{(P/S)}$  was similar to that obtained during batch cultivations (Table 1). No benzoate, catechol or *cis, cis*-muconate was detected in the cytosol of *P. putida* KT2440-JD1 that was producing *cis, cis*-muconate from benzoate during growth on glucose in shake flasks. These results indicate that some *cis, cis*-muconate was further metabolized. When the  $D$  was increased to 1.3 h<sup>-1</sup> after a steady state with *P. putida* KT2440-JD1 in the presence of 5 mM benzoate, the culture washed-out. The  $\mu_{max}$  of the mutant during the wash-out was 0.6 h<sup>-1</sup>. The highest  $q_{pm}$  was determined to be 1.4 g *cis, cis*-muconate/ (gDCW\* h) after 1 hour and 20 minutes after the increase of the  $D$  to 1.3 h<sup>-1</sup>. The  $q_{pm}$  was 8 times higher than observed during continuous cultivation at  $D$  0.2 h<sup>-1</sup>, showing that the productivity of *P. putida* KT2440-JD1 is much higher under  $\mu_{max}$  conditions and unlimited presence of benzoate.

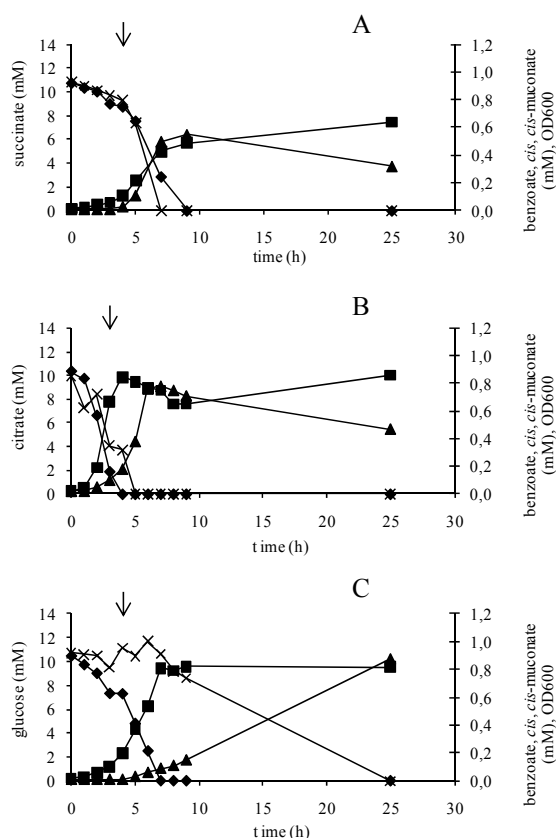


**Figure 3.** Growth of *P. putida* KT2440-JD1 during batch cultivations in MM with 1 mM benzoate and 10 mM succinate (A), citrate (B), or glucose (C). The pre-cultures were grown on the same medium. Symbols: x, growth substrate; ♦, benzoate; ■, *cis, cis*-muconate; ▲, cell density measured at OD<sub>600</sub>. The arrows show the period in which the specific production rate of *cis, cis*-muconate was maximal.

Several other mutants were reported that also convert benzoate to *cis, cis*-muconate<sup>7,12,40,41,42,43</sup>. The  $q_{pm}$  of *P. putida* KT2440-JD1 under  $\mu_{max}$  conditions was at least 8 times higher than that of the best performing strains *Pseudomonas* sp. B13<sup>12</sup> and *P. putida* BM014<sup>40</sup>, while the  $Y_{(P/S)}$  was similar, showing that *P. putida* KT2440-JD1 is a very suitable biocatalyst for the production of *cis, cis*-muconate.

**Transcriptomics of *P. putida* KT2440 and KT2440-JD1 in the presence and absence of benzoate.** The transcriptome analysis of *P. putida* KT2440 and KT2440-JD1 was conducted on steady state samples of the continuous cultivations in the presence and absence of benzoate. The transcriptomes were compared by analyzing the expression of genes via four pairwise comparisons. The genes involved in benzoate degradation (*ben*, *cat* and *pca* operons) comprised the majority of differentially expressed genes (Fig. 4)<sup>6</sup>. When the strains were grown in the absence of benzoate, the transcriptomes of both strains were very similar except for a lower expression of *catA* and a higher expression of a gene encoding a hypothetical protein (PP\_0032) in *P. putida* KT2440-JD1 (Table 2). When benzoate was present, the genes of the *ben* operon were highly induced in both strains. The genes of the *cat* operon were highly induced in *P. putida* KT2440, but their expression was very low in *P. putida* KT2440-JD1, showing that the induction of the *cat* operon is impaired in

the mutant (Fig. 4, Table 2). Furthermore, in the presence of benzoate the expression of two transporter genes (PP\_3565 and PP\_3566) was higher in *P. putida* KT2440-JD1 as compared to *P. putida* KT2440 (Table 2).

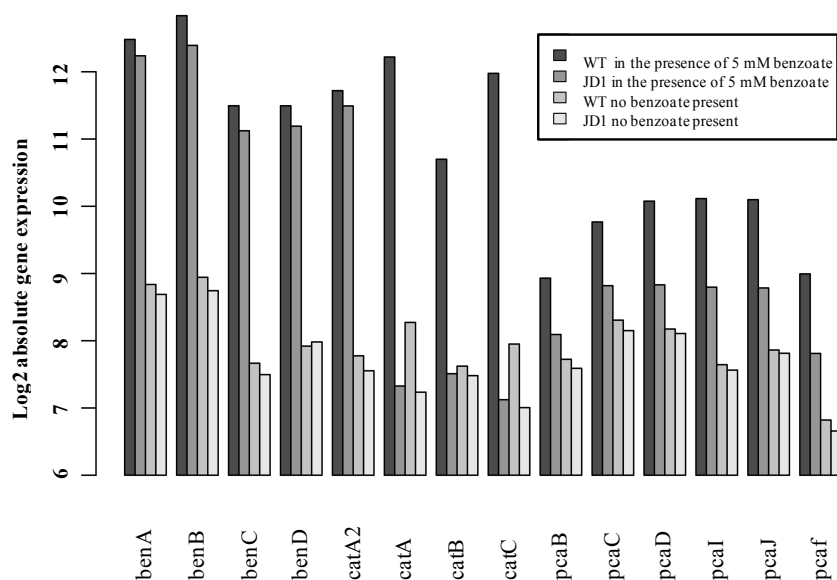


**Figure 4.** Log2 of absolute gene expression values of genes involved in benzoate metabolism in *P. putida* KT2440 (WT) and *P. putida* KT2440-JD1 (JD1) during steady states on 10 mM glucose in the presence and absence of 5mM benzoate at  $D$  0.2 h<sup>-1</sup>.

The results reveal that *P. putida* KT2440-JD1 accumulates *cis*, *cis*-muconate in the culture medium when benzoate is present due to the lack of induction of the *cat* operon. The *ben* operon contains a gene for a putative second catechol 1,2-dioxygenase (CatA2), which is probably responsible for the conversion of catechol to *cis*, *cis*-muconate in the mutant, since there were no other catechol 1,2-dioxygenase genes identified in the genome of *P. putida* KT2440<sup>2</sup>.

The function of CatA2 has not yet been shown<sup>6</sup>. CatA2 has 76 % amino acid identity with both CatA and the catechol 1,2-dioxygenase from *P. arvilla* C1, of which the three-dimensional structure has been elucidated<sup>33,34,36</sup>. Based on the protein sequence alignment and visual structural comparison, the defined active sites of the three enzymes are 100% identical. To show that CatA2 is able to convert catechol to *cis*, *cis*-muconate, *catA2* was heterologously expressed in *E. coli* BLN21, and the enzyme was purified using the His-Tag. The results revealed that CatA2 is indeed functioning as a catechol 1,2-dioxygenase with a  $K_m$  of 0.0010 mM catechol and a  $IC_{50}$  of 0.1392 mM *cis*, *cis*-muconate at a concentration of 0.05 mM catechol. From these numbers a  $K_i$  value of

0.0028 mM was calculated using the Cheng-Prusoff equation<sup>44</sup>. The  $V_{max}$  was estimated to be 0.4  $\mu\text{M}/\text{min}/\text{mg}$ .

The genes of the protocatechuate pathway (*pcaBCDIJF*) were still induced in *P. putida* KT2440-JD1, but the expression levels of the genes were approximately two times lower than those in the wildtype (Fig. 4, Table 2).  $\beta$ -keto adipate is known to induce the *pca* pathway<sup>45,46</sup> and may be generated in the mutant by some remaining activity of the enzymes encoded by the *cat* operon.  $\beta$ -keto adipate may also be formed by PcaB and PcaC, which convert  $\beta$ -carboxy-*cis*, *cis*-muconate and 7-carboxymuconolactone, respectively, but may have some activity for *cis*, *cis*-muconate and muconolactone as well, which could explain the observed  $Y_{(P/S)}$  of  $0.89 \pm 0.02$  mol *cis*, *cis*-muconate/ mol benzoate.

### **Proteomics of *P. putida* KT2440 and KT2440-JD1 in the presence and absence of benzoate.**

Proteome analysis of *P. putida* KT2440 and KT2440-JD1 was conducted on steady state samples of the continuous cultivations. An average of 400 protein spots was displayed on each 2D gel, independent of the cultivation condition. When the strains were grown in the absence of benzoate, the proteomes of *P. putida* KT2440 and *P. putida* KT2440-JD1 were similar. In the presence of benzoate the only differences between *P. putida* KT2440 and KT2440-JD1 were the lower levels of CatA and CatB in the mutant, which confirmed on the proteomic level that the *cat* operon is no longer induced in *P. putida* KT2440-JD1. Other enzymes from the *ortho*-cleavage pathway that have been shown at the proteomic level<sup>47,48,49</sup> were not identified in this study, which may be caused by a higher sensitivity of their analyses due to the use of longer IPG strips.

In both strains the same 15 proteins were differentially regulated in the presence and absence of benzoate (Table 3). In the presence of benzoate, the expression levels of the chaperones GroEL, GroES and DnaK, which belong to the RpoH regulon family, were up-regulated. These proteins are induced by aromatics and mediate the proper folding of the proteins<sup>50</sup>. The expression levels of *Catalase/ peroxidase* HPI, which is involved in the oxidative stress response, three outer membrane porin-like proteins (OprF, OmpA family protein and OprD) and a motility protein (FliC) were down-regulated. *catA* and *catB* were the only genes that were differentially expressed both at the transcriptome and proteome level. The lack of similarity of the transcriptome and proteome may be caused by post-transcriptional regulatory systems, which determine the translation efficiency, the stability of the protein and its activity by modifications, and therefore influence the protein concentration in the cell<sup>51,52,53</sup>. This illustrates the importance of multi-level studies.

**Nucleotide sequence of the *cat* operon of *P. putida* KT2440\_JD1.** The analyses of the transcriptome and proteome revealed that the *cat* operon in *P. putida* KT2440-JD1 is no longer induced in the presence of benzoate. A 4,031 bp region containing the *cat* operon was sequenced and only one single point mutation was found in *catR*. This was at the first position of the 50<sup>th</sup> codon, which changed Arg50 (CGC) to Cys50 (TGC). CatR belongs to the LysR-type transcriptional regulator (LTTR) proteins<sup>54</sup>. An alignment of the amino acid sequences of seven different LTTR proteins showed that Arg50 is highly conserved in the winged helix-turn-helix motif of the DNA-binding region. The genes *catA* and *catBC* are divergently induced by the regulatory protein CatR in the presence of *cis*, *cis*-muconate<sup>55,56</sup>. Apparently, the mutation in *catR* inhibited the expression of all genes of the *cat* operon. When *P. putida* KT2440-JD1 was

complemented with wildtype *catR*, growth on benzoate as the single carbon source was restored. These results show unequivocally that the mutation in *catR* is responsible for the observed phenotype of *P. putida* KT2440-JD1.

**Table 2.** Transcriptomic data of genes that were differentially expressed with a fold change above 2 or below 0.5 and a threshold of 5 percent of false positives. Comparison 1: *P. putida* KT2440-JD1 compared to *P. putida* KT2440 when grown in the absence of benzoate. Comparison 2: *P. putida* KT2440-JD1 compared to *P. putida* KT2440 when grown in the presence of benzoate. Comparison 3: *P. putida* KT2440 grown in the presence of benzoate compared to *P. putida* KT2440 grown in the absence of benzoate. Comparison 4: *P. putida* KT2440-JD1 grown in the presence of benzoate compared to *P. putida* KT2440-JD1 grown in the absence of benzoate.

Comparison	Locus ID	Gene name	Product name	Fold change	Percent of false positives	
1	PP_0032		hypothetical protein	2.28	0.00	
	PP_3713	<i>catA</i>	catechol 1,2-dioxygenase	0.49	0.00	
2	PP_3566		major facilitator family transporter	3.87	0.00	
	PP_1157		acetolactate synthase	2.87	0.00	
	PP_3123		3-oxoacid CoA-transferase subunit B	2.58	0.00	
	PP_2652		hydratase/decarboxylase	2.18	0.00	
	PP_0017		transcriptional regulator MvaT, P16 subunit, putative	2.30	0.00	
	PP_2244		hypothetical protein	2.13	0.00	
	PP_3122		3-oxoacid CoA-transferase subunit A	2.08	0.00	
	PP_3565		amino acid transporter LysE	2.04	0.00	
	PP_4466		TauD/TfdA family dioxygenase	2.02	0.00	
	PP_1377	<i>pcaF</i>	beta-ketoadipyl CoA thiolase	0.44	0.02	
	PP_1380	<i>pcaD</i>	3-oxoadipate enol-lactonase	0.42	0.01	
	PP_3951	<i>pcaI</i>	3-oxoadipate CoA-transferase, subunit A	0.40	0.02	
	PP_3952	<i>pcaJ</i>	3-oxoadipate CoA-transferase, subunit B	0.40	0.02	
	PP_3712		hypothetical protein	0.41	0.02	
	PP_2553		major facilitator family transporter	0.36	0.01	
	PP_2643		methyl-accepting chemotaxis sensory transducer	0.28	0.00	
	PP_3715	<i>catB</i>	muconate and chloromuconate cycloisomerase	0.11	0.00	
	PP_3714	<i>catC</i>	muconolactone isomerase	0.03	0.00	
	PP_3713	<i>catA</i>	catechol 1,2-dioxygenase	0.03	0.00	
	3	PP_3714	<i>catC</i>	muconolactone isomerase	16.29	0.00
		PP_3713	<i>catA</i>	catechol 1,2-dioxygenase	15.43	0.00
		PP_3162	<i>benB</i>	muconate and chloromuconate cycloisomerase	14.83	0.00
		PP_3166	<i>catA2</i>	catechol 1,2-dioxygenase	15.39	0.00
		PP_3163	<i>benC</i>	oxidoreductase FAD/NAD(P)-binding domain protein	14.21	0.00
		PP_3165	<i>benK</i>	major facilitator transporter	13.76	0.00
		PP_3161	<i>benA</i>	benzoate dioxygenase, alpha subunit	12.50	0.00
		PP_3164	<i>benD</i>	1,6-dihydroxycyclohexa-2,4-diene-1-carboxylate dehydrogenase	11.91	0.00
PP_3168		<i>benF</i>	benzoate-specific porin	11.01	0.01	
PP_3167		<i>benE-2</i>	benzoate transporter	9.63	0.00	
PP_3715		<i>catB</i>	muconate and chloromuconate cycloisomerase	8.44	0.01	
PP_3951		<i>pcaI</i>	3-oxoadipate CoA-transferase, subunit A	5.54	0.01	
PP_3952		<i>pcaJ</i>	3-oxoadipate CoA-transferase, subunit B	4.71	0.01	
PP_2643			methyl-accepting chemotaxis sensory transducer	4.52	0.01	
PP_1377		<i>pcaF</i>	beta-ketoadipyl CoA thiolase	4.51	0.01	
PP_1380		<i>pcaD</i>	3-oxoadipate enol-lactonase	3.74	0.02	
PP_3169			membrane-bound metal-dependent hydrolase	3.62	0.02	
PP_1376		<i>pcaK</i>	benzoate transport	3.32	0.02	
PP_1383			BenF-like porin	3.22	0.02	
PP_2553			major facilitator family transporter	3.08	0.02	
PP_1381		<i>pcaC</i>	4-carboxymuconolactone decarboxylase	2.75	0.03	
PP_3712			hypothetical protein	2.66	0.02	
PP_3671			aldo/keto reductase family oxidoreductase	2.49	0.02	
PP_1379		<i>pcaB</i>	3-carboxy- <i>cis</i> , <i>cis</i> -muconate cycloisomerase	2.31	0.03	
PP_3159		<i>benR</i>	AraC family transcriptional regulator	2.18	0.03	
PP_1742			hypothetical protein	0.34	0.04	
4		PP_3166	<i>catA2</i>	catechol 1,2-dioxygenase	15.34	0.00
	PP_3165	<i>benK</i>	major facilitator transporter	13.01	0.00	
	PP_3163	<i>benC</i>	oxidoreductase FAD/NAD(P)-binding domain protein	12.35	0.00	
	PP_3162	<i>benB</i>	muconate and chloromuconate cycloisomerase	12.54	0.00	
	PP_3161	<i>benA</i>	benzoate dioxygenase, alpha subunit	11.70	0.00	
	PP_3164	<i>benD</i>	1,6-dihydroxycyclohexa-2,4-diene-1-carboxylate dehydrogenase	9.25	0.00	

PP_3168	<i>benF</i>	benzoate-specific porin	8.93	0.00
PP_3167	<i>benE-2</i>	benzoate transporter	7.75	0.00
PP_3566		major facilitator family transporter	4.09	0.00
PP_1157		acetolactate synthase	2.97	0.00
PP_3169		membrane-bound metal-dependent hydrolase	2.72	0.01
PP_2652		hydratase/decarboxylase	2.44	0.01
PP_3123		3-oxoacid CoA-transferase subunit B	2.42	0.01
PP_3951	<i>pcaI</i>	3-oxoadipate CoA-transferase, subunit A	2.35	0.01
PP_1377	<i>pcaF</i>	beta-ketoadipyl CoA thiolase	2.22	0.02
PP_1376	<i>pcaK</i>	benzoate transport	2.06	0.02
PP_0017		transcriptional regulator MvaT, P16 subunit, putative	2.03	0.03
PP_3122		3-oxoacid CoA-transferase subunit A	2.01	0.03
PP_2006		hypothetical protein	0.49	0.01
PP_0032		hypothetical protein	0.48	0.03

**Table 3.** Proteomics data of proteins that were differentially regulated with a fold change above 1.5 or below 0.7 and a MOWSE score higher than 50 %. Comparison 1: *P. putida* KT2440-JD1 compared to *P. putida* KT2440 when grown in the absence of benzoate. Comparison 2: *P. putida* KT2440-JD1 compared to *P. putida* KT2440 when grown in the presence of benzoate. Comparison 3: *P. putida* KT2440 grown in the presence of benzoate compared to *P. putida* KT2440 grown in the absence of benzoate. Comparison 4: *P. putida* KT2440-JD1 grown in the presence of benzoate compared to *P. putida* KT2440-JD1 grown in the absence of benzoate.

Comparison	Locus ID	Protein name	Protein name	Fold change	MOWSE score
1	No differences				
2	PP_3713	CatA	catechol 1,2-dioxygenase	0.5	85
	PP_3715	CatB	muconate and chloromuconate cycloisomerase	0.4	92
3/4	PP_1361	GroEL	chaperonin GroEL	2.0	102
	PP_4849		dnaK protein, putative	1.8	163
	PP_1360	GroES	co-chaperonin GroES	1.8	57
	PP_0469	RplF	50S ribosomal protein L6	1.5	115
	PP_0454	RplC	50S ribosomal protein L3	1.5	131
	PP_5393		heavy metal transport/ detoxification protein	1.5	57
	PP_0466	RplE	50S ribosomal protein L5	0.7	144
	PP_2089	OprF	OmpF family protein	0.7	146
	PP_1001	ArcA	arginine deiminase	0.7	53
	PP_1087		OmpA family outer membrane protein	0.7	97
	PP_1206	OprD	outer membrane porin	0.7	128
	PP_4378	FliC	flagellin FliC	0.7	147
	PP_1661		dehydrogenase subunit, putative	0.6	120
	PP_0766		hypothetical protein	0.6	57
	PP_3668		catalase/ peroxidase HPI	0.6	82

## Conclusion

*P. putida* KT2440-JD1, which was derived from the typestrain *P. putida* KT2440 after NTG mutagenesis and exposure to 3-FB, accumulates *cis*, *cis*-muconate from benzoate with a very high  $q_{pm}$  of 2.0 g/(g<sub>DCW</sub>\* h) and  $Y_{(P/S)}$  of 0.89 mol (*cis*, *cis*-muconate/ mol benzoate) under  $\mu_{max}$  conditions and unlimited presence of benzoate. This  $q_{pm}$  is at least eight times higher than the  $q_{pm}$  values reported for other *cis*, *cis*-muconate-producing strains<sup>7,12,40,41,42,43</sup>, which shows that *P. putida* KT2440-JD1 is a very suitable biocatalyst for the production of *cis*, *cis*-muconate from benzoate.

*P. putida* KT2440-JD1 is the first *cis*, *cis*-muconate-accumulating mutant that was characterized at the genetic level. It contains a point mutation in *catR* that prevents the induction of the *cat* operon as a response to the presence of benzoate. The enzymes that are responsible for the conversion of benzoate to *cis*, *cis*-muconate in *P. putida* KT2440-JD1 are encoded on the *ben* operon, which contains the second catechol 1,2-dioxygenase-CatA2. CatA2 is 76% identical to other well-characterized catechol 1,2-dioxygenases, and has a fully conserved active site. It is the only

catechol 1,2-dioxygenase-like gene that is highly expressed in the mutant, and its biochemical activity was determined.

### **Acknowledgements**

We thank Kees van Kekem for his help with the HPLC system, Sanne Hoogerwerf for her help with the continuous cultivations, and Dr. Hendrik Ballerstedt for his help with the transcriptomic experiments, and Dr. Matthias Stehr for purifying CatA2, and Dr. Birgit Hoffmann, and María Suárez Diez for their help with analyzing protein structures.

This research was carried out within the research programme of the Kluyver Centre for Genomics of Industrial Fermentation, which is part of the Netherlands Genomics Initiative.

## References

1. Wackett LP. 2003. *P. putida* - a versatile biocatalyst. *Nat Biotechnol* 21:136-138.
2. Martins dos Santos VAP, Heim S, Strätz M, Timmis KN. 2004. Insights into the genomic basis of niche specificity of *Pseudomonas putida* strain KT2440. *Environ Microbiol* 6:1264-1286
3. Nelson KE, Weinel C, Paulsen IT, Dodson RJ, Hilbert H, Martins dos Santos VAP, Fouts DE, Gill SR, Pop M, Holmes M, Brinkac L, Beanan M, DeBoy RT, Daugherty S, Kolonay J, Madupu R, Nelson W, White O, Peterson J, Khouri H, Hance I, Chris Lee P, Holtzapple E, Scanlan D, Tran K, Moazzez A, Utterback T, Rizzo M, Lee K, Kosack D, Moestl D, Wedler H, Lauber J, Stjepandic D, Hoheisel J, Straetz M, Heim S, Kiewitz C, Eisen JA, Timmis KN, Dusterhöft A, Tümmler B, Fraser CM. 2002. Complete genome sequence and comparative analysis of the metabolically versatile *Pseudomonas putida* KT2440. *Environ Microbiol* 4:799-808.
4. Federal register (1982) Certified host-vector systems, 17197.
5. Ramos JL, Wasserfallen A, Rose K, Timmis KN. 1987. Redesigning metabolic routes: manipulation of TOL plasmid pathway for catabolism of alkylbenzoates. *Science* 235:593-596.
6. Jiménez JI, Miñambres B, García JL, Díaz E. 2002. Genomic analysis of the aromatic catabolic pathways from *Pseudomonas putida* KT2440. *Environ Microbiol* 4:824-841.
7. Mizuno S, Yoshikawa N, Schi M, Mikawa T, Imada Y. 1988. Microbial-production of *cis, cis*-muconic acid from benzoic-acid. *Appl Microbiol Biotechnol* 28:20-25.
8. NCBI, <http://www.ncbi.nlm.nih.gov/sites/entrez?Db=genome&Cmd=ShowDetailView&TermToSearch=266>
9. Pieper DH, Martins dos Santos VAP, Golyshin PN. 2004. Genomic and mechanistic insights into the biodegradation of organic pollutants. *Curr Opin Biotechnol* 6:4-13.
10. Nakai C, Uyeyama H, Kagamiyama H, Nakazawa T, Inouye S, Kishi F, Nakazawa A, Nozaki M. 1995. Cloning, DNA sequencing, and amino acid sequencing of catechol 1,2-dioxygenases (pyrocatechase) from *Pseudomonas putida* mt-2 and *Pseudomonas arvilla* C-1. *Arch Biochem Biophys* 321:353-362.
11. Kim BJ, Choi WJ, Lee EY, Choi CY. 1988. Enhancement of *cis, cis*-muconate productivity by overexpressing of catechol 1,2-dioxygenase in *Pseudomonas putida* BCM114. *Biotechnol Bioprocess Eng* 3:112-114.
12. Schmidt E, Knackmuss HJ. 1984. Production of *cis, cis*-Muconate from benzoate and 2-fluoro-*cis, cis*-muconate from 3-fluorobenzoate by 3-chlorobenzoate degrading bacteria. *Appl Microbiol Biotechnol* 20:351-355.
13. Schreiber A, Hellwig M, Dorn E, Reineke W, Knackmuss HJ. 1980. Critical reactions in fluorobenzoic acid degradation by *Pseudomonas sp.* B13. *Appl Environ Microbiol* 39:58-67.14. Myers AG, Siegel DR, Buzard DJ, Charest MG. 2001. Synthesis of a broad array of highly functionalized, enantiomerically pure cyclohexanecarboxylic acid derivatives by microbial dihydroxylation of benzoic acid and subsequent oxidative and rearrangement reactions. *Org Lett* 3:2923-2926.
15. van Duuren JB, Brehmer B, Mars AE, Eggink G, Dos Santos VA, Sanders JP. 2011. A limited LCA of bio-adipic acid: Manufacturing the nylon-6,6 precursor adipic acid using the benzoic acid degradation pathway from different feedstocks. *Biotechnol Bioeng.* 108:1298-1306.
16. Duetz WA, van Beilen JB, Witholt B. 2001. Using proteins in their natural environment: potential and limitations of microbial whole-cell hydroxylations in applied biocatalysis. *Curr Opin Biotechnol* 12:419-425.
17. Hartmans S, Smits JP, van der Werf MJ, Volkering F, de Bont JAM. 1989. Metabolism of styrene oxide and 2-phenylethanol in the styrene-degrading *Xanthobacter* Strain 124X. *Appl Environ Microbiol* 55:2850-2855.
18. Jeffrey WH, Cuskey SM, Chapman PJ, Resnick S, Olsen RH. 1992. Characterization of *Pseudomonas putida* mutants unable to catabolize benzoate: cloning and characterization of *Pseudomonas* genes involved in benzoate catabolism and isolation of a chromosomal DNA fragment able to substitute for *xyIS* in activation of the TOL lower-pathway promoter. *J Bacteriol* 174:4986-4996.
19. Adelberg EA, Mandel M, Chen GCC. 1965. Optimal conditions for mutagenesis by *N*-Methyl-*N*-Nitro-*N*-Nitrosoguanidine in *Escherichia coli* K12. *Biochem Biophys Res Commun* 18:788-795.
20. Ballerstedt H, Volkers RJM, Mars AE, Hallsworth JE, dos Santos VA, Puchalka J, van Duuren J, Eggink G, Timmis KN, de Bont JAM, Wery J. 2007. Genomotyping of *Pseudomonas putida* strains using *P. putida* KT2440-based high-density DNA microarrays: implications for transcriptomics studies. *Appl Microbiol Biotechnol* 75:1133-1142.

21. Gentleman RC, Carey VJ, Bates DM, Bolstad B, Dettling M, Dudoit S, Ellis B, Gautier L, Ge Y, Gentry J, Hornik K, Hothorn T, Huber W, Iacus S, Irizarry R, Leisch F, Li C, Maechler M, Rossini AJ, Sawitzki G, Smith C, Smyth G, Tierney L, Yang JYH, Zhang J. 2004. Bioconductor: open software development for computational biology and bioinformatics. *Genome Biol* 5:R80.
22. Wu Z, Irizarry RA, Gentleman R, Murillo FM, Spencer F. 2004. A Model-based background adjustment for oligonucleotide expression arrays. *J Amer Statistical Assoc* 99:909-917.
23. Breitling R, Armengaud P, Amtmann A, Herzyk P. 2004. Rank products: a simple, yet powerful, new method to detect differentially regulated genes in replicated microarray experiments. *FEBS Lett* 573:83-92.
24. Dudoit S, Popper Shaffer J, Boldrick JC. 2003. Multiple hypothesis testing in microarray experiments. *Stat Sci* 18:71-103.
25. VanBogelen RA, Neidhardt FC. 1999. Preparation of *Escherichia coli* samples for 2-D gel analysis. *Methods Mol Biol* 112:21-29.
26. Wijte D, de Jong AL, Mol MAE, van Baar BLM, Heck AJR. 2006. ProteomIQ blue, a potent post-stain for the visualization and subsequent mass spectrometry based identification of fluorescent stained proteins on 2D-gels. *J Proteome Res* 5:2033-2038.
27. Krieg RC, Paweletz CP, Liotta LA, Petricoin EF. 2003. Dilution of protein gel stain results in retention of staining capacity. *Biotechniques* 35:376-378.
28. Havlis J, Thomas H, Sebela M, Shevchenko A. 2003. Fast-response proteomics by accelerated in-gel digestion of proteins. *Anal Chem* 75:1300-1306.
29. Kovach M.E., Elzer P.H., Hill D.S., Robertson G.T., Farris M.A., Roop 2<sup>nd</sup> R.M., Peterson K.M. 1995. Four new derivatives of the broad-host-range cloning vector pBBR1MCS, carrying different antibiotic-resistance cassettes. *Gene* 166:175-176.
30. Holtwick R., von Wallbrunn A., Keweloh H., Meinhardt F. 2001. A novel rolling-circle-replicating plasmid from *Pseudomonas putida* P8: molecular characterization and use as vector. *Microbiology*. 147:337-344.
31. Uniprot, <http://www.uniprot.org>.
32. Thompson J.D., Gibson T.J., Higgins D.G., 2002. Multiple sequence alignment using ClustalW and ClustalX. *Curr Protoc Bioinformatics* Chapter 2, Unit 2.3.
33. Kiefer F., Arnold K., Künzli M., Bordoli L., Schwede T. 2009. The SWISS-MODEL Repository and associated resources. *Nucleic Acids Res* 37:D387-392.
34. Kopp J., Schwede T. 2006. The SWISS-MODEL Repository: new features and functionalities. *Nucleic Acids Res* 34:D315-318.
35. Protein data bank, <http://www.rcsb.org>.
36. Earhart C.A., Vetting M.W., Gosu R., Michaud-Soret I., Que Jr L., Ohlendorf D.H. 2005. Structure of catechol 1,2-dioxygenase from *Pseudomonas arvilla*. *Biochem Biophys Res Commun* 338:198-205.
37. Emsley P., Cowtan K. 2004. Coot: model-building tools for molecular graphics. *Acta Crystallogr D Biol Crystallogr* 60:2126-2132.
38. Suárez M., Tortosa P., Jaramillo A. 2008. PROTDES: CHARMM toolbox for computational protein design. *Syst Synth Biol* 2:105-113.
39. Göbel M, Kassel-Cati K, Schmidt E, Reineke W. 2002. Degradation of aromatics and chloroaromatics by *Pseudomonas sp.* strain B13: cloning, characterization, and analysis of sequences encoding 3-oxoadipate: succinyl-coenzyme A (CoA) transferase and 3-oxoadipyl-CoA thiolase. *J Bacteriol* 184:216-223.
40. Bang SG, Choi CY. 1995. DO-stat fed-batch production of *cis, cis*-muconic acid from benzoic-acid by *Pseudomonas putida* BM014. *J Ferment Bioeng* 79:381-383.
41. Bang SG, Choi WJ, Choi CY, Cho MH. 1996. Production of *cis, cis*-muconic acid from benzoic acid via microbial transformation. *Biotechnol Bioprocess Eng* 1:36-40.
42. Choi W J, Lee EY, Cho MH, Choi CY. 1997. Enhanced production of *cis, cis*-muconate in a cell-recycle bioreactor. *J Ferment Bioeng* 84:70-76.
43. Wu CM, Lee TH, Lee SN, Lee YA, Wu JY. 2006. Microbial synthesis of *cis, cis*-muconic acid from benzoate by *Sphingobacterium sp* GCG generated from effluent of a styrene monomer (SM) production plant. *Biochem Eng J* 29:35-40.
44. Cheng Y., Prusoff WH. 1973. Relationship between the inhibition constant (K<sub>1</sub>) and the concentration of inhibitor which causes 50 per cent inhibition (I<sub>50</sub>) of an enzymatic reaction. *Biochem Pharmacol* 22:3099-3108.
45. Parke D. 1995. Supraoperonic clustering of *pca* genes for catabolism of the phenolic compound protocatechuate in *Agrobacterium tumefaciens*. *J Bacteriol* 177:3808-3817.

46. Romero-Steiner S, Parales RE, Harwood CS, Houghton JE. 1994. Characterization of the *pcaR* regulatory gene from *Pseudomonas putida*, which is required for the complete degradation of p-hydroxybenzoate. *J Bacteriol* 176:5771-5779.
47. Cao B, Geng A, Loh KC. 2008. Induction of *ortho*- and *meta*-cleavage pathways in *Pseudomonas* in biodegradation of high benzoate concentration: MS identification of catabolic enzymes. *Appl Microbiol Biotechnol* 81:99-107.
48. Cao B, Loh KC. 2008. Catabolic pathways and cellular responses of *Pseudomonas putida* P8 during growth on benzoate with a proteomics approach. *Biotechnol Bioeng* 101:1297-1312.
49. Kim YH, Cho K, Yun SH, Kim JY, Kwon KH, Yoo JS, Kim SI. 2006. Analysis of aromatic catabolic pathways in *Pseudomonas putida* KT 2440 using a combined proteomic approach: 2-DE/MS and cleavable isotope-coded affinity tag analysis. *Proteomics* 6:1301-1318.
50. Domínguez-Cuevas P, González-Pastor JE, Marqués S, Ramos JL, de Lorenzo V. 2006. Transcriptional tradeoff between metabolic and stress-response programs in *Pseudomonas putida* KT2440 cells exposed to toluene. *J Biol Chem* 281:11981-11991.
51. de Groot MJL, Daran-Lapujade P, van Breukelen B, Knijnenburg TA, de Hulster EAF, Reinders MJT, Pronk JT, Heck AJR, Slijper M. 2007. Quantitative proteomics and transcriptomics of anaerobic and aerobic yeast cultures reveals post-transcriptional regulation of key cellular processes. *Microbiology* 153:3864-3878.
52. Kolkman A, Daran-Lapujade P, Fullaondo A, Olsthoorn MM, Pronk JT, Slijper M, Heck AJ. 2006. Proteome analysis of yeast response to various nutrient limitations. *Mol Syst Biol* 2006:0026
53. Rosen R, Ron EZ. 2002. Proteome analysis in the study of the bacterial heat-shock response. *Mass Spectrom Rev* 21:244-265.
54. Muraoka S, Okumura R, Ogawa N, Nonaka T, Miyashita K, Senda T. 2003. Crystal structure of a full-length LysR-type transcriptional regulator, CbnR: unusual combination of two subunit forms and molecular bases for causing and changing DNA bend. *J Mol Biol* 328:555-566.
55. Houghton JE, Brown TM, Appel AJ, Hughes EJ, Ornston LN. 1995. Discontinuities in the evolution of *Pseudomonas putida cat* genes. *J Bacteriol* 177:401-412.
56. Parsek MR, Shinabarger DL, Rothmel RK, and Chakrabarty AM. 1992. Roles of CatR and *cis*, *cis*-muconate in activation of the *catBC* operon, which is involved in benzoate degradation in *Pseudomonas putida*. *J Bacteriol* 174:7798-7806.



# Chapter 3

## pH-stat fed-batch process to enhance the production of *cis, cis*-muconate from benzoate by *Pseudomonas putida* KT2440-JD1

**Abstract:** *Pseudomonas putida* KT2440-JD1 is able to co-metabolize benzoate to *cis, cis*-muconate in the presence of glucose as growth substrate. *P. putida* KT2440-JD1 was unable to grow in the presence of concentrations above 50 mM benzoate or 600 mM *cis, cis*-muconate. The inhibitory effects of both compounds were cumulative. The maximum specific uptake rate of benzoate was higher than the specific production rate of *cis, cis*-muconate during growth on glucose in the presence of benzoate, indicating that a benzoate derivative accumulated in the cells, which is likely to be catechol. Catechol was shown to reduce the expression level of the *ben* operon, which encodes the conversion of benzoate to *cis, cis*-muconate. To prevent overdoses of benzoate, a pH-stat fed-batch process for the production of *cis, cis*-muconate from benzoate was developed, in which the addition of benzoate was coupled to the acidification of the medium. The maximum specific production rate during the pH-stat fed-batch process was 0.6 g (4.3 mmol) g dry cell weight<sup>-1</sup> h<sup>-1</sup>, while 18.5 g L<sup>-1</sup> *cis, cis*-muconate accumulated in the culture medium with a molar product yield of close to 100 %. Proteome analysis revealed that the outer membrane protein H1 was up-regulated during the pH-stat fed-batch process, while the expression of 10 other proteins was reduced. The identified proteins are involved in energy household, transport, translation of RNA and motility.

**Keywords:** benzoate, catechol, *cis, cis*-muconate, pH-stat, *P. putida* KT2440-JD1

Accepted for publication in Biotechnology Progress. Co-Authors: Wijte D, Karge B, Yang Y, Martins dos Santos VAP, Mars AE, Eggink G.

## Introduction

Previously, a derivative of *P. putida* KT2440 (*P. putida* KT2440-JD1) was isolated that co-metabolizes benzoate to *cis, cis*-muconate in the presence of glucose as a growth substrate<sup>1</sup> (Fig. 1). *cis, cis*-Muconate is a dicarboxylic acid with two conjugated double bonds that can be used as a raw material for fine and bulk chemicals. Hydrogenation to adipic acid, for example, yields a monomer that can be used to synthesize nylon-6,6<sup>2</sup>.

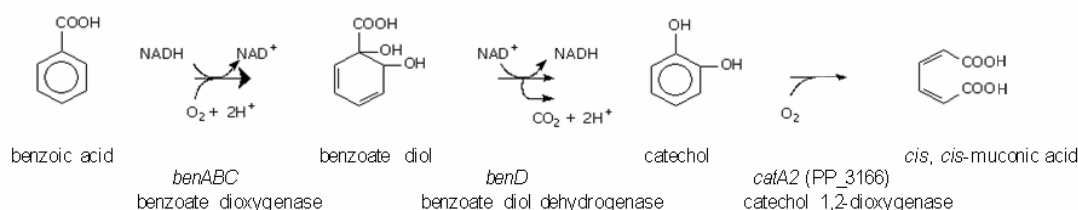


**Figure 1.** Conversion of benzoate to *cis, cis*-muconate by *P. putida* KT2440-JD1.

The ability to produce *cis, cis*-muconate from benzoate has been reported for several microorganisms: *Pseudomonas* sp. B13<sup>3</sup>, *P. putida* BM014<sup>4,5</sup>, an *Arthrobacter* sp.<sup>6</sup>, and *Spingobacterium* sp. GCG<sup>7</sup>. Compared to these strains, *P. putida* KT2440-JD1 has a very high specific production rate ( $q_{pm}$ ) of up to 2.0 g (14 mM) *cis, cis*-muconate  $\text{g dcw}^{-1} \text{h}^{-1}$ . The *cat* operon is no longer induced in *P. putida* KT2440-JD1. This operon contains the *catA* gene that encodes for a catechol 1,2-dioxygenase, which converts catechol to *cis, cis*-muconate. *P. putida* KT2440-JD1 contains a second gene for catechol 1,2-dioxygenase *catA2* that is encoded on the *ben* operon<sup>8</sup>. CatA2 is responsible for the conversion of catechol to *cis, cis*-muconate in *P. putida* KT2440-JD1<sup>1</sup>.

The aim of this research was to develop a new process for the accumulation of *cis, cis*-muconate. It will be shown that benzoate is much more toxic to *P. putida* KT2440-JD1 than *cis, cis*-muconate. Therefore, a pH-stat fed-batch process was designed in which the addition of benzoate was coupled to the pH-decrease that occurs when benzoate is converted to *cis, cis*-muconate. In this way, overdoses of benzoate are prevented. This bioprocess resulted in the production of 18.5  $\text{g L}^{-1}$  of *cis, cis*-muconate with a molar product yield of close to 100 % and a high maximum  $q_{pm}$  of 0.6 g (4.3 mmol) of *cis, cis*-muconate  $\text{g dcw}^{-1} \text{h}^{-1}$ . Furthermore, the proteome of the pH-stat culture was analyzed at 3 different stages of the pH-stat process to characterize the effects of the changing conditions on the biocatalyst.

## Material and Methods

**Strain and cultivation conditions.** *P. putida* KT2440-JD1 was grown in E-2 Mineral Medium (MM)<sup>9</sup> with glucose as carbon source at 30 °C and pH 7. Batch cultivations were done in Erlenmeyer flasks that were shaken at 160 rpm. A pH-stat fed-batch cultivation was done in a 5 L bioreactor (Sartorius BBI systems GmbH, Germany) with a working volume of 3.5 L and 10 mM glucose. The culture was sparged with air at a rate of 3.5  $\text{L min}^{-1}$ , and the oxygen concentration was maintained at >50 % saturation by adjusting the stirring speed. 0.02 % antifoam 204 (Sigma-

Aldrich, USA) was added to the medium to prevent foaming. MM with 1.4 M glucose, 0.02 % antifoam 204, and 19 g L<sup>-1</sup> ammonium sulfate was added to the culture at a linear feeding rate, which was increased every hour to obtain exponential feeding at a rate of 0.04 h<sup>-1</sup>. During operation as a pH-stat, the addition of benzoate was coupled to the pH-regulation by titrating with a solution containing MM with 1.2 M benzoic acid, 2.4 M sodium hydroxide, and 0.02 % of antifoam 204.

**Analytical methods.** Benzoate and *cis, cis*-muconate were determined in the supernatant of the batch cultures and washed cell suspensions by HPLC using a Varian Microsorb<sup>tm</sup>-MVHPLC column (length, 250 nm; inside diameter, 4.6 mm; particle size, 5 μm) (Varian, USA), with a mobile phase that consisted (per 1 L) of: 130 ml methanol, 130 ml acetonitril, 740 ml demineralized water, 26 μl trifluoroacetic acid (TFA) and 67.5 μl H<sub>3</sub>PO<sub>4</sub> (85 %) (1.25 ml/ min), and a Waters 2487 UV detector (Waters, USA). Benzoate was measured at 207 nm and *cis, cis*-muconate at 260 nm. The supernatants were filtered (pore size of 0.2 μm) prior to analysis to remove solids and precipitated proteins. The glucose concentration in the pH-stat fed-batch culture was determined by a spectrophotometric enzyme assay kit (cat. no. 10139041035, Boehringer Mannheim, Germany). Benzoate, catechol, and *cis, cis*-muconate concentrations were determined in the culture supernatant as previously described by Cámara *et al.*<sup>10</sup>.

The cell density of the cultures was determined by measuring the optical density (OD) of the culture against a water blank at 600 nm on a Eppendorf Biophotometer (Eppendorf AG, Germany). The relation between the OD<sub>600</sub> and dry cell weight concentration ( $C_x$ ) in g dcw L<sup>-1</sup> was determined to be  $C_x = 0.35 \times OD_{600} + 0.21$  by measuring the OD<sub>600</sub> in 7 batch cultures of *P. putida* KT2440 in MM with 0 to 12.5 mM glucose, and measuring  $C_x$  by filtering 10 ml of the culture over a 0.2 μm cellulose acetate filter (Whatmann, United Kingdom). The filters were dried at 80°C for 24 hours and weighed before usage. The cells were washed with 5 ml of 0.9 % NaCl after filtration to discard salts, dried at 80°C for 24 hours, and weighed.

**Batch cultures.** *P. putida* KT2440-JD1 was grown in batch cultures in MM with 10 mM of glucose for 25 hours, after which 2 % of the cultures were transferred to the same medium with various concentrations of benzoate as a substrate ( $C_{sb}$ ) (0-50mM) and/or *cis, cis*-muconate as a product ( $C_{pm}$ ) (0-600mM) to determine the maximum growth rate ( $\mu_{max}$ ), the specific uptake rate of benzoate ( $q_{sb}$ ) and  $q_{pm}$ . The  $\mu_{max}$  was determined from the slope of the natural logarithm of  $C_x$  over time during the exponential growth phase. The maximal  $q_{sb}$  and  $q_{pm}$  in the batch cultures were

$$q_{sb} = \frac{dC_{sb_t}}{(C_{x_t} \times dt)} \quad \text{and} \quad q_{pm} = \frac{dC_{pm_t}}{(C_{x_t} \times dt)}$$

calculated by using the following formulas:

**Expression of *benA*.** The expression of *benA* was determined by using quantitative real-time polymerase chain reaction (RT-PCR) to amplify cDNA products that were reversely transcribed from mRNA. The experiment was done in triplicate. For each experiment, 7 batch cultures were grown in MM with 10 mM of glucose and 2.5 mM of benzoate. The cultures were inoculated (2 % volume) with a pre-culture that was grown in MM with 10 mM of glucose and 1 mM of benzoate. During mid-logarithmic growth, various concentrations of catechol (0-12 mM) and 2.5 mM benzoate were added to the cultures. After 1.5 h, 0.5 ml samples were taken from the cultures and mixed with 1 ml RNeasy Protect Bacteria Reagent (Qiagen, USA). RNA was isolated from the cells by using the RNeasy kit (Qiagen, USA) together with RNase-Free DNase (Qiagen, USA). RNA was quantified by spectrophotometry at 260 nm. Quantitative RT-PCRs were carried out in duplicate in 20-μl reaction mixtures with 10 ng of RNA using SYBR green as a nucleic acid stain (Qiagen, USA)<sup>10</sup> and the primers: *benA*-F (GAAGGCAACTGGAAGCTCAC) and *benA*-R

(CCGTGGTCGAAGGAATAGAA) for *benA*; and *catA-F* (CTCGTCCTCGGTAATCTCCA) and *catA-R* (CCGTGAAAATTTCCCACT) for *catA*. The expression of *benA* was normalized by dividing the expression level of *benA* by that of *catA* using the standard calculation described by Pfaffl<sup>11</sup>. *catA* is still transcribed but no longer regulated in *P. putida* KT2440-JD1<sup>1</sup>.

**Conversion of benzoate by washed cells in the presence of various concentrations of *cis, cis*-muconate.** The effect of *cis, cis*-muconate on the conversion of benzoate by washed cells of *P. putida* KT2440-JD1 was determined. For each concentration of *cis, cis*-muconate, *P. putida* KT2440-JD1 was pre-grown on 10 mM glucose with 2.5 mM benzoate, after which 4 Erlenmeyer flasks with 120 ml of the same medium were inoculated with 10 % of the pre-culture. After 3.5 hours of cultivation, 2.5 mM of benzoate was added to each flask, and the cells were cultivated for another 1.5 hours. Then, the cells were harvested by centrifugation at 10,410 g at 4°C for 10 min, washed with 100 mM phosphate buffer (pH 6.9) at 4°C, equally divided into two tubes, and again centrifuged. After that the two cell pellets were separately re-suspended in 50 ml phosphate buffer in a Erlenmeyer flask of 250 ml. The flasks were incubated at 30°C. The oxygen concentration was measured in the cell suspensions by using a DO-electrode, and kept above 80 % by stirring with a magnetic stirrer. *cis, cis*-Muconate (0-200 mM) was added to one of the two cell suspensions, after which conversion of benzoate was started by adding 5 mM of benzoate to both cell suspensions. The cell density was measured at the start of the conversion. The  $q_{sb}$  was determined by measuring the concentration of benzoate in the cell suspensions during two hours. The effect of *cis, cis*-muconate on the  $q_{sb}$  was normalized with respect to the  $q_{sb}$  in the absence of *cis, cis*-muconate to allow the comparison of different cell suspensions.

**Proteomics.** Protein extracts of the *P. putida* KT2440-JD1 were prepared for analysis with 2-D gel electrophoresis using a sodium dodecyl sulfate (SDS) extraction protocol for *E. coli*<sup>12</sup>. The protein pellet was resolved by sonication (4 × 5 sec) in rehydration buffer (9.5 M urea, 4 % (w/v) 3-[(3-cholamidopropyl)dimethylammonio]-1-propan sulfonat (CHAPS), 25 mM dithiothreitol (DTT), pH 8.5). Protein concentrations were determined with the RC/DC protein-assay (Bio-Rad, USA) according to the manufacturer's instructions. The protein samples were stored in 100 µl aliquots at -80 °C. Protein samples were prepared and labeled with CyDyes according to the manufacturer's protocol (GE Healthcare, UK). For the first dimension electrophoresis, 75 µg aliquots of Cy2, Cy3, and Cy5-labelled proteins were mixed and loaded on a 24 cm Immobiline Dry-Strip at pH 4-7 in 450 µl rehydration buffer (9.5 M urea, 4 % (w/v) CHAPS, 1 % Destreak (GE Healthcare, UK), pH 8.5). Strips were rehydrated overnight in a rehydration tray. Isoelectric focusing was carried out using an IPGphor (GE Healthcare, UK) for a total of 60-67 kVh, with the current set to 50 µA per strip, at 20 °C. Prior to the second dimension, the immobilized pH gradient (IPG) strips were incubated for 15 min in equilibration buffer (50 mM Tris-HCl, pH 8.8, 6 M urea, 30 % (v/v) glycerol, 2 % (w/v) SDS) containing 1 % (w/v) DTT, followed by 15 min incubation in equilibration buffer containing 2.5 % (w/v) iodoacetamide instead of DTT. Second dimension electrophoresis was performed on lab-cast 12.5 % polyacrylamide gels in a DALTsix<sup>TM</sup> electrophoresis unit (GE Healthcare, UK). The IPG strips were placed on the top of 12.5 % polyacrylamide gels and sealed with a solution of 1 % (w/v) agarose, with a trace of bromophenol blue. Gels were run at 1 W per gel for 60 min, followed by 2 W per gel, until the bromophenol blue had migrated to the bottom of the gel. Difference In Gel Electrophoresis (DIGE) gels with CyDye-labelled proteins were scanned with a Molecular Imager FX (Bio-Rad, USA) (100 µm resolution, middle sensitivity, Cy2: 488 nm laser, Cy3: 532 nm laser and Cy5: 635 nm laser) and converted with Quantity-One 4.4.0 software (Bio-Rad, USA) to TIFF file format. Image analysis was performed using Decyder software version 6.5 (GE Healthcare, UK). To enable a proper statistical analysis, five gels were used, so that every stage of the pH-stat culture was represented in three gels. For each of the 5 gels, a Cy2 labeled mixture of all protein samples was used as the internal

standard minimizing the gel-to-gel variation in the five gels<sup>13</sup>. After cropping and filtering, images were subjected to automated Difference In-gel Analysis (DIA) and Biological Variation Analysis (BVA) with the Decyder 6.5 software (GE Healthcare, United Kingdom). After one-way analysis of variance (student's *t* test with a *p* value of 0.05), significantly changed proteins were selected that had an average fold-change difference of at least 1.5 up-regulation or 0.7 down-regulation between the conditions. Next, the DIGE gels were fixed for 60 min in MeOH/ acetic acid (25 %/10 % in Milli-Q) prior to post-staining with ProteomIQ Blue (Proteome Systems, USA)<sup>14</sup>. Protein spots that were differentially expressed were excised and digested in-gel with trypsin, using the protocol of Havlis *et al.*<sup>15</sup>. Protein digests were solubilised in 50 % acetonitrile and 0.1 % (v/v) TFA, and applied onto the MALDI-target by applying 1  $\mu$ L of a saturated solution of cyano-4-hydroxycinnamic acid in 50 % acetonitrile and 0.1 % (v/v) TFA. Peptides were first subjected to MALDI MS using a Biflex III instrument (Bruker Daltonics), using delayed extraction and reflectron mode with positive ion detection. The mass scale was calibrated with the trypsin autodigestion product of known  $[M+H]^+$  mass, 2211.1 Da, and the keratin 9 fragment  $[M+H]^+$ , 2705.2 Da.

## Results

**Effect of benzoate and *cis, cis*-muconate on growth and production of *cis, cis*-muconate.** The  $\mu_{max}$  of *P. putida* KT2440-JD1 was determined during batch cultivations in MM with 10 mM of glucose in the presence of increasing concentrations of benzoate or *cis, cis*-muconate. The  $\mu_{max}$  decreased linearly at increasing concentrations of benzoate and was reduced by 50 % at 24 mM of benzoate. Growth was completely arrested when the concentration of benzoate was higher than 48 mM (Fig. 2). The  $\mu_{max}$  also decreased linearly at increasing concentrations of *cis, cis*-muconate, although the inhibition occurred at much higher concentrations. At 300 mM of *cis, cis*-muconate the  $\mu_{max}$  was decreased to 50 %, while growth no longer occurred at concentrations higher than 600 mM (Fig. 2).

*P. putida* KT2440-JD1 co-metabolized benzoate to *cis, cis*-muconate during the batch cultivations on glucose. The maximum  $q_{sb}$  steeply increased at increasing concentrations of benzoate up to 25 mM, after which it suddenly decreased to a much lower constant level (Fig. 3). In the same period the  $q_{pm}$  of *cis, cis*-muconate was much lower than the  $q_{sb}$ , suggesting that benzoate or a benzoate-derivative accumulated. A dark coloration was observed in the batch cultures that indicated the accumulation of catechol, which is known to spontaneously form coloured polymers<sup>16</sup>.

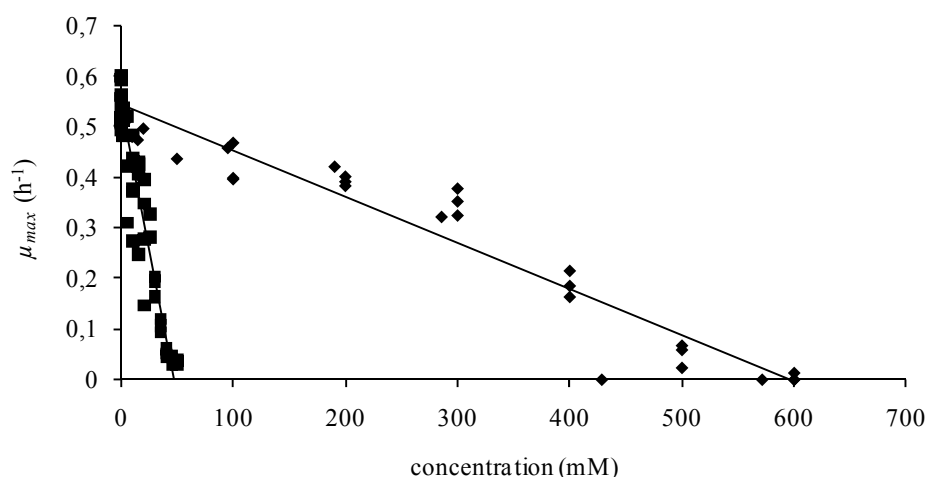


**Figure 2.**  $\mu_{max}$  of *P. putida* KT2440-JD1 during batch cultivations in MM with 10 mM of glucose in the presence of increasing concentrations of benzoate (0-50 mM) (■) or *cis, cis*-muconate (0-600mM) (◆).

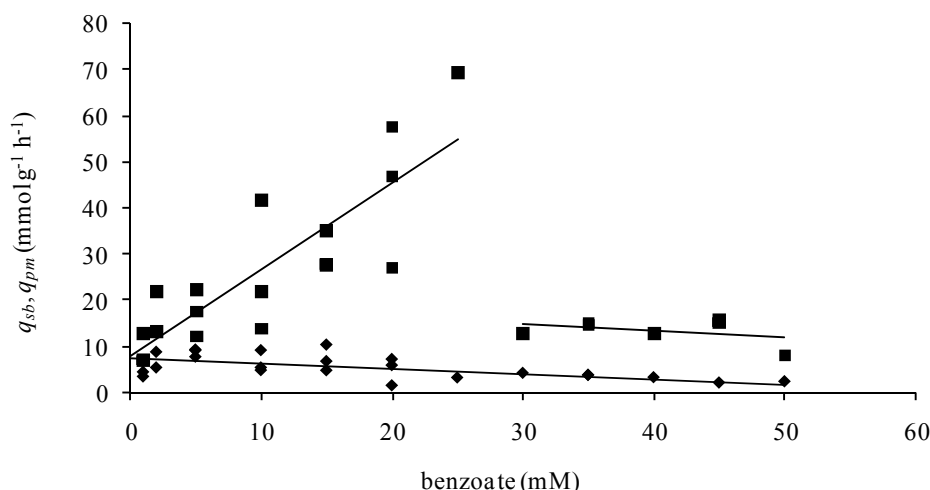


**Figure 3.** Maximum specific uptake rate of benzoate ( $q_{sb}$ ) (■) and concurrent specific production rate of *cis, cis*-muconate ( $q_{pm}$ ) (◆) of *P. putida* KT2440-JD1 during batch cultivations in MM with 10 mM of glucose in the presence of increasing concentrations of benzoate (0-50 mM).

To characterize the combined effect of benzoate and *cis, cis*-muconate on the  $\mu_{max}$  of *P. putida* KT2440-JD1, the strain was grown on glucose in the presence of different concentrations of both compounds. A  $2^2$ -factorial central composite design<sup>17</sup> was used to determine the concentrations of both compounds (Table 1). The spectrum of the concentrations was chosen based on the individual inhibiting effects of benzoate and *cis, cis*-muconate. Six independent batch cultivations were done with 200 mM *cis, cis*-muconate and 10 mM benzoate representing the middle point of the central composite design to determine the standard deviation. The average  $\mu_{max}$  was  $0.23 \pm 0.05 \text{ h}^{-1}$ . The other cultivations were done once. Figure 4 represents the contour plot of the  $\mu_{max}$  of *P. putida*

KT2440-JD1 grown in the presence of the different combinations of benzoate and *cis, cis*-muconate. Since the regression lines are parallel, the inhibitory effects of both compounds are cumulative and do not have any synergistic effects.

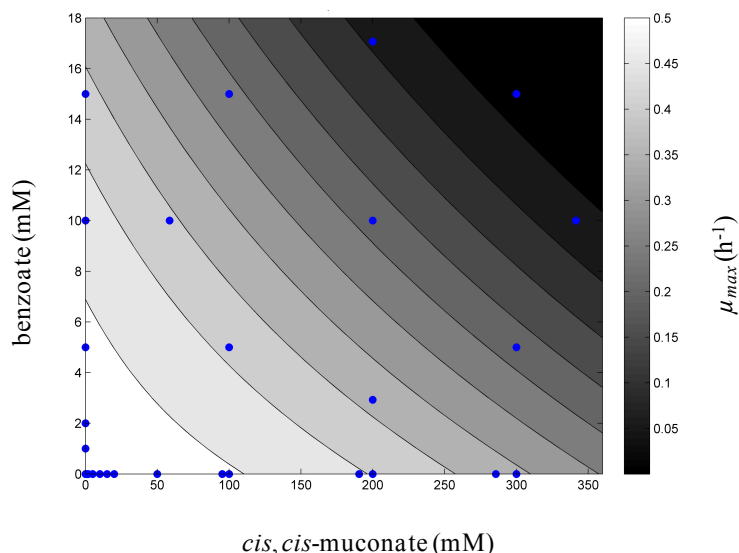


**Figure 4.** Contour plot of the  $\mu_{max}$  of *P. putida* KT2440-JD1 during batch cultivations in MM with 10 mM of glucose in the presence of various concentrations of benzoate (2.5-17.5 mM) and *cis, cis*-muconate (50-350 mM).

**Table 1.** Variables used for the  $2^2$ -factorial central composite design to determine the inhibiting effects of combinations of benzoate and *cis, cis*-muconate on the  $\mu_{max}$  of *P. putida* KT2440-JD1.

Variable	Component	Concentration range (mM)	Levels of variables (mM)				
			$-\alpha$	-1	0	1	$+\alpha$
$\chi_1$	benzoate	2.5-17.5	2.5	5	10	15	17.5
	<i>cis, cis</i> -muconate	50-350	50	100	200	300	350

$-\alpha, +\alpha$  = lowest and highest chosen concentration, -1, +1 = intermediate concentrations, 0 = central point

**Effect of catechol on the expression of the *ben* operon.** Since catechol may accumulate during the conversion of benzoate to *cis, cis*-muconate, the effect of catechol on the expression of the *ben* operon was determined. For this, the expressions of *benA* and *catA* were measured with RT-PCR in cultures of *P. putida* KT2440-JD1 that were exposed to catechol during exponential growth on glucose in the presence of benzoate. The expression of gene *catA* was used for normalization, since it is still transcribed but no longer regulated in *P. putida* KT2440-JD1<sup>1</sup>. The results showed that the expression of *benA* was reduced in the presence of catechol (Fig. 5), indicating that accumulation of catechol will lead to a reduction of the  $q_{sb}$ . The sudden drop in the maximum  $q_{sb}$  in Figure 3 may be explained by the inhibition of the *ben* operon due to the accumulation of catechol at high concentrations of benzoate.

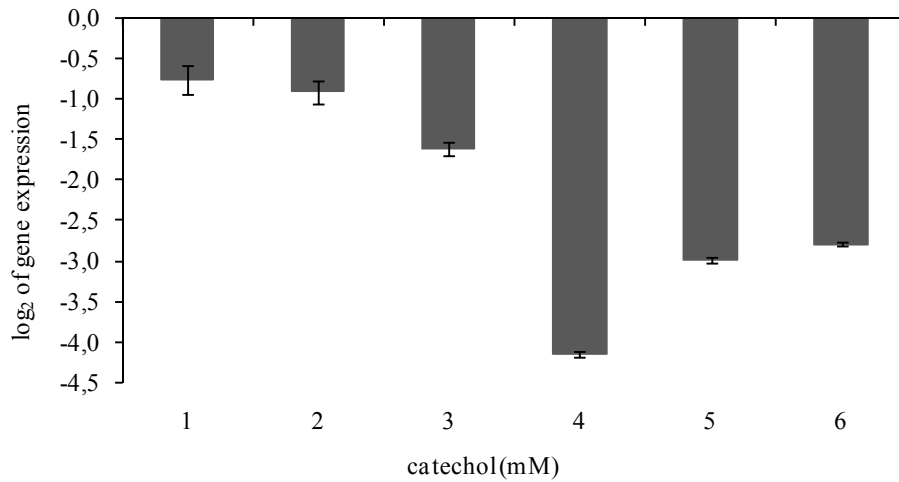


**Figure 5.** Log<sub>2</sub> of the expression of *benA* in *P. putida* KT2440-JD1 after various pulses of catechol (0-12 mM) and 2.5 mM benzoate during mid-logarithmic growth of batch cultivations in MM with 10 mM glucose and 2.5 mM benzoate. Data were normalized to the expression level of *catA*. The experiments were done in triplicate.

**Effect of *cis*, *cis*-muconate on the uptake of benzoate by washed cells of *P. putida* KT2440-JD1.** The effect of *cis*, *cis*-muconate on the  $q_{sb}$  was determined with washed cells of *P. putida* KT2440-JD1 that were pre-grown on glucose in the presence of benzoate. The  $q_{sb}$  increased at increasing concentrations of *cis*, *cis*-muconate up to 100 mM, after which it decreased to become completely arrested at approximately 240 mM *cis*, *cis*-muconate (Fig. 6).

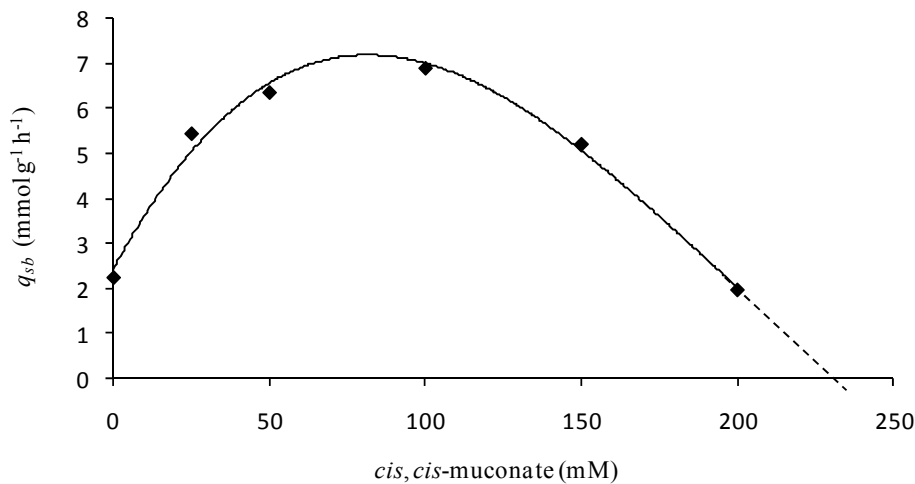


**Figure 6.** Specific uptake rate of benzoate ( $q_{sb}$ ) (■) of washed cells of *P. putida* KT2440-JD1 in 100 mM phosphate buffer and 5 mM benzoate at increasing concentrations of *cis*, *cis*-muconate (0-200 mM). The cells were harvested during batch cultivations in MM with 10 mM of glucose and 2.5 mM benzoate. An extra pulse of 2.5 mM benzoate was added 1.5 h. before sampling.

**pH-stat fed-batch process.** When *P. putida* KT2440-JD1 is applied for the production of *cis, cis*-muconate, it is important to prevent its exposure to high concentrations of benzoate, since it reduces the  $\mu_{max}$  and probably leads to the accumulation of catechol, which reduces the expression of the *ben* operon and may be toxic to *P. putida* KT2440-JD1 since catechol generates reactive oxygen species and spontaneously forms coloured polymers<sup>16,18,19,20,21</sup>.

Since the medium is acidified when benzoate is converted to *cis, cis*-muconate, it is possible to prevent the accumulation of benzoate by coupling the addition of benzoate to the pH-regulation. Therefore, a pH-stat fed-batch process was designed in which the addition of benzoic acid was coupled to the pH-regulation with NaOH at a benzoic acid:NaOH molar ratio of 1:2. For this, a bioreactor containing MM with 10 mM of glucose was inoculated with *P. putida* KT2440-JD1. 1 mM of benzoate was added after 1 hour to induce the cells. Continuous addition of glucose started when glucose was depleted. The feeding rate of glucose was increased every hour to obtain exponential feeding, which resulted in a growth rate of 0.04 h<sup>-1</sup> (Fig. 7A). During this period the glucose concentration never exceeded 0.3 mM (Fig. 7B). After 13 hours, production of *cis, cis*-muconate was started by adding 20 mM benzoate to the culture to maximally induce the cells. The pH was maintained at 7.0 by the automated addition of 10 M of NaOH. Catechol accumulated in the culture up to 6 mM but disappeared within 6 h. The temporary presence of catechol confirmed that catechol accumulates in the culture medium when benzoate is present in high concentrations. When benzoate was almost completely converted to *cis, cis*-muconate (as determined by HPLC), the feeding of benzoate was coupled to the acidification of the culture by titrating the culture to pH 7.5 with a solution of 1.2 M benzoic acid and 2.4 M NaOH as soon as the pH became lower than 7.0. In this way, the concentrations of benzoate and catechol were kept low (Fig. 7B).

After the pulse of 20 mM benzoate, the  $q_{pm}$  increased to a maximum value of 0.6 g (4.3 mmol) g dcw<sup>-1</sup> h<sup>-1</sup>, which resulted in a maximal volumetric productivity of 0.8 g L<sup>-1</sup> h<sup>-1</sup>. The  $q_{pm}$  gradually decreased during the accumulation of *cis, cis*-muconate and completely stopped at a concentration of 18.5 g L<sup>-1</sup> (130 mM) (Fig. 7C). The overall molar product yield ( $C_{pm} C_{sb}^{-1}$ ) was close to 100 %. The production of biomass continued when the production of *cis, cis*-muconate became completely inhibited, indicating that *P. putida* KT2440-JD1 was still able to grow at this concentration of *cis, cis*-muconate. Extra benzoate was added to stimulate *cis, cis*-muconate production, but the concentration of *cis, cis*-muconate did not increase. Instead, benzoate, catechol, and glucose accumulated in the medium and growth of *P. putida* KT2440-JD1 stopped. Due to the conversion of benzoate to catechol, the pH of the medium increased from 7.5 to 8.5.

**Proteomics.** To characterize the expression of proteins during the different stages of the pH-stat fed-batch process, protein samples were taken to determine the proteome of *P. putida* KT2440-JD1 just before the pulse of 20 mM benzoate (t=13 h, sample 1), during the production of *cis, cis*-muconate (t=36 h, sample 2) and after the final concentration of 18.5 g L<sup>-1</sup> *cis, cis*-muconate was reached (t=56 h, sample 3). BVA revealed that a total of 540 to 620 detected protein spots in each gel could be matched under all three conditions, from which 36 spots were found to be significantly ( $p < 0.05$ ) different. Interestingly, no significant differences were observed between the protein expression patterns of samples 2 and 3. The 36 differentially expressed spots were identified by MALDI-TOF MS which revealed that these 36 protein spots were originated from 11 different proteins. This indicates that several proteins have different isoforms, like the outer membrane protein H1 (OprH) which was up-regulated in 8 protein spots in samples 2 and 3. Unfortunately, no data could be extracted from our MALDI-TOF MS analysis to identify the difference in isoform for OprH. The other 10 identified proteins were down-regulated and their functions are related to energy household, transport, translation of RNA, and motility (Table 2).

**Table 2.** Differentially expressed proteins of samples 2 and 3 compared to sample 1.

Locus ID	Protein name	Protein name	regulation	Number of peptides
PP_0849	Ndk	<b>Energy household related proteins</b> nucleoside-diphosphate kinase	0.6	5
PP_5413	AtpD	FOF1 ATP synthase subunit beta	0.7	8
PP_1185	OprH	<b>Outer membrane proteins</b> outer membrane protein H1	3.5	8
PP_1206	OprD	<b>Transport proteins</b> outer membrane porin	0.5	9
PP_1015		sugar ABC transporter, periplasmic sugar-binding protein	0.7	6
PP_1297	AapJ	general amino acid ABC transporter, periplasmic binding protein	0.7	5
PP_0452	Tuf	<b>Translation related proteins</b> Elongation factor Tu-B	0.6	13
PP_0440	Tuf	Elongation factor Tu-A	0.6	11
PP_4877	RpsF	30S ribosomal protein S6	0.7	5
PP_4874	RplI	50S ribosomal protein L9	0.7	5
PP_4378	fliC	<b>Motility</b> flagellin FliC	0.5	8

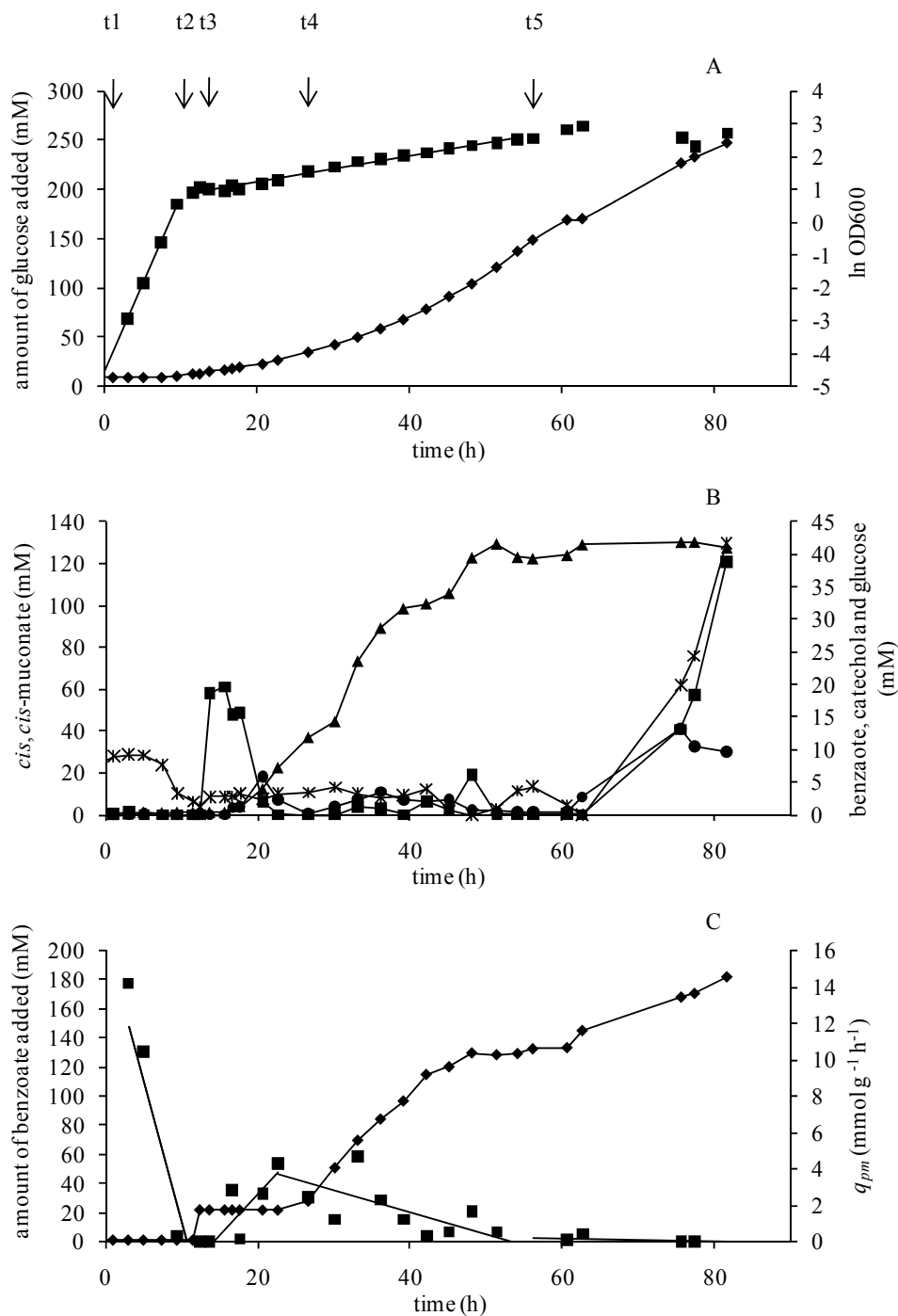


**Figure 7.** Parameters of the pH-stat fed-batch process with *P. putida* KT2440-JD1. Panel A: natural logarithm of cell density, measured as  $OD_{600}$  (■); cumulative amount of glucose that was added to the culture (◆). Panel B: concentrations of *cis,cis*-muconate (▲), benzoate (■), catechol (●) and glucose (\*) in the culture supernatant. Panel C: specific production rate of *cis,cis*-muconate ( $q_{pm}$ ) (■); cumulative amount of benzoate that was added to the culture (◆). Arrows indicate the time points at which 1 mM of benzoate was added ( $t_1$ ), exponential feeding of glucose started ( $t_2$ ), 20 mM of benzoate was added ( $t_3$ ), benzoate addition was coupled to the acidification of the culture ( $t_4$ ) and manual additions of benzoate started ( $t_5$ ).

## Discussion

Various processes have been reported for the accumulation of *cis*, *cis*-muconate from benzoate using aerobic bacteria (Table 3). The exposure of the culture to high concentrations of benzoate was avoided by feeding under controlled conditions at a low constant rate or in pulses<sup>3,5,6,7</sup>, or by coupling the addition of benzoate to the depletion of oxygen (DO-stat)<sup>4</sup> or the decrease of the pH (pH-stat) (this study). The advantage of a pH-stat compared to a DO-stat is the decoupling of the feeding of benzoate from the feeding of the growth substrate (glucose), because benzoate is only replenished when the medium acidifies by its own conversion to *cis*, *cis*-muconate.

**Table 3.** Maximum specific productivities ( $q_{pm}$ ), maximum volumetric productivities and final concentrations of *cis*, *cis*-muconate of various production processes of *cis*, *cis*-muconate from benzoate using different strains.

Process	Strain	Maximum $q_{pm}$ (g g dcw <sup>-1</sup> h <sup>-1</sup> )	Maximum volumetric productivity (g L <sup>-1</sup> h <sup>-1</sup> )	Final concentration (g L <sup>-1</sup> )
pH-stat fed-batch	<i>P. putida</i> KT2440-JD1 (this research)	0.60	0.8	18.5
fed-batch	<i>Spingobacterium</i> sp. GCG <sup>7</sup>	>0.10	>0.1	>0.1
cell-recycle system	<i>P. putida</i> BM014 <sup>5</sup>	0.14**	5.5**	12.0**
DO-stat fed-batch	<i>P. putida</i> BM014 <sup>4</sup>	0.21	2.2	32.0
fed-batch	<i>Arthrobacter</i> sp. <sup>6</sup>	n.d.*	1.1	44.0
fed-batch	<i>Pseudomonas</i> sp. B13 <sup>3</sup>	0.24	0.8	7.0

\* not determined; \*\* steady values.

The highest volumetric productivity of 5.5 g *cis*, *cis*-muconate L<sup>-1</sup> h<sup>-1</sup> was obtained in a system which used a constant inflow rate of benzoate in combination with a membrane to retain the cells, resulting in a culture with a high cell density of 40 g L<sup>-1</sup><sup>5</sup>. This productivity could be maintained during the whole process and yielded a fermentation effluent of 12 g *cis*, *cis*-muconate L<sup>-1</sup>. An *Arthrobacter* sp. was able to accumulate the highest concentration of *cis*, *cis*-muconate of 44 g L<sup>-1</sup> during a fed-batch process, but the  $q_{pm}$  was not determined<sup>6</sup> (Table 3). During the pH-stat fed-batch process the highest  $q_{pm}$  was observed soon after the initial pulse of 20 mM of benzoate, but the productivity was lower than the maximum rates that were previously observed under  $\mu_{max}$  conditions<sup>1</sup>, and the  $q_{pm}$  decreased during the pH-stat process. The  $q_{pm}$  was also much lower than the  $q_{sb}$  that was determined in this study. The discrepancy between the  $q_{sb}$  and the  $q_{pm}$  is probably caused by the accumulation of the metabolic intermediate catechol, which was formed during the pH-stat fed-batch process, especially after the pulse of 20 mM benzoate. The conversion of catechol can be rate limiting<sup>3,20</sup>, and over-expression of catechol 1,2-dioxygenase in *P. putida* BCM114 resulted an increased  $q_{pm}$  from benzoate<sup>22</sup>. Catechol down-regulates the expression of the *ben* operon in *P. putida* KT2440-JD1, and is known to be a toxic compound<sup>16,18,19,20,21</sup>. The accumulation of catechol at higher concentrations of benzoate may therefore explain the higher sensitivity of *P. putida* KT2440-JD1 to benzoate compared to *cis*, *cis*-muconate. *P. putida* KT2440 contains two genes for two catechol 1,2-dioxygenases (*catA2* and *catA*), which are both induced during growth on benzoate<sup>1,8</sup>. One of these genes (*catA*) is no longer induced in *P. putida* KT2440-JD1. It is therefore likely that the conversion of benzoate to *cis*, *cis*-muconate can be improved by enhancing the catechol 1,2-dioxygenase activity in this strain.

The analyses of the proteome identified only a few proteins that were differentially expressed before and after the start of the production of *cis*, *cis*-muconate within the pH-stat fed-batch process. Proteins such as OprH (an outer membrane protein) and AtpD (an energy household related protein) were found to be up- and down-regulated, respectively. A similar response was also observed during toluene stress, indicating the prevention of influx by membrane stabilization<sup>23</sup>. The

loss of a motility protein (Flic), translation related proteins (Tuf (PP\_0452, PP\_0440), RpsF, RplI) and energy household-related proteins (Ndk, AtpD) are likely part of a stress response mechanism to minimize energy expenditure<sup>24,25</sup>. OprH is associated with resistance to polymyxin B, gentamicin, and EDTA under Mg<sup>2+</sup> deficiency<sup>26</sup>. The relatively high up-regulation of OprH is most likely a primary reaction to the accumulation of *cis*, *cis*-muconate and/or the presence of benzoate and catechol in the culture medium, which probably results in a lower permeability of the cell membrane, thereby increasing the resistance of the bacteria to these compounds<sup>23,26</sup>. Catechol is formed during the conversion of benzoate, which is known to generate reactive oxygen species that cause oxidative stress<sup>17</sup>. Proteins of *P. putida* that are involved in oxidative stress responses (e.g. AhpC, SodB and catalase/oxidase HPI) and proteins involved in heat shock stress responses (e.g. ATP-binding region, ATPase-like)<sup>25,27</sup> were not differentially expressed between the samples of the pH-stat fed-batch process, which were taken after 13, 36, and 56 h of cultivation. Induction of these and other proteins might already have started after the addition of 1 mM benzoate after 1 hour of cultivation, which may have resulted in indistinguishable concentrations in the different proteome samples.

The  $q_{pm}$  of *P. putida* KT2440-JD1 decreased during the pH-stat fed-batch process with increasing concentrations of *cis*, *cis*-muconate and became completely arrested at 18.5 g L<sup>-1</sup> *cis*, *cis*-muconate. At this concentration of *cis*, *cis*-muconate, the growth of *P. putida* KT2440-JD1 and uptake of benzoate was still observed, but catechol started to accumulate in the growth medium instead of *cis*, *cis*-muconate. The latter may be caused by product inhibition of *cis*, *cis*-muconate.

## Conclusion

The coupling of the addition of benzoate to the decrease of the pH (pH-stat) proved to be a very suitable method to prevent the overdoses of benzoate to the culture. The process may be further improved by i) enhancing the catechol 1,2-dioxygenase activity in *P. putida* KT2440-JD1 e.g. by genetic engineering; ii) enhancing the volumetric productivity by increasing the  $C_x$  in the bioreactor, e.g. by using a cell retention system; iii) preventing the accumulation of *cis*, *cis*-muconate by an efficient removal of *cis*, *cis*-muconate. These improvements could lead to a process that optimally exploit the high potential productivity of this strain to convert benzoate to *cis*, *cis*-muconate.

## Acknowledgments

We would like to acknowledge Dr. Eric Boer for his assistance in applying the 2<sup>2</sup>-factorial central composite design, Dr. Piotr Bielecki for his assistance with molecular biology, Dr. Christoph Ulmer for his assistance with the pH-stat fed-batch process, and Iris Plumeier for her assistance with the HPLC. This research was carried out within the research programme of the Kluyver Centre for Genomics of Industrial Fermentation, which is part of the Netherlands Genomics Initiative (NGI) and by the Bundesministerium für Bildung und Forschung (BMBF, Project PSYSMO, #0313980A).

## References

1. vanDuuren JBJH, Wijte D, Leprince A, Karge B, Puchalka J, Wery J, Martins dos Santos VAP, Eggink G, Mars AE. Generation of a *catR* deficient mutant of *P. putida* KT2440 that produces *cis, cis*-muconate from benzoate at high rate and yield. *J Biotechnol*. 2011;in press.
2. van Duuren, JB, Brehmer, B, Mars, AE, Eggink, G, Dos Santos, VA, Sanders, JP. 2011. A limited LCA of bio-adipic acid: Manufacturing the nylon-6,6 precursor adipic acid using the benzoic acid degradation pathway from different feedstocks. *Biotechnol Bioeng* 108:1298-1306.
3. Schmidt E, Knackmuss HJ. 1984. Production of *cis, cis*-muconate from benzoate and 2-fluoro-*cis, cis*-muconate from 3-fluorobenzoate by 3-chlorobenzoate degrading bacteria. *Appl Microbiol Biotechnol* 20:351-355.
4. Bang SG, Choi CY. 1995. Do-stat fed-batch production of *cis, cis*-muconic acid from benzoic-acid by *Pseudomonas putida* Bm014. *J Ferment Bioeng* 79:381-383.
5. Choi WJ, Lee EY, Cho MH, Choi CY. 1997. Enhanced production of *cis, cis*-muconate in a cell-recycle bioreactor. *J Ferment Bioeng* 84:70-76.
6. Mizuno S, Yoshikawa N, Schi M, Mikawa T, Imada Y. 1988. Microbial-production of *cis, cis*-muconic acid from benzoic-acid. *Appl Microbiol Biotechnol* 28:20-25.
7. Wu CM, Lee TH, Lee SN, Lee YA, Wu JY. 2006. Microbial synthesis of *cis, cis*-muconic acid from benzoate by *Sphingobacterium* sp GCG generated from effluent of a styrene monomer (SM) production plant. *Biochem Eng J*, 29:35-40.
8. Jiménez JI, Miñambres B, García JL, Díaz E. 2002. Genomic analysis of the aromatic catabolic pathways from *Pseudomonas putida* KT2440. *Environ Microbiol* 4:824-841.
9. Hartmans S, Smits JP, van der Werf MJ, Volkering F, de Bont JAM. 1989. Metabolism of styrene oxide and 2-phenylethanol in the styrene-degrading *Xanthobacter* Strain 124X. *Appl Environ Microbiol* 55:2850-2855.
10. Cámara B, Bielecki P, Kaminski F, Martins dos Santos V, Plumeier I, Nikodem P, Pieper DH. 2007. A gene cluster involved in degradation of substituted salicylates via *ortho* cleavage in *Pseudomonas* sp. strain MT1 encodes enzymes specifically adapted for transformation of 4-methylcatechol and 3-methylmuconate. *J Bacteriol* 189:1664-1674.
11. Pfaffl MW. 2001. A new mathematical model for relative quantification in real-time RT-PCR. *Nucleic Acids Res* 29:e45.
12. Van Bogelen RA, Neidhardt FC. 1999. Preparation of *Escherichia coli* samples for 2-D gel analysis. *Methods Mol Biol* 112:21-29.
13. Alban A, David SO, Bjorkesten L, Andersson C, Sloge E, Lewis S, Currie I. 2003. A novel experimental design for comparative two-dimensional gel analysis: two-dimensional difference gel electrophoresis incorporating a pooled internal standard. *Proteomics* 3:36-44.
14. Wijte D, de Jong AL, Mol MAE, van Baar BLM, Heck AJR. 2006. ProteomIQ blue, a potent post-stain for the visualization and subsequent mass spectrometry based identification of fluorescent stained proteins on 2D-gels. *J Proteome Res* 5:2033-2038.
15. Havlis J, Thomas H, Sebela M, Shevchenko A. 2003. Fast-response proteomics by accelerated in-gel digestion of proteins. *Anal Chem* 75:1300-1306.
16. Benndorf D, Thiersch M, Loffhagen N, Kunath C, Harms H. 2006. *Pseudomonas putida* KT2440 responds specifically to chlorophenoxy herbicides and their initial metabolites. *Proteomics* 6:3319-3329.
17. Pujari V, Chandra TS. 2000. Statistical optimization of medium components for improved synthesis of riboflavin by *Eremothesium ashbyii*. *Bioprocess Biosyst Eng* 23:303-307.
18. Benndorf D, Loffhagen N, Babel W. 2001. Protein synthesis patterns in *Acinetobacter calcoaceticus* induced by phenol and catechol show specificities of responses to chemostress. *FEMS Microbiol Lett* 200:247-252.
19. de Bont JAM. 1998. Solvent-tolerant bacteria in biocatalysis. *Tibtech*. 16:493-499.
20. Schreiber A, Hellwig M, Dorn E, Reineke W, Knackmuss HJ. 1980. Critical reactions in fluorobenzoic acid degradation by *Pseudomonas* sp. B13. *Appl Environ Microbiol* 39:58-67.
21. Smith JT, Vinjamoori DV. 1995. Rapid determination of logarithmic partition coefficients between n-octanol and water using micellar electrokinetic capillary chromatography. *J Chromatogr B Biomed Appl* 669:59-66.
22. Kim BJ, Choi WJ, Lee EY, Choi CY. 1988. Enhancement of *cis, cis*-muconate productivity by overexpressing of catechol 1,2-dioxygenase in *Pseudomonas putida* BCM114. *Biotechnol Bioprocess Eng* 3:112-114.

23. Volkers RJ, de Jong AL, Hulst AG, van Baar BL, de Bont JA, Wery J. 2006. Chemostat-based proteomic analysis of toluene-affected *Pseudomonas putida* S12. *Environ Microbiol* 8:1674-1679
24. Domínguez-Cuevas P, González-Pastor JE, Marqués S, Ramos JL, de Lorenzo V. 2006. Transcriptional tradeoff between metabolic and stress-response programs in *Pseudomonas putida* KT2440 cells exposed to toluene. *J Biol Chem* 281:11981-11991.
25. Cao B, Loh KC. 2008. Catabolic pathways and cellular responses of *Pseudomonas putida* P8 during growth on benzoate with a proteomics approach. *Biotechnol Bioeng*. 101:1297-1312.
26. Bell A, Bains M, Hancock RE. 1991. *Pseudomonas aeruginosa* outer membrane protein OprH: expression from the cloned gene and function in EDTA and gentamicin resistance. *J Bacteriol* 173:6657-6664.
27. Kim YH, Cho K, Yun SH, Kim JY, Kwon KH, Yoo JS, Kim SI. 2006. Analysis of aromatic catabolic pathways in *Pseudomonas putida* KT 2440 using a combined proteomic approach: 2-DE/MS and cleavable isotope-coded affinity tag analysis. *Proteomics*. 6:1301-1318.



# Chapter 4

## Modeling carbon-limited growth of *Pseudomonas putida* KT2440 on glucose

**Abstract:** One of the most common assumptions underlying simulations built upon genome-scale, constraint-based metabolic reconstructions is that bacteria try to maximize their growth yield. Consequently, such simulations require experimentally determined biomass composition and energetic maintenance values. In most reconstructions, due to the lack of appropriate measurements, these parameters are simply assumed to be equal to those of *E. coli*. Yet, their value can have a substantial impact on the prediction, for example, of the production yields of industrially relevant chemicals, which influences the usefulness of these models. Therefore, in order to increase the ability of a genome-scale metabolic model of *Pseudomonas putida* KT2440 (iJP815) to make accurate predictions, we determined the biomass composition and maintenance values, originally adopted from the *E. coli* model, and tested the impact of this refinement on the model forecasts. To this end, continuous fermentations on a mineral medium with glucose were carried out at a number of dilution rates and the macromolecular composition of the biomass was measured for each of them. Besides, the maximum growth yield, maximum growth rate, and maintenance coefficient were determined. The biomass composition remained stable through the whole range of dilution rates tested. Only the DNA fraction increased with the growth rate. The maximum yield turned out to be lower and the maintenance coefficient higher than originally assumed. Consequently, Growth-Associated Maintenance was increased fivefold and Non Growth-Associated Maintenance decreased 1.5-fold. The revalidation with  $^{13}\text{C}$  flux measurements showed an improvement in the model predictions. The model predictions were also compared with transcriptomic data and overall good consistency was observed. Thus, altogether, and by measuring carefully key biological parameters, this work enabled to explain missing links and inconsistencies, and improved considerably the accuracy of the model previously developed, providing a more solid basis for its use in designing biotechnological processes.

**Keywords:** biomass composition, continuous cultivation, flux balance analysis, glucose, metabolic modeling, *P. putida* KT2440, transcriptomics

Submitted for publication. Co-Authors: Puchalka J\*, Mars AE, Eggink G, Martins dos Santos VAP.

\*joint first authorship

## Introduction

*Pseudomonas putida* is a non-pathogenic, soil bacterium that developed a notably flexible metabolism and thus can inhabit versatile environmental niches. Numerous strains, some of them being solvent tolerant<sup>1,2</sup>, are able to produce efficiently a range of bulk and fine chemicals or, conversely, degrade various substances that are by products or waste of industrial processes<sup>3,4</sup>. These features, along with the amenability for genetic manipulation and suitability as a host for the expression of heterologous genes have rendered *P. putida* an attractive object of research for biotechnological applications<sup>5</sup>.

The sequencing of the genome of *P. putida* brought a significant leap in developing its applications by unveiling the metabolic potential encoded in the genome<sup>6</sup>. In an effort to enable the analysis of *P. putida* KT2440 from a systems biology perspective and to foster the development of its biotechnological applications, we built recently a constraint-based metabolic reconstruction (iJP815) of this strain<sup>7</sup>. Although a lot of knowledge pertaining to this strain was collected while building the model, some information had to be approximated from the *Escherichia coli* model<sup>8</sup>.

The information approximated included the biomass composition of the bacterium and the energetic expenses related to growth and the maintenance of life-functions (the so called Growth-Associated and Non-Growth Associated Maintenance value (GAM and NGAM)<sup>9</sup>. These parameters need to be specified prior to performing simulations of the growth, which provide a basis for numerous applications of metabolic reconstructions including rational strain design for biotechnological (and other) applications. Furthermore, these parameters influence significantly the outcome of such simulations, as they confine fluxes of important parts of the metabolism<sup>10,11,12,13</sup>. Moreover, they may vary significantly not only among organisms, but also among different growth conditions. Thus, for applications of metabolic reconstructions in biotechnology, the knowledge of maintenance values is pivotal as their values determine how much of the supply is “wasted” for the activities not related to the investigated application itself.

Therefore, to strengthen the ability of the metabolic model of *P. putida* (iJP815) to provide useful predictions, we characterized experimentally the macromolecular composition of *P. putida* KT2440 by numerous continuous fermentations under glucose-limited condition at varying dilution rates ( $D$ ). Furthermore, growth parameters as the maximal growth rate ( $\mu_{max}$ ), maximal yield ( $Y_{x/s}^{max}$ ) and maintenance coefficient ( $m_s$ ) were determined, from which maintenance values were derived. The updated model was revalidated by linking the Flux Variability Analysis (FVA) and Flux Balance Analysis (FBA) of the constraint-based model with available <sup>13</sup>C-flux batch measurements<sup>14</sup> and transcriptomics of continuous cultures at a  $D$  of 0.2 h<sup>-1</sup><sup>15</sup>, respectively. The revalidation showed that the model predictions improved and suggested a number of changes leading to further model development.

## Material and Methods

**Strain and culture conditions.** *P. putida* KT2440 (code name DSM6125) was aerobically grown in Biostat B bioreactors (Sartorius AG, Germany) at a working volume of 0.75 L, at 30 °C, and pH

7 that was regulated with 1 M NaOH. The bacterium was grown on E-2 mineral medium (MM)<sup>16</sup> with 10 mM glucose. The bioreactor was sparged with air at 0.75 L·min<sup>-1</sup>. The stirring of the bioreactor was adjusted to 550 rpm, to ensure that the dissolved oxygen level was above 50% saturation. Antifoam 204 Sigma (an entirely organic anti-foaming agent, Sigma-Aldrich, USA) was added to the medium at a concentration of 0.02%. Fifteen fermentations were performed at various  $D$  ranging from 0.05 to 0.64 h<sup>-1</sup>. All fermentations were started separately and were inoculated at 5% with a fresh pre-culture that was grown on a similar medium. After at least five residence times the desired growth rate was equal to  $D$ , at which time samples were taken.

**Analytical methods.** The cell density of the cultures was determined by measuring the optical density (OD) of the culture against a water blank at 600 nm on a Eppendorf Biophotometer (Eppendorf AG, Germany). The dry cell weight concentration ( $C_x$ ) in g<sub>DCW</sub>·L<sup>-1</sup> was measured by filtering 10 ml of a culture over a MF mixed cellulose esters filter with 0.22 μm pores (Millipore, Ireland). Before usage the filters were dried at 80°C for 24 hours and weighted. To discard salts and anti-foaming agent that might have stuck to the cells during filtration, the filters were subsequently washed with 5 ml of 0.9% NaCl. Subsequently they were dried again at 80°C for 24 hours and weighted. Both OD<sub>600</sub> and  $C_x$  measurements were done in triplicate for each  $D$ . To test whether the filter retracts any non-cell material (salts and/or anti-foaming agent) the dry cell weight determination procedure was repeated for pure medium (with anti-foaming agent and without carbon source). The measurements were repeated five times and yielded a residue of 0.356 (±0.023) g L<sup>-1</sup>. This residue was subtracted from  $C_x$  measurements obtained in the previous step. Parallel, the OD<sub>600</sub> and the  $C_x$  from 7 batch cultures of *P. putida* KT2440 in E-2 MM with 0 to 12.5 mM glucose were measured in triplicate. The following linear relation between the two measurements was determined:  $C_x=0.35 \cdot OD_{600}$ , with a  $r^2$  of 1. However, the directly measured dry cell weight measurements showed a relation of 0.399 OD<sub>600</sub>. In batch cultures it was shown that anti foam also has a significant positive influence on the filtration at the measured cell density. Therefore, the dry cell weight was compensated by multiplying with 0.35 divided by 0.399. The mean was taken from 2 to 3  $C_x$ -values measured by applying the OD<sub>600</sub>- $C_x$  relationship as determined above. This was also done for 2 or 3  $C_x$ -values measured directly and corrected afterwards as described above. From these two means an average was taken. The off-gas was analyzed on CO<sub>2</sub> content with the gas analyzer Servomex Xentra 4900 (Spectris, United Kingdom). The total amount of produced CO<sub>2</sub> during each continuous fermentation was calculated by analyzing the difference of its concentration in in- and outflowing gas and applying the gas law:  $pV=nRT$ .

The cell viability was determined by live and dead cell discrimination assay using a standardized cell viability kit (BD Biosciences, USA). The measurements were carried out using a FACSCalibur flow cytometer (BD Biosciences, USA). The liquid samples were beforehand diluted 100-fold in Tween 20-containing (0.01% w·v<sup>-1</sup>) phosphate buffered saline (PBS) (pH 7.4). The cell count was carried out at the flow of 60 μL·min<sup>-1</sup>.

To measure the glucose and ammonium concentrations, samples were taken from the feed medium and the supernatant sampled during the steady state of the fermentations. The samples were centrifuged at 16,873·g for 2 min and filter sterilized (pore size of 0.2 μm), to preserve them and to remove solids and precipitated proteins, and stored at -20°C. The ammonium concentrations were measured in 15-fold diluted samples using the LCK 303 kit of Hach Lange (Danaher, USA).

According to the manufacturer the kit has the detection limit of  $0.5 \text{ mg L}^{-1}$  and standard deviation of  $0.3 \text{ mg L}^{-1}$ . The glucose concentrations were determined using the glucose kit of Merck (Darmstadt, Germany), by measuring the absorbance at 340 nm in 10-fold diluted samples. According to the manufacturer the kit has the detection limit of  $0.4 \text{ mg L}^{-1}$  and a standard deviation of  $0.4\text{-}0.8 \text{ mg L}^{-1}$ . The same samples were used to assess the presence of possible other metabolites in the efflux medium using nuclear magnetic resonance (NMR). This was performed in duplicate for the  $D$  of 0.26, 0.44 and  $0.49 \text{ h}^{-1}$ . 1D  $^1\text{H}$  NMR spectra of aqueous supernatant containing 10%  $\text{D}_2\text{O}$  or of supernatant containing a standard solution of sodium 3-(trimethylsilyl)propane-1-sulphonate dissolved in  $\text{D}_2\text{O}$  to give a final volume of 0.66 ml were recorded on a Bruker AVANCE DMX600 NMR spectrometer at 300 K. The water signal was suppressed using standard Bruker software. For comparison purposes spectra of solutions of initial medium containing Antifoam 204 Sigma (Sigma-Aldrich, USA), glucose, sodium acetate and sodium 2-ketogluconate were recorded<sup>17,18</sup>. For quantitative analysis signals were referenced to the singlet signal of sodium 3-(trimethylsilyl)propane-1-sulphonate at a chemical shift of 0 ppm. In order to reach an appropriate signal to noise ratio, the spectra were recorded under standard conditions (sweep width: 20 ppm, acquisition time: 1.36 s, pulse delay: 1 s, number of scans: 1000, Bruker program noesypr1d). The detection limit for glucose was below 0.02 mM, for other metabolites below 0.2 mM.

To prepare samples for the measurement of RNA, carbohydrates, and lipids fractions, three medium samples of 5 ml each were taken and centrifuged at  $1,557 \cdot g$  at  $4^\circ\text{C}$  for 25 min. The supernatants were discarded and the pellets were stored in  $-70^\circ\text{C}$ . The total concentration of RNA, carbohydrates and lipids in bacterial cells were determined according to the procedures as described by Benthin *et al.*<sup>19</sup>, Herbert *et al.*<sup>20</sup> and Izard *et al.*<sup>21</sup>, respectively.

For the analyses of the protein and DNA concentration in the biomass, one sample of 15 ml culture was taken and centrifuged at  $20,201 \cdot g$  at  $4^\circ\text{C}$  for 12 min. The pellet was washed with PBS (pH 7.4) and stored at  $-70^\circ\text{C}$ . Prior to the analysis, the frozen cell pellet was re-suspended in 3 ml PBS and aliquoted in 3 equal-sized batches. One batch was used to determine the protein concentration in the cells. For this, the suspension was centrifuged at  $16,873 \cdot g$  at room temperature for 2 minutes and re-suspended in 200  $\mu\text{l}$  protein extraction solution that consists per 10 mL re-swelling solution, of 46 mg 1,4-Dithiothreitol and a half tablet of protease inhibitor cocktail (Roche Diagnostics GmbH, Germany). Re-swelling solution consists of 84 g Urea (Mallinkrodt Baker, Inc., USA) dissolved in 200 ml distilled water, a big spoon of Serdolit (SERVA Electrophoresis GmbH, Germany), 30.4 g thio-urea (Sigma-Aldrich, USA), 8 g 3-[(3-Cholamidopropyl)dimethylammonio]-1-propansulfonat (Carl Roth GmbH, Germany), and 0.48 g tris base (Sigma-Aldrich, USA). After the re-suspension 2  $\mu\text{l}$  lysozyme ( $100 \text{ mg} \cdot \text{ml}^{-1}$ ) was added and the cells were incubated at  $37^\circ\text{C}$  for 30 min while shaking at 400 rpm. During the incubation the samples were frozen three times with liquid nitrogen. Next, the incubation was continued at  $37^\circ\text{C}$  for 10 min while shaking at 1400 rpm. 50  $\mu\text{l}$  of the supernatant was taken and centrifuged at  $16,873 \cdot g$  for 15 min at  $4^\circ\text{C}$ . The supernatant was diluted 50 times with the QL lysis buffer. Standards of bovine serum albumin of 0.5, 0.25, and  $0.125 \text{ mg} \cdot \text{mL}^{-1}$  were prepared in triplicate. 10  $\mu\text{l}$  aliquots of the diluted supernatants and the three standards were separately mixed with 200  $\mu\text{l}$  of fivefold diluted (with distilled water) Biorad protein assay solution (Bio-Rad laboratories GmbH, Germany). The absorbance of samples and standards was measured at 595 nm with a microplate reader (Bio-Rad model 3550-UV, USA). The

absorbance values of the samples were recomputed to the concentrations using a regression line estimated from the absorbance of the standards.

The second batch of suspended cells was used to determine the concentrations of genomic DNA using the genomic DNA purification kit #K0512 (Fermentas, Canada). The procedure described by the manufacturer was followed until the step in which the DNA was dissolved in 100  $\mu\text{l}$  of 1.2 M NaCl by gently vortexing. Then, 0.2  $\mu\text{l}$  of 100  $\text{mg}\cdot\text{ml}^{-1}$  RNaseA (Qiagen, The Netherlands) was added, and the mixture was incubated at 37°C for 10 min under regular mixing by vortexing. To ensure the complete RNA degradation, the samples were analyzed with a formaldehyde agarose gel electrophoresis. The concentration of 20-fold diluted sample of DNA was measured at  $\text{OD}_{260}$  with an Eppendorf Biophotometer (Eppendorf AG, Germany).

From the continuous fermentation with *P. putida* KT2440 at a  $D$  of 0.2  $\text{h}^{-1}$  the amino acid composition of 1.5 mL medium was analyzed by an amino acid analyzer equipped with a ninhydrin detection system (Biochrom Ltd., UK) at Ansynth Service B.V. (The Netherlands). The samples were centrifuged at 16,873  $\cdot\text{g}$  at room temperature for 2 min and the supernatant was discarded before sending the samples off.

**Growth parameters.** To calculate the  $m_s$  in  $\text{g}_{\text{Glc}}\cdot\text{g}_{\text{DCW}}^{-1}\cdot\text{h}^{-1}$  and  $Y_{x/s}^{\text{max}}$  in  $\text{g}_{\text{DCW}}\cdot\text{g}_{\text{Glc}}^{-1}$  of *P. putida* KT2440 the following formula of Pirt was used:  $Y_{(x/s)}^{-1} = m_s \cdot D^{-1} + Y_{(x/s)}^{\text{max}-1}$  <sup>22</sup>. The  $\mu_{\text{max}}$  was determined by a wash out experiment. For this, the  $D$  was increased to 1.2  $\text{h}^{-1}$  after cultivation at the  $D$  of 0.13  $\text{h}^{-1}$  for five generation times. Within 3 hours the cell density was determined 10 times by measuring the  $\text{OD}_{600}$  of the culture. The  $\mu_{\text{max}}$  was calculated by fitting the decrease of the cell density to the formula:  $C_{xt} = C_{x0} \cdot e^{(\mu-D)\cdot t}$ .

**Calculation of carbon and nitrogen-balance.** To determine the carbon percentage in the biomass, the difference between carbon inflow (in form of glucose) and carbon outflow (in form of  $\text{CO}_2$ ) was calculated in  $\text{g}_{\text{carbon}}\cdot\text{L}^{-1}\cdot\text{h}^{-1}$ . Dividing this value by the biomass production rate ( $R_x$ ) ( $\text{g}_{\text{DCW}}\cdot\text{L}^{-1}\cdot\text{h}^{-1}$ ) yielded the carbon percentage in the biomass. To determine the nitrogen percentage of the biomass the difference between the nitrogen concentrations in the influx and efflux medium in  $\text{g}\cdot\text{L}^{-1}$  was divided by the  $C_x$ .

**Metabolic model.** The metabolic model of *P. putida* model (iJP815)<sup>7</sup> was used. Several minor modifications that resulted from further development of the model were introduced. These are summarized in Supplementary Material.

**Creation of new Biomass equation for *P. putida* model (iJP815).** The new biomass equation for the iJP815 model was created based on a number of sources. First, the fraction of each type of macromolecule (Protein, DNA, RNA, Lipids, and Carbohydrates) was determined as described in Analytical methods. Since our protein determination method accounts only for water-soluble proteins, the fraction of proteins was increased by 13.0 percentage points—the amount of water-insoluble proteins. This value was assessed based on the fraction of proteins in the outer and cytoplasmic membranes of *P. aeruginosa* (51.0%  $\text{w}\cdot\text{w}^{-1}$ )<sup>23</sup> which in turn constitutes 24-27% ( $\text{w}\cdot\text{w}^{-1}$ ) of the total dry mass in *E.coli*<sup>24</sup>. Equivalence between water-insoluble proteins and membrane-bound proteins was assumed. Next, the composition of each type of macromolecule with regard to its building blocks (e.g. amino acids for proteins) was elucidated. The fractions were recomputed to

represent the molar coefficients that are used in stoichiometric equations in the constraint-based models. The biomass equation was designed to produce 1 gram of biomass when the flux reaction equals to 1 and the fluxes are expressed in  $\text{mmol g}_{\text{DCW}}^{-1} \cdot \text{h}^{-1}$ .

**Proteins:** The amino acid composition was based on the experimental values obtained in continuous culture analyzed by Ansynth Service B.V. The amino acids that were not identified in this assay (Cysteine, Methionine, Tryptophan) were assumed to have identical molar fraction as in the *E. coli* biomass<sup>8</sup>.

**DNA:** The fraction of each of four deoxyribonucleotide moieties was determined using the genomic sequence of the bacterium. Although replication forks of the genome are formed during growth it is assumed that the DNA sequence is equal for all cells.

**RNA:** The RNA composition was assumed to be identical to *E. coli* at a *D* of  $0.6 \text{ h}^{-1}$ <sup>25</sup>.

**Lipids:** The lipids were assumed to consist of two subclasses – lipopolysaccharide (LPS) and phospholipids. As the information regarding LPS was missing it was assumed that its fraction and molecular composition is the same as in *E. coli*<sup>8</sup>. The *in silico* LPS molecule in the constraint-based model consists only of lipid A and core oligosaccharide. The polysaccharide chains were not included, since their molecular composition and length are not well-defined, and, furthermore, they are accounted for in the carbohydrate biomass constituents. In addition, the CDP ethanoloamine moiety was removed from the *in silico* LPS molecule as any evidence of the ability of *P. putida* KT2440 to synthesize this compound is missing. The composition of phospholipids was defined with regard to both head-groups and fatty-acid compositions. The composition of the former was identified from the measurements of the very close relative *Pseudomonas putida* S12 (phosphatidylethanolamine – 73.7%, cardiolipin – 21.3%, phosphatidylglycerol – 4.9%; measured by Mylnefield Lipid Analysis, United Kingdom; Rita Volkers, personal communication), while the *in silico* fatty acid composition was based on experimental measurements of Stead<sup>26</sup>.

**Carbohydrates:** The carbohydrate pool was assumed to be present entirely in the form of glycogen as a proxy for all sugar polymers.

In addition to these macromolecules peptidoglycan was assumed to be present<sup>27</sup>. Due to lacking information the mass fraction and exact composition were adopted from the *E. coli* biomass composition<sup>8</sup>. Similarly, the biomass was augmented with vitamins and co-factors, albeit with several differences – the spermidine and UDP-Glucose were removed as there was no evidence that these two compounds can be produced by *P. putida* KT2440. As the small molecules are represented in minimal amounts in the biomass, the influence of their coefficients in the biomass equation on model predictions such as  $Y_{(x/s)}$  or flux-distribution is negligible. Important is only whether they are considered to be present or not as this influences, for example, the essentiality predictions for genes and reactions.

**Computation of maintenance values.** The GAM and NGAM are two values that need to be fit in the model in order to make accurate flux predictions<sup>9</sup>. GAM – the amount of ATP that is dissipated when  $1 \text{ g}_{\text{DCW}}$  is synthesized – was adjusted so that FBA-predicted (see below)  $Y_{x/s}^{\text{max}}$  is equal to the experimentally measured value. NGAM – the amount of ATP that is dissipated for maintenance

purposes by an amount of living cells (corresponding to  $1g_{DCW}$ ) in a unit time (1h) – was computed from the experimentally measured  $m_s$  by multiplying it by maximal theoretical (computed using the stoichiometry of the reactions within the model) ATP yield ( $Y_{ATP}$ ) of  $19.25 \text{ mol}_{ATP} \text{ mol}_{Glc}^{-1}$ . The latter value was determined computationally using the metabolic model (by finding the maximal ATP production from glucose) and thus depends on the P:O ratio (1.33) assumed within the model.

***In silico* flux predictions – FVA.** FVA was used to predict flux values using the model. FVA is a variant of FBA. FBA finds a flux distribution (values of fluxes of all reactions belonging to the model) that maximizes or minimizes a previously defined objective (usually  $R_x$  or substrate uptake rate) and calculates value of this objective given the constraints included into the model. This is achieved by means of linear optimization (maximization of a linear objective in constraint-based stoichiometric models poses a linear problem). In flux predictions reported here the objective was to minimize the glucose uptake rate of *P. putida* KT2440 while maintaining the specific  $\mu$  at  $0.2 \text{ h}^{-1}$  (one of the  $D$  used in the continuous culture experiments). For more details on FBA, see Puchałka *et al.*, and Kauffman *et al.*<sup>7,28</sup>. Metabolic networks of living organisms are usually considerably underdetermined. This means that not all reaction fluxes can be uniquely determined by the FBA approach. FVA is a method that allows for rough top estimation of the allowed flux variability of each reaction, given by the FBA optimization. FVA computes for each reaction an interval of values inside of which the flux of the reaction can change without influencing the value of the objective function, provided that other fluxes are allowed to vary freely within their constraints<sup>29,30,31</sup>.

When FBA/FVA simulations are compared to real data, it is often observed that cells do not operate fully optimally. Therefore, a variant of the FVA approach called suboptimal FVA<sup>29</sup> is sometimes informative, in which the objective value is allowed to vary within a predetermined limit instead of fixing the objective to its optimal value from the initial FBA run (as in standard FVA). For every suboptimal FVA presented in this paper the objective upper limit was set at 110% of the initial objective value.

**Comparison of the model output with <sup>13</sup>C flux measurement data.** The FVA predictions were compared with <sup>13</sup>C flux measurements of Fuhrer *et al.*<sup>14</sup>, similarly to the comparisons done in Puchałka *et al.*<sup>7</sup>. In these measurements fluxes of the reactions belonging to central metabolic pathways (Pentose phosphate Pathway, Entner-Doudoroff Pathway TCA Cycle) were determined for *P. putida* KT2440 grown in Erlenmeyer flasks in minimal medium with glucose. To assess the agreement between the experimental measurements and FVA-predictions, the minimal and maximal square distance between the experimental data and FVA-results were computed. For each FVA-simulation the sums of the minimal and maximal distances provide two distance values (minimal and maximal). This pair of values will be called a “FVA distance”. Some fluxes were not included in the computation of the FVA-distance. For details, see Supplementary Material.

**Generation of hypotheses pertaining to the increase of Acetyl-CoA production.** The hypotheses were generated identically as in Puchałka *et al.*<sup>7</sup>. Modified OptKnock algorithm was used<sup>7,32</sup> to identify double mutants in combination of a specific carbon source. Compared to the WT these mutants are expected to show increased Acetyl-CoA production flux, as predicted by either “production” or “pooling” method<sup>7</sup>, and maintained defined minimal  $Y_{(x/s)}$ .

**Comparison of model predictions with transcriptomic data.** The transcriptomic data were used as one of the sources for model validation<sup>15</sup>. The transcriptomic analysis was performed for *P. putida* grown continuously under glucose limitation at  $D$  0.2 h<sup>-1</sup>. Four microarray experiments were used for the validation. These included mutant *P. putida* KT2440-JD1 and WT strains. The inclusion of the mutant strain was motivated by the lack of significant expression differences under these conditions (the mutant contains a mutation in gene *catR* that is the regulator of the *cat* operon). Various methods were used for estimating the consistency between the transcriptomic data and the model predictions. These are described later in the manuscript.

## Results

**Macromolecular components.** The molecular composition of the *P. putida* KT2440 cell remained fairly stable over the whole measured range of  $D$ . The biomass fractions of RNA, lipids, water-soluble proteins, and carbohydrates showed no significant dependency on the  $\mu$  (Fig. 1), while the DNA exhibited an increase. The macromolecular composition of the biomass is summarized in Table 1. About 96.1% of the  $C_x$  was identified with the measurements of the macromolecules. The mass missing in the macromolecular measurements justified the addition of 13.0% hydrophobic proteins<sup>33</sup>. The water-insoluble proteins, peptidoglycan and micro-molecules were not included in the measurements. By balancing carbon and nitrogen measurements of the continuous fermentations, the average fraction of these compounds in the  $C_x$  was computed to be 52.5% ( $\pm 3.70$ ) and 14.2% ( $\pm 1.81$ ), respectively.

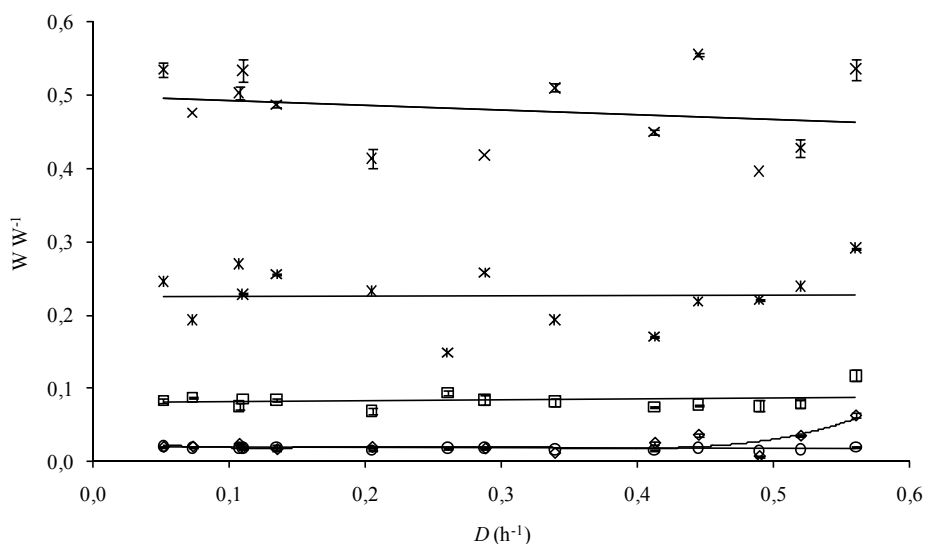


**Figure 1.** Macromolecular composition of *P. putida* KT2440 grown in continuous culture on glucose at different  $D$  (h<sup>-1</sup>). The percentages of water-soluble proteins (×), lipids (□), carbohydrates (○), RNA (\*), and DNA (◇) in the total biomass in W W<sup>-1</sup> are given.

The amino acid composition of the water-soluble proteins of the cells grown at a  $D$  of  $0.2 \text{ h}^{-1}$  was analyzed (Table 2). By dividing the total concentration of amino acids by the measured  $C_x$  the mass of proteins constituted 52.3% of the biomass.

**Table 1.** The comparison of macromolecular composition of the *P. putida* KT2440 biomass.

Macro-molecule	W W <sup>-1</sup> <i>P. putida</i> KT2440 ± standard deviation (this study)	W W <sup>-1</sup> iJP815 ( <i>E. coli</i> ) biomass <sup>6</sup>	W W <sup>-1</sup> PpuMBEL1071 <i>P. putida</i> KT2440 <sup>41</sup>
Proteins	61.0 ± 5.4*	55.3*	50.6*
Lipids	8.5 ± 1.2	13.0	7.4***
Carbohydrates	1.8 ± 0.2	2.5	
RNA	22.9 ± 4.0	20.7	20%
DNA	1.8±0.4**	3.1	2.8%

(\*Pertains to all proteins, \*\* $D$  of 0,2, \*\*\*phospholipid and polysaccharide)

**Table 2.** Amino acid composition of the water-soluble proteins of *P. putida* KT2440 at a  $D$  of  $0.2 \text{ h}^{-1}$ .

Amino Acid	Mol % (this study)	Mol % PpuMBEL1071 <sup>41</sup>
Ala	12	10
Arg	5	6
Asx	10	9
Cys		2
Glx	12	10
Gly	10	12
His	2	2
Ile	4	5
Leu	10	8
Lys	5	6
Met		3
Phe	4	4
Pro	5	4
Ser	5	4
Thr	5	5
Trp		1
Tyr	3	3
Val	7	8

**Creation of *P. putida* specific biomass equation.** A new biomass equation for the metabolic model (iJP815) was computed based on the cell composition at a  $D$  of  $0.2 \text{ h}^{-1}$  and other sources (see methods). This new equation differed only to some extent from the old one, with respect to both macromolecular and elemental composition (Tables 1 and 3). The main difference for the macromolecular composition is the lower fraction of lipids and the higher fraction of RNA (see Table 1). From the *in silico* biomass equation the elemental composition of *P. putida* KT2440 was computed, which is shown in Table 3. This composition corresponded well with the elemental compositions that were calculated from the C and N balances and the values that were reported for *P. putida* ATCC 29735 grown on peptone-yeast extract medium<sup>34</sup>. The lower carbon fraction in the *in silico* biomass and the appropriate nitrogen concentration could suggest that the lipids fraction was underestimated since this macromolecule has a carbon fraction exceeding 50% and contains a relative low concentration of nitrogen<sup>11</sup>.

**Table 3.** Elemental composition of the biomass  $W W^{-1}$ : computed from the *in silico* *P. putida* KT2440 specific biomass equation created in this work, the determined carbon and nitrogen-balance of *P. putida* KT2440, the ashing and chemical determination of the biomass is from *P. putida* ATCC 29735 grown in continuous culture on peptone-yeast extract<sup>34</sup>, and computed from the *in silico* biomass equation used in the original iJP815 model (*E. coli* biomass).

	Calculated from <i>in silico</i> <i>P. putida</i> specific biomass (this study)	C-/N-balance (this study)	Ashing and chemical preparation	Calculated from <i>in silico</i> original iJP815 ( <i>E. coli</i> ) biomass
C	48.8	52.5	52.1	50.0
H	6.3		7.4	6.6
N	15.6	14.6	14.3	15.1
O	25.8			25.2
P	2.7		1.8	2.8
S	0.8		0.5	0.7

In order to assess the effect of change of the biomass equation on the accuracy of predicted flux values, the FVA-distances were computed from simulations performed using either biomass equation (Table 4). The new biomass equation caused a small decrease of optimal FVA-distances, which is in agreement with the small differences between the biomass equations. The maximal suboptimal FVA-distance increased to small extent, which was unexpected, as the new biomass equation was expected to increase the fidelity of the model.

**Growth related factors.** Not only biomass composition, but also growth-related parameters were determined during the continuous fermentations of *P. putida* KT2440 on glucose at different  $D$ . The  $R_x, R_{CO_2}, R_{glc}$  increased until  $D$  0.49  $h^{-1}$  (Fig. 2) with the highest measured  $Y_{(x/s)}$  of 0.389  $g_{DCW} \cdot g_{Glc}^{-1}$ . The  $\mu_{max}$  was determined to be 0.59  $h^{-1}$  by a wash out experiment ( $r^2$  of 0.98). This means that when *P. putida* KT2440 was cultivated with the highest  $D$  of 0.64  $h^{-1}$  the  $\mu$  was equal to  $\mu_{max}$  and as a consequence no steady state was reached. Above  $D$  of 0.52  $h^{-1}$  increasing glucose concentrations were observed. This is most probably a consequence of approaching the  $\mu_{max}$ , whereas the classical Monod-relationship<sup>35</sup> was not observed (the relationship between glucose concentration and  $D$  ( $\mu_{max}-D$ )<sup>-1</sup> was rather exponential as linear). The  $Y_{x/s}^{max}$  and the  $m_s$  of *P. putida* KT2440 were determined with high accuracy to be 0.393 ( $\pm 0.0029$ )  $g_{DCW} \cdot g_{Glc}^{-1}$  and 0.031 ( $\pm 0.0021$ )  $g_{Glc} \cdot g_{DCW}^{-1} \cdot h^{-1}$ , respectively (Fig. 3). The linear relationship was very strong, as  $r^2 = 0.95$ .

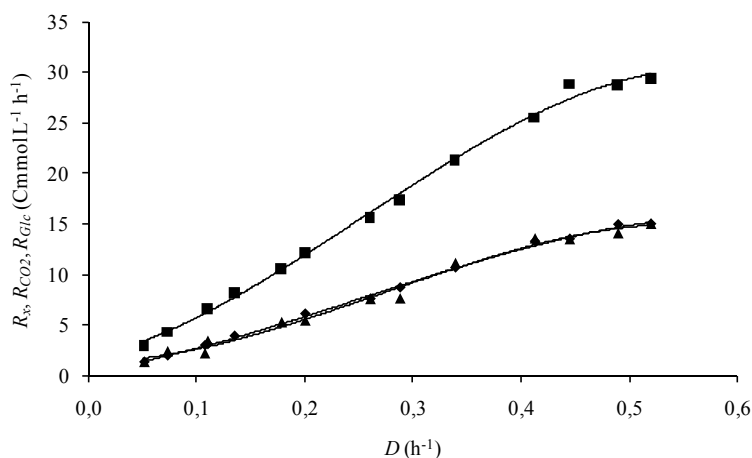


**Figure 2.** The  $R_x$  ( $\blacklozenge$ ),  $R_{CO_2}$  ( $\blacktriangle$ ),  $R_{glc}$  ( $\blacksquare$ ) ( $Cmmol \cdot L^{-1} \cdot h^{-1}$ ) of *P. putida* KT2440 at various  $D$  ( $h^{-1}$ ) on MM with 10 mM glucose.

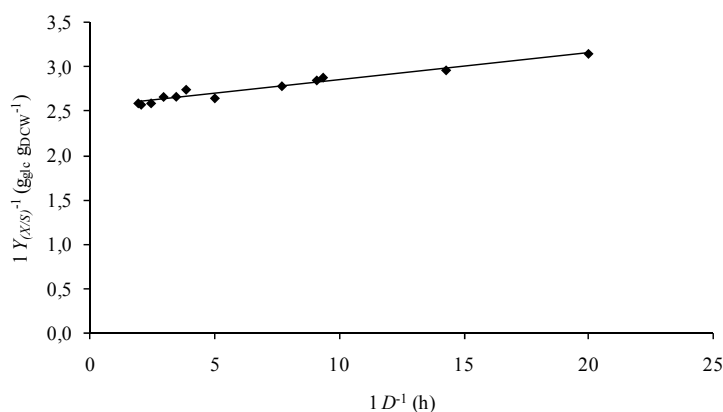


**Figure 3.** Reciprocal values of the  $Y_{x/s}$  ( $\text{g}_{\text{DCW}} \cdot \text{g}_{\text{glc}}^{-1}$ ) plotted against the related reciprocal values of the  $D$  ( $\text{h}^{-1}$ ) (Pirt diagram)<sup>22</sup>.

The average concentration of cells was  $6.94\text{E}+08$  ( $\pm 6$ ) % cells per ml. On average 95 ( $\pm 2$ ) % of the cells were alive and 2 ( $\pm 2$ ) % were dead. Only the fermentation with a  $D$  of  $0.05 \text{ h}^{-1}$  had a distinct percentage of dead cells of 11%. Since  $0.05 \text{ h}^{-1}$  is a relatively low  $D$ , this deviation is most likely due to a higher relative cell death rate caused by the increased generation time of *P. putida* KT2440<sup>36</sup>. With increasing  $D$  the cell size increases, thus leading to higher  $Y_{(X/S)}$  as indicated by the increased scatter values during the flow cytometry measurements. The analysis of feed medium by NMR showed strong characteristic signals of the  $\alpha$ - and  $\beta$ -anomeric forms of D-glucopyranose together with those of the antifoam, as well as very small signals of impurities associated with the technical grade materials used. During steady state of the fermentation the signals for glucose had completely disappeared and only antifoam and those of the small impurity signals could be detected. The signal-to-noise ratio was high enough to show that neither acetate nor any other organic metabolites accumulated during the fermentation. The position of such signals was in regions of the spectrum that were essentially free from overlap. Because no other metabolites were found in the medium by  $^1\text{H-NMR}$  at a  $D$  of 0.26, 0.44 and  $0.49 \text{ h}^{-1}$ , it was concluded that there is no accumulation of any intermediates of anabolism or catabolism in the range of  $D$  under carbon limited conditions.

**New maintenance values.** The estimated  $Y_{x/s}^{\text{max}}$  and  $m_s$  were used to fit the NGAM and GAM parameters of iJP815. These were computed to be  $85 \text{ mmol}_{\text{ATP}} \text{ g}_{\text{DCW}}^{-1}$  and  $4.96 \text{ mmol}_{\text{ATP}} \text{ g}_{\text{DCW}}^{-1} \text{ h}^{-1}$  for GAM and NGAM, respectively. The main change was a 2.5-fold increase of the GAM value (the old value was  $33 \text{ mmol}_{\text{ATP}} \text{ g}_{\text{DCW}}^{-1}$ ), which was due to the use of a much lower value of the  $Y_{x/s}^{\text{max}}$  than assumed in the original version of the model. The NGAM was decreased approximately 1.5-fold<sup>8,9</sup> as a consequence of lower value of the  $m_s$ . The change of GAM and NGAM values caused larger changes to the flux distribution than the change of biomass equation. These changes manifested themselves by a small decrease of the minimal FVA-distance.

**Evaluation of limits within the central metabolism.** When inspecting the FVA results for the reactions whose fluxes were identified via  $^{13}\text{C}$ -measurements<sup>14</sup>, three enzymes were identified that showed high possible variability, namely 2-oxoglutarate dehydrogenase (AkgDH, EC:1.2.4.2),

pyruvate dehydrogenase (PyrDH, EC: 1.2.4.1), and pyruvate kinase (Pyk, EC: 2.7.1.40). It was therefore tested, how restricting the fluxes of the respective reactions would influence the output of FVA simulations as measured with FVA-distances. The reactions were constrained either to their maximal FVA values or to the experimentally measured ones based on  $^{13}\text{C}$  measurements. Imposing these limits had a strong impact on the flux predictions (Table 4). The drop in the FVA-distances was much higher than implied by the limits on the particular reaction(s). This drop was only observed in values of maximal distances. Therefore constraining these reactions did not lead to identification of a solution that is significantly closer to the experimental values, but it excluded flux distributions that are far from the experimental. The best combination was parallel limitation of flux through AkgDH and Pyk. Imposing *in silico* constraints on AkgDH also caused that the flux through PyrDH was defined (i.e. the fluxes through these reactions are coupled *in silico*). Interestingly, better (with smaller FVA-distances) results were obtained when the reactions were limited to their maximal FVA values than to the values measured in the  $^{13}\text{C}$  experiments.

$^{13}\text{C}$  measurements showed that glucose-6-phosphate isomerase (EC: 5.3.1.9) operated in the reverse direction. This cannot be predicted by optimal FVA, as this would decrease  $Y_{x/s}$ . Limiting this enzyme to its experimentally measured values caused a small decrease of the FVA-distances.

When inspecting the distances for suboptimal FVA computations, the same trend as for optimal FVA can be observed. Due to the relaxed optimality, the minimal distance always reached zero. This however does not mean that a flux distribution with minimal distance will be feasible, since the FVA computations for every reaction are not independent of each other.

**Table 4.** Distances between FVA solutions and  $^{13}\text{C}$  flux measurements: FVA-distances (see Text) computed for different combinations of biomass composition, GAM, NGAM, and limitations of the reactions *AkgDH*, *Pyk* and, or *Pgi* based on maximal FVA or experimental values.

Model modifications	FVA – optimal	FVA – suboptimal	
	Min	Max	Max
Original model	36.8	415.37	2532.96
New Biomass, old GAM and NGAM	35.02	366.19	2580.44
New Biomass, GAM, and NGAM	34.35	470.65	3371.76
AkgDH limited to max	34.8	138.46	974.4
AkgDH limited to experimental	40.59	152.56	1242.01
AkgDH & Pyk limited to max	35.79	36.37	974.4
AkgDH & Pyk limited to experimental	40.19	43.66	788.95
AkgDH & Pgi limited (AkgDH – max)	36.15	123.79	1435.97
AkgDH & Pgi limited (AkgDH – experimental)	36.66	144.53	1281.93
AkgDH, Pyk & Pgi limited (max)	35.09	35.65	910.63
AkgDH, Pyk & Pgi limited (experimental)	36.75	39.38	810.84

**Influence of biomass composition and maintenance values changes on model predictions.** The original *P. putida* model was used to generate hypotheses pertaining to increasing the production of acetyl-CoA. This compound is an entry metabolite for the synthesis of polyhydroxyalkanoates – biodegradable plastics of industrial and medical relevance<sup>37,38</sup>. In order to evaluate, how the changes of biomass composition and maintenance values influenced these predictions, the same hypothesis-generation procedure was repeated using the updated model. The comparison of the old and the new results is presented in Table 5. Mutants 1-3 were generated with ‘acetyl-CoA

production' method, while mutants 4-6 with 'acetyl-CoA pooling flux' method. The acetyl-CoA production flux values are not comparable between these two mutant hypothesis groups<sup>7</sup>. The update of the model caused the identification of the novel mutant 6 that showed a higher 'pooling' flux than the mutant suggested with the original version of the model. Mutant 6 has a predicted  $Y_{x/s}$  higher than  $6.66 \text{ g}_{\text{DCW}} \text{ molC}^{-1}$  and a maximal acetyl-CoA 'pooling' flux of  $10.29 \text{ mmol} \cdot \text{g}_{\text{DCW}}^{-1} \cdot \text{h}^{-1}$ . Furthermore, the predicted values of Acetyl-CoA production/pooling fluxes were in all cases increased, yet these changes did not exceed 10%. In those cases where the same mutations were predicted in the original and updated model, the change of the flux anti-correlated strongly with the change of the  $Y_{x/s}$  value (correlation coefficient of -0.99).

**Table 5.** Predictions of maximal acetyl-CoA production flux and  $Y_{x/s}$  as a result of at least two suggested mutations in combination of a specific carbon source.

Mutant	$Y_{x/s}$ bottom limit [ $\text{g}_{\text{DCW}} \cdot \text{molC}^{-1}$ ]	Blocked enzymatic activity	Loci to be blocked	Carbon source(s)	Identical with Old	Max AcCoA production flux [ $\text{mmol} \cdot \text{g}_{\text{DCW}}^{-1} \cdot \text{h}^{-1}$ ]		$Y_{x/s}^{\text{max}}$ [ $\text{g}_{\text{DCW}} \cdot \text{molC}^{-1}$ ]	
						Old	New	Old	New
WT	0.83	WT	WT	L-Serine	Yes	22.26	25.67	11.16	9.13
1	0.83	- triose-phosphate isomerase	PP4715	D-Fructose	Yes	29.74	30.63	3.5	2.82
		- 6-phosphogluconolactonase	PP1023						
2	0.83	- glucose dehydrogenase (membrane)	PP1444	D-Glucose	Yes	28.51	29.64	4.17	3.49
		- 6-phosphogluconolactonase	PP1023						
3	6.66	- isocitrate dehydrogenase	PP4011 or PP4012	L-Serine	Yes	23.01	26.14	10.67	8.8
		- formate dehydrogenase	PP0490 or PP0491 PP2183 or PP2184 or PP2185 or PP2186						
4	0.83	- citrate synthase	PP4194	L-Valine	Yes	21.85	21.98	1.00	1.00
		- 2-methylcitrate dehydratase	PP2338						
5	3.33	- glycine hydroxymethyl transferase	PP0322 PP0671	L-Leucine, L-Lysine, L-Phenylalanine	Yes	16.75	17.51	4.00	4.00
		- citrate synthase	PP4194						
6	6.66	- phosphoglycerate kinase	PP4963	L-isoleucine	No	9.35	10.29	9.33	7.14
		- citrate synthase	PP4194						

**Evaluating the consistency between the transcriptomic data and the model.** To further validate the model, the consistency between model predictions and the transcriptomics data, generated at steady-state, was assessed. The FBA-predicted fluxes and the levels of respective mRNA transcripts showed overall good agreement with each other. It should be emphasized, however, that measured abundances of mRNA transcripts cannot be directly translated into fluxes. The consistency was evaluated by analyzing the expression levels of: i) genes essential for growth, ii) non-essential genes with low expression that are involved in reactions with non-zero flux, and iii) genes with high expression values that are only involved in the catalysis of the reactions with predicted zero flux.

**Expression of the genes essential for growth.** The first assessment aimed at identifying genes essential for growth *in silico* that are actually not expressed. From genes identified by the model as essential those were selected and termed as potentially not expressed that complied with at least one of the following criteria: i) the number of “absent” calls (as defined by Affymetrix analysis Manual) was higher than 2 (out of 4 arrays), or ii) the number of “present” calls was lower than 3, (out of 4 arrays) or iii) the mean  $\log_2$  absolute gene expression value was lower than 7.5. Out of 147 essential genes 33 were selected that were potentially not expressed. They are listed in Supplementary Table 2. Inspection of these genes showed that the overlap between the methods is limited. The “present” call condition is the least restrictive one, while the mean condition is the most restrictive. Many of the genes that fulfilled one of the “call” conditions show  $\log_2$  absolute gene expression values higher than 8, whereas the average over all arrays was 8.29. This suggests that the call methods are relatively untrustworthy and that, in many cases, it rather points out the genes for which experimental problems possibly occurred, e.g. due to cross-hybridization of the respective probes with mRNA from some other gene. A cluster of genes PP0237-PP0240 (rows marked blue) that was originally annotated to be involved in sulfate transport was consistently identified as absent. After close inspection, these genes appeared to be miss-assigned, since there was a group of other genes that is responsible for sulfate transport (PP5168-PP5171). The model was updated accordingly.

Inspecting the genes that complied with at least two of the criteria revealed that there were a number of those involved in biosynthesis of cofactors (red rows). The corresponding reactions usually have a low flux so it may be that low protein levels suffice for the required enzymatic activity. There are also six genes involved in the synthesis of LPS (green). The majority of these genes has relatively high expression levels and were selected due to the presence/absence criteria. LPS is needed in rather limited amounts so a low expression may be sufficient for the required enzymatic activity. Furthermore these six genes constitute only around 50% of the genes involved in LPS synthesis, so this also suggests that the expression levels are sufficient. PP2458, PP2460, and PP4266 (yellow) are genes that were labeled as essential due incompleteness of the metabolic model. S-adenosyl homocysteine is produced during the synthesis of cyclo-fatty acids. This compound needs to be converted further. Apparently the only way is to convert it into ribose and adenine which are then phosphorylated to ribose-6-phosphate and AMP, respectively. This route seems, however, not to be the proper one.

**Expression of non-essential genes required for optimal growth.** The second assessment was an extension to the previous one. Here reactions with non-zero minimal fluxes in FVA simulations were identified. For these reactions the “expression value” was computed and reactions with a  $\log_2$  expression value below 7.5 were selected. There were only five such reactions identified. They were all involved in fatty acid biosynthesis and all catalyzed by the same pair of isozymes (PP3553 and PP2795-acyl-CoA synthetases) whose mean expression values did both not exceed 7.5.

**Highly expressed genes not required for growth.** Finally, genes with high expression levels were identified that only catalyze reactions with a low flux (this threshold was arbitrarily set to  $0.1 \text{ mmol} \cdot \text{g}_{\text{DCW}}^{-1} \cdot \text{h}^{-1}$ , when the  $\mu$  was  $0.2 \text{ h}^{-1}$ ). These genes are listed in Supplementary Table 3. Several interesting observations could be made out of it. First, branched-chain amino acids ABC transporters constituted a significant fraction of these genes (blue rows), suggesting that the bacterium is actively searching for alternative nutrition sources. Second, a number of genes are

involved in the synthesis of cofactors (yellow rows). These include biotin, pyridoxal phosphate (Vitamin B6), thiamin pyrophosphate, and riboflavin. For the last one, only a single gene from its biosynthesis pathway showed high expression and, as riboflavin is included into biomass composition, there is a flux going through the reactions involved in its synthesis. This flux depends on the share of the riboflavin in the biomass. The high expression of this gene may suggest that this coefficient should be higher, yet the evidence is weak, as other genes belonging to the pathway did not show high expression. The other three compounds are not included in the biomass equation, but the expression levels of respective genes suggest that they should be included. The mechanism (biosynthetic reactions and genes catalyzing them) of the synthesis of pyridoxal phosphate in *P. putida* KT2440 is known, whereas it is not the case for the other two compounds. Third, reactions involved in rhamnosugars synthesis (red rows) are also highly expressed. These are used for synthesis of rhamnolipids that are a constituent of the bacterial envelope and are not part of the biomass in the current version of the model. This assay suggests that they should be included. This requires however the determination of the exact composition of these metabolites and their share in the biomass. The reason of higher expression of remaining genes could not be elucidated.

## Discussion

Constraint-based modeling provides a valuable framework for navigating microbial metabolic networks and for identification and prediction of intra-cellular flux distributions, thereby aiding the discovery and application of bacteria e.g. in biotechnology. However, to be predictive, the metabolic reconstructions created within this framework require proper and accurate input information. Striving to improve the metabolic reconstruction of *P. putida* KT2440, we characterized experimentally the macromolecular composition of the bacterium cultivated continuously on a minimal medium with glucose as the sole carbon and energy source at a range of  $D$  (0.05-0.6 h<sup>-1</sup>). These measurements showed that the macromolecular biomass composition does not change significantly when the  $D$  and thus the  $\mu$  varies. The only macromolecule that did change significantly upon increasing  $D$  was the DNA. This might have been a consequence of the appearance of a higher number of replication forks. In other organisms like *E. coli* K12 ( $D$  range: 0.05-1.7 h<sup>-1</sup>)<sup>10</sup>, *E. coli* B/r ( $D$  range: 0.6-2.5 h<sup>-1</sup>)<sup>25</sup> and *P. denitrificans* ( $D$  range: 0.06-0.6 h<sup>-1</sup>)<sup>10</sup>, the DNA fraction was observed to decrease at increasing  $D$ , or remain stable as in *S. cerevisiae* ( $D$  range: 0.02-0.2 h<sup>-1</sup>)<sup>11</sup>, and *A. calcoaceticus*<sup>39</sup>. Baart *et al.*<sup>40</sup> observed however that in *N. meningitidis* ( $D$  range: 0.04-0.16 h<sup>-1</sup>) the DNA fraction increases too. The stability of the RNA and protein fractions in *P. putida* KT2440 also contradicts to some extent previous findings, as in some other organisms – *E. coli* and *P. denitrificans* – these fractions increased and decreased with the  $D$ , respectively<sup>10,25</sup>. However, no significant changes were observed for the RNA and protein fractions in *E. coli* K12 at the  $D$  range of 0.05-0.6 h<sup>-1</sup> and *N. meningitidis* ( $D$  range: 0.04-0.16 h<sup>-1</sup>)<sup>10,40</sup>. In *A. calcoaceticus*<sup>39</sup> only the RNA fraction increased and in *S. cerevisiae* ( $D$  range: 0.02-0.2 h<sup>-1</sup>)<sup>11</sup> both the RNA and protein fractions increased. The increase of the RNA fraction most probably reflects the extra need for ribosomal RNA for the synthesis of proteins<sup>41</sup>. However, besides the increase of the number of ribosomes, the higher need for proteins can be fulfilled by an increase in the efficiency of their synthesis<sup>39</sup>.

Based on these results and a multitude of different sources, including our amino acid composition measurements, a new *P. putida* specific biomass equation was created. The differences between the new and old biomass equation were relatively small, showing that the biomass compositions of *P. putida* and *E. coli* do not differ significantly. This supports the assumption made in many reconstruction efforts that *E. coli* biomass composition approximates well that of other gram-negative bacteria when grown at the same  $D$ . The protein composition is comparable to that determined by Sohn *et al.*<sup>42</sup>. On the contrary, the peptidoglycan concentration reached 22.7% of the biomass weight in the macro molecular biomass composition. This concentration was surprisingly high as the sum of the fractions exceeded 100%. Of the determined growth related factors, the specific glucose uptake rate increased linearly with the  $D$  when the culture was glucose-limited. This is in agreement with the  $Y_{x/s}/m_s$  model of Pirt<sup>22</sup>.  $Y_{x/s}^{max}$  and  $m_s$  were used to update the values of GAM and NGAM in the model. In contrast to the biomass composition, the new values differed substantially from the old ones. Particularly the  $Y_{x/s}^{max}$  was significantly lower and, consequently, the GAM higher, than assumed before. This means that the energy required for assembly of a cell of *P. putida* is much higher than in *E. coli*, which GAM value was used in the original version of the model. This resulted in an overall higher maintenance leading to higher costs of biotechnological processes. On the other hand even at a  $D$  of  $0.49\text{ h}^{-1}$ , no overflow metabolism was observed, i.e. no by-products (e.g. acetate) were accumulated. The opposite is the case for many organisms at higher  $\mu$  and is a result of limitations in the TCA cycle or respiratory NADH turnover<sup>10,43,44</sup>. For example, in *E. coli* cultures at  $D$  above  $0.4\text{ h}^{-1}$  acetate accumulates in the medium<sup>43</sup>. The lack of overflow metabolism is of great importance as it points out the capacity of *P. putida* KT2440 as biocatalyst. The ability to generate sufficient energy and the availability of NADH and NAD<sup>+</sup> are of importance for applications of a strain in biocatalysis, especially for a cofactor dependent conversion and the primary export of the product out of the cell. These results confirm earlier presented data that *P. putida* can meet high energy demands<sup>45</sup>. After implementing the new biomass equation and the new values of GAM and NGAM the model was revalidated using <sup>13</sup>C-flux measurement (used also for the validation of the original model). When looking at the minimum FVA distances these changes did cause an improvement of the model simulations. Interesting to see was that the minimum FVA distance did not decrease anymore, even when the maximum FVA distance did after restricting certain fluxes. Possibly the best agreement was reached within limitations of constraint-based modeling. Given the fairly stable macro-molecular composition in the measured  $\mu$  range it can be assumed that the flux distribution does not significantly change in *P. putida* KT2440 when the growth rate varies. This is relevant for the phenotype in case the strain is subjected to gene deletion. The experimental data used for validation encompass only a small part of the metabolic network. Consequently, the validation does not cover metabolic pathways outside the central metabolism.

The changes in the model influenced also its predictions for double mutations that increase the production of Acetyl-CoA. In all cases the values predicted with the updated model were higher than the original ones, while  $Y_{x/s}$  were lower. As the higher GAM value is generally responsible for the lower growth yields of the updated model, it seems that the increase of GAM caused also the increased predicted AcCoA-flux. In one case a different pair of genes was suggested to be mutated. This confirms the importance of knowledge of biomass composition and maintenance values for the predictive force of constraint-based models.

The validation with transcriptomic data showed good agreement between the revalidated model and the experimental results. More than 90% of genes identified by the transcriptomics as potentially not expressed were involved in the catalysis of reactions not required for growth. For the reactions catalyzed by proteins of which zero-flux was predicted, only a limited number of genes were expressed. A lot of them are involved in the transport of amino acids, and the synthesis of co-factors, indicating that the bacterium tries to reduce the nutrient limitation. In general, with transcriptomic assays reproducible results are obtained<sup>46</sup>. Yet, the translation of the expression values into fluxes and *vice versa* needs to be done with care. For example, some genes might be expressed constitutively, consequently they do not always correspond with metabolic fluxes. Also there is no linear correspondence between the abundance of the mRNA transcript, as measured by transcriptomics, and the activity of the enzyme. This is due to a multitude of factors that influence the efficiency of protein production from mRNA as post-transcriptional regulation<sup>47</sup>.

Summarizing, by measuring carefully key biological parameters, this work enabled to explain missing links and inconsistencies in the previously developed model, and improved considerably its accuracy, providing thereby a more solid basis for its use in designing biotechnological metabolic processes.

### **Acknowledgements**

We thank Rui Marinho for his help with the continuous fermentations, Bianka Karge and Agata Bielecka for their help with the experimental analysis, María Suárez-Diez for reviewing the article, and Christel Kakoschke and Dr. Victor Wray for NMR data.

## References

1. de Bont JAM. 1998. Solvent-tolerant bacteria in biocatalysis. *Tibtech* 16:493-499.
2. Ramos JL, Duque E, Gallegos MT, Godoy P, Ramos-Gonzalez MI, Rojas A, Teran W, Segura A. 2002. Mechanisms of solvent tolerance in gram-negative bacteria. *Annu Rev Microbiol* 56:743-768.
3. Wackett LP. 2003. *P. putida*-a versatile biocatalyst. *Nat. Biotechnol* 21:136-138.
4. Martins dos Santos VAP, Heim S, Strätz M, Timmis KN. 2004. Insights into the genomic basis of niche specificity of *Pseudomonas putida* strain KT2440. *Environ Microbiol* 6:1264-1286
5. Ramos JL, Wasserfallen A, Rose K, Timmis KN. 1987. Redesigning metabolic routes: manipulation of TOL plasmid pathway for catabolism of alkylbenzoates. *Science* 235:593-596.
6. Nelson KE, Weinel C, Paulsen IT, Dodson RJ, Hilbert H, Martins dos Santos VAP, Fouts DE, Gill SR, Pop M, Holmes M, Brinkac L, Beanan M, DeBoy RT, Daugherty S, Kolonay J, Madupu R, Nelson W, White O, Peterson J, Khouri H, Hance I, Chris Lee P, Holtzapple E, Scanlan D, Tran K, Moazzez A, Utterback T, Rizzo M, Lee K, Kosack D, Moestl D, Wedler H, Lauber J, Stjepandic D, Hoheisel J, Straetz M, Heim S, Kiewitz C, Eisen JA, Timmis KN, Düsterhöft A, Tümmler B, and Fraser CM. 2002. Complete genome sequence and comparative analysis of the metabolically versatile *Pseudomonas putida* KT2440. *Environ Microbiol* 4:799-808.
7. Puchalka J, Oberhardt MA, Godinho M, Bielecka A, Regenhardt D, Timmis KN, Papin JA, Martins dos Santos VA. 2008. Genome-scale reconstruction and analysis of the *Pseudomonas putida* KT2440 metabolic network facilitates applications in biotechnology. *PLoS Comput Biol* 4.
8. Reed JL, Vo TD, Schilling CH, Palsson BO. 2003. An expanded genome-scale model of *Escherichia coli* K-12 (iJR904 GSM/GPR). *Genome Biol* 4.
9. Varma A, Palsson BO. 1994. Stoichiometric flux balance models quantitatively predict growth and metabolic by-product secretion in wild-type *Escherichia coli* W3110. *Appl Environ Microbiol* 60:3724-3731.
10. Hanegraaf PP, Muller EB. 2001. The dynamics of the macromolecular composition of biomass. *J Theor Biol* 212:237-251.
11. Lange HC, Heijnen JJ. 2001. Statistical reconciliation of the elemental and molecular biomass composition of *Saccharomyces cerevisiae*. *Biotechnol Bioeng* 75:334-344.
12. Pramanik J, Keasling JD. 1997. Stoichiometric model of *Escherichia coli* metabolism: Incorporation of growth-rate dependent biomass composition and mechanistic energy requirements. *Biotechnology and Bioengineering* 56:398-421.
13. Pramanik J, Keasling JD. 1998. Effect of *Escherichia coli* biomass composition on central metabolic fluxes predicted by a stoichiometric model. *Biotechnology and Bioengineering* 60:230-238.
14. Fuhrer T, Fischer E, Sauer U. 2005. Experimental identification and quantification of glucose metabolism in seven bacterial species. *J Bacteriol* 187:1581-1590.
15. vanDuuren JBJH, Wijte D, Leprince A, Karge B, Puchalka J, Wery J, Martins dos Santos VAP, Eggink G, Mars AE. Generation of a *catR* deficient mutant of *P. putida* KT2440 that produces *cis*, *cis*-muconate from benzoate at high rate and yield. *J Biotechnol*. 2011; in press.
16. Hartmans S, Smits JP, van der Werf MJ, Volkering F, de Bont JA. 1989. Metabolism of Styrene Oxide and 2-Phenylethanol in the Styrene-Degrading Xanthobacter Strain 124X. *Appl Environ Microbiol* 55:2850-2855.
17. del Castillo T, Ramos JL, Rodríguez-Herva JJ, Fuhrer T, Sauer U, Duque E. 2007. Convergent peripheral pathways catalyze initial glucose catabolism in *Pseudomonas putida*: genomic and flux analysis. *J Bacteriol* 189:5142-5152.
18. Latrach Tlemçani L, Corroler D, Barillier D, Mosrati R. 2008. Physiological states and energetic adaptation during growth of *Pseudomonas putida* mt-2 on glucose. *Arch Microbiol* 190:141-150.
19. Benthin S, Nielsen J, Villadsen J. 1994. Galactose Expulsion during Lactose Metabolism in *Lactococcus lactis* subsp. *cremoris* FD1 Due to Dephosphorylation of Intracellular Galactose 6-Phosphate. *Appl Environ Microbiol* 60:1254-1259.
20. Herbert D, Phipps PJ, Tempest DW. 1965. The chemostat: design and instrumentation. *Lab Pract* 14:1150-1161.
21. Izard J, Limberger RJ. 2003. Rapid screening method for quantitation of bacterial cell lipids from whole cells. *J Microbiol Methods* 55:411-418.

22. Pirt SJ. 1982. Maintenance energy: a general model for energy-limited and energy-sufficient growth. *Arch Microbiol* 133:300-302.
23. Mizuno T, Kageyama M. 1978. Separation and characterization of the outer membrane of *Pseudomonas aeruginosa*. *J Biochem* 84: 179-191.
24. Miura T, Mizushima S. 1968. Separation by density gradient centrifugation of two types of membranes from speroplast membrane of *Escherichia coli* K12. *Biochim Biophys Acta* 150:159.
25. Bremer H, Dennis P. 1996. Modulation of chemical composition and other parameters of the cell by growth rate. In: Neidhardt F, editor. *Escherichia coli* and *Salmonella*: Cellular and Molecular Biology: ASM Press. pp. 1553–1569.
26. Stead DE. 1992. Grouping of plant-pathogenic and some other *Pseudomonas* spp. by using cellular fatty acid profiles. *Int J Syst Bacteriol* 42:281-295.
27. Forsberg CW, Ward JB. 1972. *N*-acetylmuramyl-*L*-alanine amidase of *Bacillus licheniformis* and its L-form. *J Bacteriol* 110:878-888.
28. Kauffman KJ, Prakash P, Edwards JS. 2003. Advances in flux balance analysis. *Curr Opin Biotechnol* 14: 491-496.
29. Mahadevan R, Schilling CH. 2003. The effects of alternate optimal solutions in constraint-based genome-scale metabolic models. *Metab Eng.* 5:264-276.
30. Reed JL, Palsson BØ. 2003. Thirteen years of building constraint-based *in silico* models of *Escherichia coli*. *J Bacteriol* 185:2692-2699.
31. Teusink B, Wiersma A, Molenaar D, Francke C, de Vos WM, Siezen RJ, Smid EJ. 2006. Analysis of growth of *Lactobacillus plantarum* WCFS1 on a complex medium using a genome-scale metabolic model. *J Biol Chem* 281:40041-40048.
32. Burgard AP, Pharkya P, Maranas CD. 2003. Optknock: a bilevel programming framework for identifying gene knockout strategies for microbial strain optimization. *Biotechnol Bioeng.* 84:647-657.
33. Martin E, MacLeod R. 1971. Isolation and chemical composition of the cytoplasmic membrane of a gram-negative bacterium. *J Bacteriol* 105:1160-1167.
34. Passman FJ, Jones GE. 1985. Preparation and analysis of *Pseudomonas putida* cells for elemental composition. *Geomicrobiol J* 4:191-206.
35. Monod J. 1950. La technique de la culture continue, théorie et applications. *Annales de Institute Pasteur Paris* 79:390-410.
36. Mason C, Hamer G, Bryers J. 1986. The death and lysis of microorganisms in environmental processes. *FEMS microbiol lett* 39:373-401.
37. Hazer B, Steinbüchel A. 2007. Increased diversification of polyhydroxyalkanoates by modification reactions for industrial and medical applications. *Appl Microbiol Biotechnol.* 74:1-12.
38. Klinke S, Dauner M, Scott G, Kessler B, Witholt B. 2000. Inactivation of isocitrate lyase leads to increased production of medium-chain-length poly(3-hydroxyalkanoates) in *Pseudomonas putida*. *Appl Environ Microbiol.* 66:909-913.
39. Du Preez JC, Lategan PM, Toerien DF. 1984. Influence of the growth rate on the macromolecular composition of *Acinetobacter calcoaceticus* in carbon-limited chemostat culture. *FEMS Microbiol Lett* 23:71-75.
40. Baart GJ, Willemsen M, Khatami E, de Haan A, Zomer B, Beuvery EC, Tramper J, Martens DE. 2008. Modeling *Neisseria meningitidis* B metabolism at different specific growth rates. *Biotechnol Bioeng.* 101:1022-1035.
41. Kjeldgaard N, Gausing K. 1974. Regulation of biosynthesis of ribosomes. In: Nomura M, Tissieres A, Lengyel P, editors. *Ribosomes*. New York: Cold Spring Harbor. pp. 369-392.
42. Sohn SB, Kim TY, Park JM, Lee SY. 2010. *In silico* genome-scale metabolic analysis of *Pseudomonas putida* KT2440 for polyhydroxyalkanoate synthesis, degradation of aromatics and anaerobic survival. *Biotechnol J* 5:739-50.
43. Kayser A, Weber J, Hecht V, Rinas U. 2005. Metabolic flux analysis of *Escherichia coli* in glucose-limited continuous culture. I. Growth-rate-dependent metabolic efficiency at steady state. *Microbiology.* 151:693-706.
44. Varma A, Boesch BW, Palsson BO. 1993. Stoichiometric interpretation of *Escherichia coli* glucose catabolism under various oxygenation rates. *Appl Environ Microbiol.* 59:2465-2473
45. Blank LM, Iondis G, Ebert BE, Bühler B, Schmid A. 2008. Metabolic response of *pseudomonas putida* during redox biocatalysis in the presence of a second octanol phase. *Febs j* 275:5173-5190.

46. MAQC Consortium, Shi L, Reid LH, Jones WD, Shippy R, Warrington JA, Baker SC, Collins PJ, de Longueville F, Kawasaki ES, Lee KY, Luo Y, Sun YA, Willey JC, Setterquist RA, Fischer GM, Tong W, Dragan YP, Dix DJ, Frueh FW, Goodsaid FM, Herman D, Jensen RV, Johnson CD, Lobenhofer EK, Puri RK, Schrf U, Thierry-Mieg J, Wang C, Wilson M, Wolber PK, Zhang L, Amur S, Bao W, Barbacioru CC, Lucas AB, Bertholet V, Boysen C, Bromley B, Brown D, Brunner A, Canales R, Cao XM, Cebula TA, Chen JJ, Cheng J, Chu TM, Chudin E, Corson J, Corton JC, Croner LJ, Davies C, Davison TS, Delenstarr G, Deng X, Dorris D, Eklund AC, Fan XH, Fang H, Fulmer-Smentek S, Fuscoe JC, Gallagher K, Ge W, Guo L, Guo X, Hager J, Haje PK, Han J, Han T, Harbottle HC, Harris SC, Hatchwell E, Hauser CA, Hester S, Hong H, Hurban P, Jackson SA, Ji H, Knight CR, Kuo WP, LeClerc JE, Levy S, Li QZ, Liu C, Liu Y, Lombardi MJ, Ma Y, Magnuson SR, Maqsoodi B, McDaniel T, Mei N, Myklebost O, Ning B, Novoradovskaya N, Orr MS, Osborn TW, Papallo A, Patterson TA, Perkins RG, Peters EH, Peterson R, Philips KL, Pine PS, Puztai L, Qian F, Ren H, Rosen M, Rosenzweig BA, Samaha RR, Schena M, Schroth GP, Shchegrova S, Smith DD, Staedtler F, Su Z, Sun H, Szallasi Z, Tezak Z, Thierry-Mieg D, Thompson KL, Tikhonova I, Turpaz Y, Vallanat B, Van C, Walker SJ, Wang SJ, Wang Y, Wolfinger R, Wong A, Wu J, Xiao C, Xie Q, Xu J, Yang W, Zhang L, Zhong S, Zong Y, Slikker W Jr. 2006. The MicroArray Quality Control (MAQC) project shows inter- and intraplatform reproducibility of gene expression measurements. *Nat Biotechnol* 24:1151-1161.
47. Rosen R, Ron EZ. 2002. Proteome analysis in the study of the bacterial heat-shock response. *Mass. Spectrom Rev* 21:244-265.

## Supplementary Material

### Modifications to the original iJP815 model:

1. Addition of the following reactions responsible for the synthesis of fatty acids which the original biomass equation did not account for:
  - a. S-2-hydroxy-lauroyl-ACP synthase:  
(2) Dodecanoyl-ACP (n-C12:0ACP) + Oxygen --> (2) 2-hydroxydodecanoyl-[acyl-carrier protein]
  - b. cis-9,10-methylene hexadecanoyl-ACP synthase:  
Hexadecanoyl-ACP (n-C16:1ACP) + S-Adenosyl-L-methionine --> S-Adenosyl-L-homocysteine + cis-9,10-methylene hexadecanoyl-ACP
2. Modification of the stoichiometry of the phosphatidate synthase reaction to account for the new composition of the acyl residues in phospholipids:  
*old:* (2) Myristoyl-ACP (n-C14:0ACP) + (7) cis-9-hexadecanoyl-ACP + (5) cis-7-tetradecanoyl-ACP + (36) Palmitoyl-ACP (n-C16:0ACP) + (50) sn-Glycerol 3-phosphate + (50) cis-11-octadecanoyl-ACP --> (100) acyl carrier protein + phosphatidate (E.coli) \*\*  
*new:* (7) (R)-3-Hydroxydecanoyl-[acyl-carrier protein] + (26) cis-9-hexadecanoyl-ACP + (6) cis-9,10-methylene hexadecanoyl-ACP + (50) sn-Glycerol 3-phosphate + (3) Dodecanoyl-ACP (n-C12:0ACP) + (6) (R)-3-Hydroxydodecanoyl-[acyl-carrier protein] + (29) Palmitoyl-ACP (n-C16:0ACP) + (6) 2-hydroxydodecanoyl-[acyl-carrier protein] + (17) cis-11-octadecanoyl-ACP --> Phosphatidic acid (PPU) + (100) acyl carrier protein
3. Modification of the elemental composition of the following phospholipid compounds to account for the new composition of the acyl residues in phospholipids:
  - a. phosphatidate, old: C1836H3398O400P50, new: C1682H3116O413P50
  - b. phosphatidylglycerol, old: C1986H3748O500P50, new: C1832H3466O513P50
  - c. phosphatidylserine, old: C1986H3698N500O500P50, new: C1832H3416N500O513P50
  - d. CDP-diacylglycerol, old: C2286H3998N150O750P100, new: C2132H3716N150O763P100
  - e. cardiolipin, old: C3822H7096O850P100, new: C3514H6532O876P100
  - f. phosphatidylglycerol phosphate, old: C1986H3698O650P100, new: C1832H3416O663P100
4. Substitution of multi-step mechanism of the following enzymes with a single-step lumped reaction:
  - a. Pyruvate dehydrogenase
  - b. 2-oxoglutarate dehydrogenase
  - c. 2-oxoadipate dehydrogenase
  - d. Acetolactate synthase
  - e. (S)-2-Aceto-2-hydroxybutanoate synthase

This change was made to separate better the fluxes between these multi-step reactions, as some of the sub-steps overlap between them. This influences the computation of the FVA-distances. Since all these reactions are catalyzed by enzyme complexes, it can be assumed that the

intermediates are not exchanged between different reactions and the approximation by lumped reactions is a correct one.

### **Computation of FVA-distances:**

The following reactions which fluxes were reported by Fuhrer et al. were not included in the computation of FVA-distances:

1.  $\text{GLC} \rightarrow \text{GCLi}$ ,  $\text{GLCi} + \text{ATP} \rightarrow \text{G6P}$  –  $^{13}\text{C}$ -flux measurements are not able to distinct between the three possible glucose uptake routes in *P. putida*. The flux values of these reactions were not predicted but assumed. Therefore they should not be used when comparing predictions.
2.  $\text{MAL} \rightarrow \text{OAA} + \text{NADH}$  – this reaction is a part of a closed loop in the iJP815 model. The FVA predicts in such a case infinite fluxes.
3.  $\text{OAA} + \text{ATP} \rightarrow \text{PEP} + \text{CO}_2$  – this reaction was not included in the iJP815 model, as no evidence for its operation could have been found.

**Supplementary Table 2.** Genes predicted essential by the iJP815 model for which transcriptomics data suggest a lack of expression. Colors mark distinctive groups discussed in the text.

Gene	# Absent	# Present	Mean Exp	Corresponding reaction	Pathway
PP0237	0	2	6.74	Sulfate transport via ABC system	ABC transporters
PP0239	4	0	6.33	Sulfate transport via ABC system	ABC transporters
PP0240	4	0	7.48	Sulfate transport via ABC system	ABC transporters
PP0293	0	2	7.70	Imidazole-glycerol-3-phosphate synthase	Histidine metabolism
PP0514	2	0	8.29	5-amino-6-(5-phosphoribosylamino)uracil reductase [EC: 1.1.1.193]	Riboflavin metabolism
PP0530	4	0	7.14	3,4 Dihydroxy-2-butanone-4-phosphate synthase	Riboflavin metabolism
PP0631	1	1	8.06	ATP:dephospho-CoA 3'-phosphotransferase [EC: 2.7.1.24]	Pantothenate and CoA biosynthesis
PP0786	4	0	8.96	thioredoxin reductase	Pyrimidine metabolism
PP0860	1	2	6.73	sulfite reductase [EC: 1.8.1.2]	Sulfur metabolism
PP1338	1	2	8.63	UDP-N-acetylmuramoyl-L-alanine synthetase [EC: 6.3.2.8]	D-Glutamine and D-glutamate metabolism
PP1525	2	2	7.78	N-Succinyl-L-2,6-diaminoheptanedioate amidohydrolase [EC: 3.5.1.18]	Lysine biosynthesis
PP1588	1	2	7.92	N-Succinyl-L-2,6-diaminoheptanedioate:2-ocoglytarateamino-transferase [EC: 2.6.1.17]	Lysine biosynthesis
PP1601	3	1	8.57	UDP-3-O-(3-hydroxymyristoyl)glucosamine acyltransferase	Lipopolysaccharide biosynthesis
PP1603	1	2	8.24	UDP-N-acetylglucosamine acyltransferase	Lipopolysaccharide biosynthesis
PP1750	4	0	7.13	Pyridoxamine:oxygen oxidoreductase (deaminating) [EC: 6.3.5.4]	Alanine and aspartate metabolism, Nitrogen metabolism
PP1815	4	0	7.45	Orotidine-5'-phosphate carboxy-lyase [EC: 4.1.1.23]	Pyrimidine metabolism
PP1900	4	0	8.44	Tetraacyldisaccharide 4'kinase [EC: 2.7.1.130]	Lipopolysaccharide biosynthesis
PP1902	0	0	7.89	CTP:3-deoxy-D-manno-octulosonate cytidyltransferase [EC: 2.7.7.38]	Lipopolysaccharide biosynthesis
PP2012	3	1	7.88	ATP:NAD <sup>+</sup> 2'-phosphotransferase [EC: 2.7.1.23]	Nicotinate and nicotinamide metabolism
PP2329	4	0	7.10	Chorismate:L-glutamine amido-ligase [EC: 6.3.5.8]	Folate biosynthesis
PP2458	4	0	7.71	ATP:D-ribose 5-phosphotransferase [EC: 2.7.1.15]	Pentose phosphate pathway
PP2460	4	0	8.27	Adenosine ribohydrolase [EC: 3.2.2.1]	Purine metabolism, Nicotinate and nicotinamide metabolism
PP2902	4	0	7.86	UDP-2,3-bis(3-hydroxytetradecanoyl)glucosamine diphosphatase	Lipopolysaccharide biosynthesis
PP4266	4	0	7.72	AMP:pyrophosphate phosphoribosyltransferase [EC: 2.4.2.8]	Purine metabolism
PP4822	0	2	8.54	IMP 1,2-hydrolase (decyclizing) [EC: 3.5.4.10]	Purine metabolism, One carbon pool by folate
PP4869	0	1	8.96	Deamido-NAD <sup>+</sup> :L-glutamine amido-ligase (AMP-forming) [EC: 6.3.5.1]	Nicotinate and nicotinamide metabolism
PP4928	0	4	6.66	3-deoxy-D-manno-octulosonic acid transferase	Lipopolysaccharide biosynthesis
PP5097	2	2	8.20	Homoserine O-acetyltransferase [EC: 2.3.1.31]	Methionine metabolism, Sulfur metabolism
PP5132	4	0	7.47	5,6,7,8-Tetrahydrofolate:NADP <sup>+</sup> oxidoreductase [EC: 1.5.1.3]	One carbon pool by folate, Folate biosynthesis
PP5291	3	1	7.55	Orotidine-5'-phosphate:pyrophosphate phosphoribosyltransferase [EC: 2.4.2.10]	Pyrimidine metabolism
PP5296	1	1	8.63	ATP:(d)GMP phosphotransferase [EC: 2.7.4.8]	Purine metabolism
PP5409	4	0	8.31	L-Glutamine:D-fructose-6-phosphate aminotransferase (hexoseisomerizing) [EC: 2.6.1.16]	Glutamate metabolism, Aminosugars metabolism

**Supplementary Table 3.** Genes predicted to be involved in the catalysis of reactions with predicted zero flux, for which the transcriptomics data suggest high expression. Colors mark distinctive groups discussed in the text.

Gene	Expression value	Gene Annotation	Pathway
PP0188	9.28	uroporphyrin-III C-methyltransferase, putative	Porphyrin and chlorophyll metabolism
PP0226	9.01	cysteine ABC transporter, permease protein, putative	ABC transporters
PP0227	9.74	cysteine ABC transporter, periplasmic cysteine-binding protein, putative	ABC transporters
PP0362	9.99	biotin synthetase	Biotin metabolism
PP0363	9.27	8-amino-7-oxononanoate synthase	Biotin metabolism
PP0402	9.05	pyridoxal phosphate biosynthetic protein PdxA	Vitamin B6 metabolism
PP0517	9.63	riboflavin synthase, beta subunit	Riboflavin metabolism
PP0543	9.23	ethanolamine ammonia-lyase, heavy subunit	Glycerophospholipid metabolism
PP0548	9.07	3-octaprenyl-4-hydroxybenzoate carboxy-lyase	Ubiquinone and menaquinone biosynthesis
PP0723	9.76	4-diphosphocytidyl-2C-methyl-D-erythritol kinase	Biosynthesis of steroids
PP0853	9.12	1-hydroxy-2-methyl-2-(E)-butenyl 4-diphosphate synthase	Biosynthesis of steroids
PP0897	9.60	fumarate hydratase, class I	Citrate cycle (TCA cycle)
PP0964	9.79	UDP-N-acetylglucosamine 1-carboxyvinyltransferase	Aminosugars metabolism
PP1031	9.58	inosine-5-monophosphate dehydrogenase	Purine metabolism
PP1037	9.18	phosphoribosylformylglycinamide synthase	Purine metabolism
PP1068	9.59	amino acid ABC transporter, ATP-binding protein	ABC transporters
PP1070	9.28	amino acid ABC transporter, permease protein	ABC transporters
PP1071	12.24	amino acid ABC transporter, periplasmic amino acid-binding protein	ABC transporters
PP1129	9.38	pyridoxamine-phosphate oxidase	Vitamin B6 metabolism
PP1137	9.08	branched-chain amino acid ABC transporter, ATP-binding protein	ABC transporters
PP1138	9.79	branched-chain amino acid ABC transporter, ATP-binding protein	ABC transporters
PP1139	9.11	high-affinity branched-chain amino acid transport protein	ABC transporters
PP1140	9.31	branched-chain amino acid ABC transporter, permease protein	ABC transporters
PP1141	11.79	branched-chain amino acid ABC transporter, periplasmic amino acid-binding protein	ABC transporters
PP1179	9.34	ribonucleoside reductase, alpha subunit	Purine metabolism
PP1240	9.84	phosphoribosylaminoimidazole-succinocarboxamide synthase	Purine metabolism
PP1303	10.16	sulfate adenylyltransferase, subunit 2	Purine metabolism
PP1304	9.53	sulfate adenylyltransferase, subunit 1/adenylylsulfate kinase	Purine metabolism, Sulfur metabolism
PP1343	9.44	UDP-3-0-acyl N-acetylglucosamine deacetylase	Lipopolysaccharide biosynthesis
PP1348	9.05	MutT/nudix family protein/thiamine-phosphate pyrophosphorylase, putative	#N/A
PP1755	9.24	fumarate hydratase, class II	Citrate cycle (TCA cycle)
PP1771	9.51	cytidylate kinase	Pyrimidine metabolism
PP1783	9.33	glucose-1-phosphate thymidyltransferase	Nucleotide sugars metabolism
PP1784	9.02	dTDP-4-dehydrorhamnose reductase	Nucleotide sugars metabolism
PP1799	10.31	GDP-mannose 4,6 dehydratase	Fructose and mannose metabolism
PP1995	9.57	N-(5'-phosphoribosyl)anthranilate isomerase	Phenylalanine, tyrosine and tryptophan biosynthesis
PP2000	9.21	Amidophosphoribosyltransferase	Purine metabolism, Glutamate metabolism
PP2335	9.31	methylcitrate synthase, putative	Propanoate metabolism
PP2371	9.71	sulphite reductase hemoprotein, beta subunit	Sulfur metabolism
PP3511	9.66	branched-chain amino acid aminotransferase	Valine, leucine and isoleucine degradation, Valine, leucine and isoleucine biosynthesis, Pantothenate and CoA biosynthesis
PP3755	9.07	3-hydroxybutyryl-CoA dehydrogenase	Benzoate degradation via CoA ligation, Butanoate metabolism
PP3775	12.26	sarcosine oxidase, putative	Glycine, serine and threonine metabolism
PP3821	10.25	UTP-glucose-1-phosphate uridylyltransferase	Pentose and glucuronate interconversions, Galactose metabolism, Starch and sucrose metabolism
PP3839	9.84	alcohol dehydrogenase, zinc-containing	Glycolysis / Gluconeogenesis
PP4034	12.00	N-carbamoyl-beta-alanine amidohydrolase, putative	Pyrimidine metabolism, Pantothenate and CoA biosynthesis,

			beta-Alanine metabolism
PP4549	9.63	long-chain-fatty-acid-CoA ligase	Fatty acid metabolism
PP4571	9.18	cysteine synthase A	Cysteine metabolism, Sulfur metabolism
PP4863	9.52	branched-chain amino acid ABC transporter, ATP-binding protein	ABC transporters
PP4864	9.52	branched-chain amino acid ABC transporter, ATP-binding protein	ABC transporters
PP4865	9.10	branched-chain amino acid ABC transporter, permease protein	ABC transporters
PP4866	9.57	branched-chain amino acid ABC transporter, permease protein	ABC transporters
PP4867	11.38	branched-chain amino acid ABC transporter, periplasmic amino acid-binding protein	ABC transporters
PP4922	9.22	thiamin biosynthesis protein ThiC	Thiamine metabolism
PP4967	11.28	S-adenosylmethionine synthetase	Methionine metabolism
PP4977	10.29	5,10-methylenetetrahydrofolate reductase	One carbon pool by folate, Methane metabolism



# Chapter 5

## **A limited LCA of bio-adipic acid: manufacturing the nylon-6,6 precursor adipic acid using the benzoic acid degradation pathway from different feedstocks**

**Abstract:** A limited life cycle assessment (LCA) was performed on a combined biological and chemical process for the production of adipic acid, which was compared to the traditional petrochemical process. The LCA comprises the biological conversion of the aromatic feedstocks benzoic acid, impure aromatics, toluene or phenol from lignin to *cis, cis*-muconic acid, which is subsequently converted to adipic acid through hydrogenation. Apart from the impact of usage of petrochemical and biomass-based feedstocks, the environmental impact of the final concentration of *cis, cis*-muconic acid in the fermentation broth was studied using 1.85% and 4.26% *cis, cis*-muconic acid. The LCA focused on the cumulative energy demand (CED), cumulative exergy demand (CExD) and the CO<sub>2</sub> equivalent (CO<sub>2</sub>eq) emission, with CO<sub>2</sub> and N<sub>2</sub>O measured separately. The highest calculated reduction potential of CED and CExD were achieved using phenol, which reduced the CED by 29% and 57% with 1.85% and 4.26% *cis, cis*-muconic acid, respectively. A decrease in the CO<sub>2</sub>eq emission was especially achieved when the N<sub>2</sub>O emission in the combined biological and chemical process was restricted. At 4.26% *cis, cis*-muconic acid, the different carbon backbone feedstocks contributed to an optimized reduction of CO<sub>2</sub>eq emissions ranging from 14.0 to 17.4ton CO<sub>2</sub>eq/ton adipic acid. The bulk of the bioprocessing energy intensity is attributed to the hydrogenation reactor, which has a high environmental impact and a direct relationship with the product concentration in the broth.

**Keywords:** Adipic acid, Biotechnology, *cis, cis*-Muconic acid, Energy, Exergy, LCA

Published by Biotechnology and Bioengineering. 2011. 108:1298-1306. Co-authors: Brehmer B, Mars AE, Eggink G, Dos Santos VAP, Sanders JPM.

## Introduction

Ever since its discovery in the late 1930's, nylon-6,6 has been intrinsically linked to the production of adipic acid, being the main intermediate reactant. Adipic acid is a high volume bulk petrochemical commodity as is reflected in its low selling price, 1315 – 1385\$/ton (2008), 1120 – 1190\$/ton (2009) and high consumption volumes, 2.6 Mton worldwide (2006)<sup>1</sup>. Adipic acid has several commercial production route options, all of which originate from fossil fuels. The most common is the nitric acid oxidation of a cyclohexanol/cyclohexanone mixture derived from cyclohexane. Cyclohexane itself originates from naphtha benzene and nitric acid originates from ammonia, which in turn is most commonly produced from natural gas. N<sub>2</sub>O is a byproduct in the process of nitric acid oxidation<sup>2</sup>. Adipic acid is thus associated with a high fossil fuel energy demand and a high level of N<sub>2</sub>O greenhouse gas emission. The cumulative energy demand (CED), which includes the total fossil fuel feedstock cost and all subsequent process energy inputs, has been reported to be 104.2GJ/ton<sup>3</sup>. As a consequence of modern catalytic decomposition techniques and tail gas treatment, on average the current state-of-the-art will reduce the 301kg/ton N<sub>2</sub>O by 80%, which will be selected for comparison in this study<sup>4</sup>.

An alternative production route for adipic acid could occur via biological conversion of benzoic acid or other aromatics to *cis, cis*-muconic acid, which can be easily converted to adipic acid by hydrogenation under slightly elevated pressure (3.5bar) and electric potential for 3 hours<sup>5</sup>. Several bacteria have been described that convert benzoic acid to *cis, cis*-muconic acid<sup>6,7,8</sup>. Recently a derivative of *P. putida* KT2440 (*P. putida* KT2440-JD1), which can no longer use benzoic acid as a carbon source, but still co-metabolizes benzoic acid to *cis, cis*-muconic acid when grown on glucose was isolated<sup>9</sup>. *P. putida* KT2440 is a soil bacterium with a versatile metabolism. It is able to convert several aromatic compounds, such as derivatives of lignin proceeding from the recycling of plant derived material<sup>10</sup>. Furthermore, the genome has been sequenced, the strain is genetically accessible, and it is the first Gram-negative soil bacterium that was certified as a safety strain by the Recombinant DNA Advisory Committee<sup>11,12,13</sup>. In this respect, it has significant potential for biotechnological applications, particularly those involving bioremediation and biotransformation<sup>14</sup>. One of the most influential parameters in the life cycle performance of chemical production systems is the feedstock<sup>15</sup>. Various *P. putida* species have been described that can metabolize other aromatic compounds<sup>14,16,17,18</sup>. Since *P. putida* is genetically accessible, it is likely that *P. putida* KT2440-JD1 can be modified in such a way that it can convert the petrochemical feedstocks benzoic acid, toluene, and impure aromatics (e.g. collected from waste of the benzene, toluene, xylene (BTX) process), as well as phenol from the biomass-based feedstock lignin to *cis, cis*-muconic acid<sup>19</sup>.

*P. putida* KT2440-JD1 has the highest measured specific production rate of *cis, cis*-muconic acid<sup>1</sup>. The highest final concentration of *cis, cis*-muconic acid that has been achieved was 4.4% in a bioprocess with a fed-batch process using *Arthrobacter* sp.<sup>7</sup>. A final concentration of *cis, cis*-muconic acid of 1.85% with *P. putida* KT2440-JD1 during a small-scale pH-stat fed-batch process was reached. At this concentration, benzoic acid was only converted to the intermediate catechol; known to be toxic to cells<sup>20</sup>. It may be possible to optimize this conversion leading to a higher final concentration of *cis, cis*-muconic acid, because benzoic acid can be converted by *P. putida* KT2440-JD1 in the presence of up to 4.26% of *cis, cis*-muconic acid<sup>20</sup>.

In this study, the overall goal was to assess the possibility to reduce the environmental impact of the current petroleum-based adipic acid production by comparing different carbon backbone feedstocks (petrochemical and biomass-based) for the combined biological and chemical production of adipic acid using a limited life cycle assessment (LCA). Moreover, the environmental impact of an increase in the final concentration of *cis, cis*-muconic acid was studied at two final fermentation broth concentrations of 1.85% (option 1) and 4.26% (option 2). At 104.2GJ/ton, 60.2kgN<sub>2</sub>O/ton and 5.1tonCO<sub>2</sub>/ton there is a large potential to reduce the environmental impact of adipic acid production by employing bio-processing techniques based on aqueous solutions.

## Material and Methods

**Biological production of *cis, cis*-Muconic Acid.** *cis, cis*-Muconic acid has been produced by *P. putida* KT2440-JD1 in a small-scale pH-stat fed-batch process using benzoic acid as a feedstock<sup>20</sup>. The data rendered from this study were used in the limited LCA as a model process regarding the assessment of conditions of biological production systems.

**Release of N<sub>2</sub>O in the Petrochemical Industry.** Catalytic techniques to decompose N<sub>2</sub>O to elemental nitrogen and oxygen (an exothermic reaction) operate at elevated temperatures and can effectively reduce the overall N<sub>2</sub>O emission and if the decomposition of the tail gas is performed under adiabatic conditions the heat of the reaction will continue the decomposition to a total emissions reduction of 99.9%<sup>2</sup>. In these recently outfitted production plants the resulting emission of N<sub>2</sub>O can be as low as 0.3kg per ton of adipic acid<sup>4</sup>. On a worldwide scale, only an average of 80% N<sub>2</sub>O emission reduction is actually realized with these tail-gas abatement technologies. In this respect, the production of adipic acid is still associated with for more than 44.8Mton CO<sub>2</sub> equivalent (CO<sub>2</sub>eq) or about 60.2kg N<sub>2</sub>O emission per ton of adipic acid. This average will be used to denote the current state-of-the-art reduction potential in this study.

**LCA Goal and Scope.** The standard methodology of LCA based on the ISO14040 series for environmental management systems was followed to a great extent with the exception that only the CED and cumulative exergy demand (CExD) were documented with the CO<sub>2</sub>eq emission (CO<sub>2</sub> and N<sub>2</sub>O measured separately) as the only environmental considerations<sup>21</sup>. This specific setup of LCA was performed due to the interest of the study. The apparent environmental impact, namely the reduction of fossil fuel and greenhouse gas emissions of the compared production routes was to be assessed. Exergy, the quality of energy or maximum obtainable work, was mainly included to provide further depth in the energy efficiency of the processes and as an indication of future energy efficiency improvements. The cradle was set at the point of base fossil fuel delivery (naphtha, diesel, natural gas, etc.) including their respective extraction values. The grave was set at the factory gate for nylon-6,6 production, essentially the delivery point of a pure adipic acid. The boundary was effectively confined to the process. This particular LCA technique is called an exergetic life cycle assessment (or E-LCA), but is in essence a limited exergetic cradle-to-factory gate assessment.

**Data and System.** GaBi and its associated datasets were used to accumulate life cycle inventory (LCI) data<sup>22</sup>. It is vital to set realistic and comparable factory gates in the LCI. The carbon contained in feedstocks of naphtha products from the petrochemical route is not yet released into

the environment but is contained in the chemical end product. With this perspective, the analysis was partially taken beyond the factory gate and to the grave, when decades or centuries from now the nylon is presumably disintegrated or incinerated. Only at this stage will the petrochemical material feedstocks receive an extra emission charge, which was already incorporated according to common LCA practice. As the final products are identical, any other emissions associated with combustion would be the same and cancel each other out.

**Bioprocessing Demands.** Aspen<sup>+</sup> was used to calculate the internal process energy requirements of the experimental set-up. Figure 1 highlights the system, unit operations and input streams involved. Two final broth concentrations of *cis*, *cis*-muconic acid of 1.85% (option 1) and 4.26% (option 2) were studied. Several process considerations were made in light of the experimental bioreactor, hydrogen reactor, and the succeeding separation and product isolation techniques:

- “FERMENT” – Bioreactor: 30°C, 1bar and 51 hours residence time
- “HYDROGEN” – Hydrogenation reactor: 30°C, 3.5bar, 3h and electrically charged
- “EVAPORAT” – Evaporator: 100°C, 3.5bar to remove water
- “CONDENSE” – Condenser: 20°C, 1bar to recover a large portion of the evaporator duty
- “CRYSTAL” – Crystallizer: 50°C, 1bar to isolate product

The heat streams were based on a simple fuel boiler system that has a heating efficiency of 85% energy and 45% exergy<sup>23</sup>. The hydrogenation reactor is pressurized and electrically charged having an overall electric production efficiency mix of 45% energy and 35% exergy.

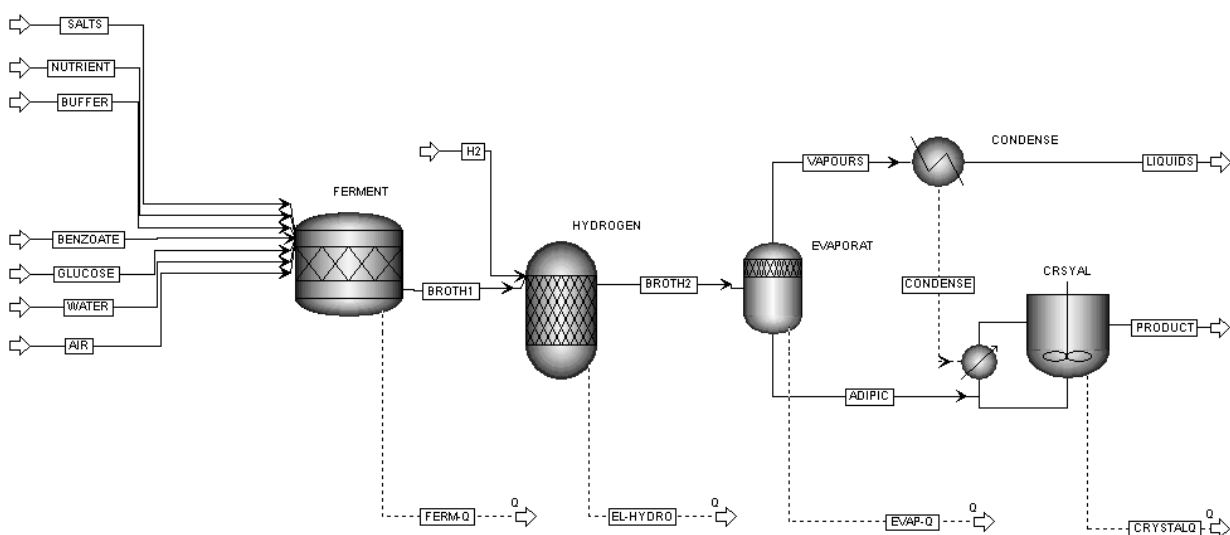


**Figure 1.** Aspen+ process flow diagram.

**Feed-Level Demands for Bacterial Growth.** For each mol *cis, cis*-muconic acid produced, 2 mol sodium hydroxide, and 2.28 mol (option 1) or 2.12 mol (option 2) hydrogen chloride were incorporated to maintain the fermentation broth at pH 7 during the fermentation and to acidify the fermentation broth to pH 2.5. Benzoic acid and *cis, cis*-muconic acid dissociate in water at pH 7 to the more soluble form of benzoate and *cis, cis*-muconate. The various streams flowing into the bioreactor need to be handled individually to assess their CED, CExD and emissions levels:

- Salts, nutrients and buffer: based on best available technology of the fertilizer industry<sup>24,25</sup>
  - Salts:  $\text{MgCl}_2 \cdot \text{H}_2\text{O}$  – dolomite limestone mining<sup>26,27</sup>
    - CED: 0.1GJ/ton, CExD: 0.2GJ/ton
    - $\text{CO}_2$ : 5.4kg/ton,  $\text{N}_2\text{O}$ : 0.0kg/ton
  - Nutrient:  $(\text{NH}_4)_2\text{SO}_4$  – ammonia and sulphuric acid production<sup>26,28</sup>
    - CED: 3.7GJ/ton, CExD: 4.1GJ/ton
    - $\text{CO}_2$ : 228.0kg/ton,  $\text{N}_2\text{O}$ : 208.0kg/ton
  - $\text{K}_2\text{HPO}_4$  – phosphorous acid and potassium oxide production<sup>26</sup>
    - CED: 1.8GJ/ton, CExD: 2.6GJ/ton
    - $\text{CO}_2$ : 117.0kg/ton,  $\text{N}_2\text{O}$ : 0.0kg/ton
  - Buffer:  $\text{NaH}_2\text{PO}_4 \cdot 2\text{H}_2\text{O}$  – mineral mining and phosphorous acid production<sup>26,27</sup>
    - CED: 0.5GJ/ton, CExD: 1.0GJ/ton
    - $\text{CO}_2$ : 33kg/ton,  $\text{N}_2\text{O}$ : 0.0kg/ton
- Sodium hydroxide<sup>4,22</sup>
  - CED: 24.8GJ/ton, CExD: 32.1GJ/ton
  - $\text{CO}_2$ : 1063.6kg/ton,  $\text{N}_2\text{O}$ : 0.0kg/ton
- Hydrogen chloride<sup>4,22</sup>
  - CED: 4.1GJ/ton, CExD: 4.5GJ/ton
  - $\text{CO}_2$ : 235.3kg/ton,  $\text{N}_2\text{O}$ : 6.8kg/ton

Glucose, like any biomass feedstock, is commonly believed to be carbon neutral consuming as much atmospheric  $\text{CO}_2$  as is emitted through its eventual decomposition (biological combustion). Nevertheless, because fossil fuels still are consumed, greenhouse gases are emitted throughout the agricultural cultivation and feedstock preparation process chain. Figure 2 is a simple process diagram of the steps involved in glucose production with the following results:

- Glucose: based on sucrose content of sugar beets for glucose production in Holland<sup>29,30</sup>
  - CED: 8.3GJ/ton, CExD: 8.7GJ/ton
  - $\text{CO}_2$ : 508.0kg/ton,  $\text{N}_2\text{O}$ : 23.3kg/ton

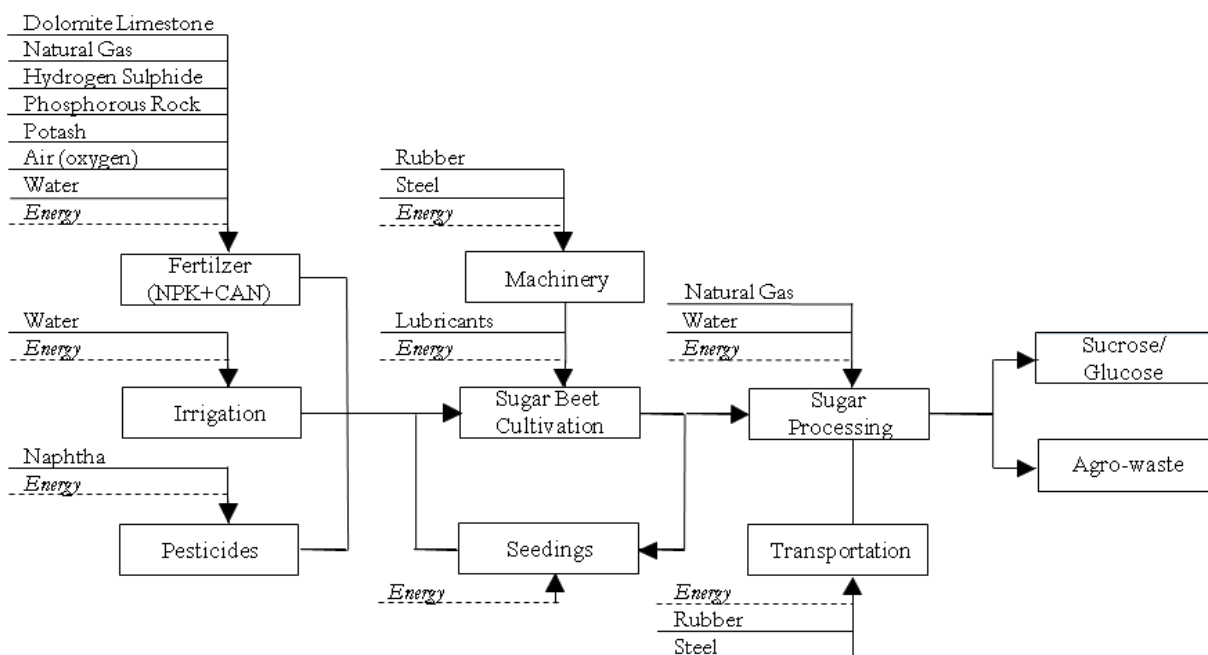


**Figure 2.** Simplified glucose production scheme.

**Bioreactor-Feedstock Demands.** Four different potential feedstocks were used in the LCA: benzoic acid, impure aromatics, and toluene are petrochemical based and phenol from lignin is biomass based. Since these feedstocks have different energetic and exergetic values and various sources of origin, along with the additional process energy needed to acquire the fraction, their CED, CExD and CO<sub>2</sub>eq emission values must be assessed separately.

To obtain benzoic acid and toluene, oil production and refinery are taken into account. Furthermore, as described the stoichiometric carbon content was included in the carbon dioxide emission calculations. An exergy ratio of 1.05 was adapted for the naphtha-based chemicals benzoic acid and toluene, which corresponds to the standard ratio of chemical energy/exergy of naphtha products.

Impure aromatics have the potential to be converted to *cis*, *cis*-muconic acid by *P. putida* KT2440-JD1. These compounds (e.g. benzoic acid) are primarily collected during the BTX purification process. Therefore impure aromatics are considered a major waste product, as they are an uneconomical residue from the distillation of crude oil. Being a waste product, no additional processing inputs are allocated to their production. Consequently, impure aromatics have a CED and CExD demand coupled directly to their chemical formation energy/exergy and no extra CO<sub>2</sub>eq emissions are considered.

Lignin is a special case being a highly complex molecule. Cleaving lignin via biological delignification (white rot fungi) will release countless different types of aromatic molecules. Due to the vast quantity and diversity of the molecules, economic delignification and isolation techniques are currently unavailable. In any case, phenol derived from lignin is present in higher concentrations and will receive its own theoretical energetic process burden based on its chemical formation energy/exergy and associated agricultural system. The potential feedstocks are:

Benzoic acid: derived from oxidized toluene<sup>3,23</sup>

- CED: 62.4GJ/ton, CExD: 65.5GJ/ton
- CO<sub>2</sub>: 3735.0kg/ton, N<sub>2</sub>O: trace ≈ 0.0kg/ton
- Impure aromatics: derived from an oil cracker (Internal calculations)
  - CED: 25.4GJ/ton, CExD: 27.4GJ/ton
  - CO<sub>2</sub>: 0.0kg/ton, N<sub>2</sub>O: 0.0kg/ton
- Toluene: derived from benzene<sup>3,17,23</sup>
  - CED: 56.4GJ/ton, CExD: 59.2GJ/ton
  - CO<sub>2</sub>: 4190.0kg/ton, N<sub>2</sub>O: trace ≈ 0.0kg/ton
- Phenol derived from lignin: derived from wheat stover grown under Dutch conditions<sup>26,29</sup>
  - CED: 11.2GJ/ton, CExD: 13.8GJ/ton
  - CO<sub>2</sub>: 682.0kg/ton, N<sub>2</sub>O: 3.9kg/ton

**Limitations.** For the conversion of benzoic acid to *cis, cis*-muconic acid no net consumption of co-factors like NADH are required, while for each mol toluene or phenol one mol NADH is produced or consumed, respectively. Hence the biomass yield (g dry cell weight (dcw)/g glucose) might increase with toluene and decrease with phenol. This hypothesis and its impact on the overall system dynamics were not taken into account. Furthermore, other aromatic feedstocks are also foreseeable, but were not assessed.

Apolar compounds such as phenol and toluene are generally not well soluble in water and often toxic to whole cells as they accumulate in the cytoplasmic membrane. As a consequence the membrane loses its integrity and increases its permeability<sup>31</sup>. Technical solutions to this problem are two-liquid-phase media, gas-phase biocatalysis and feeding under controlled conditions such as the pH-stat fed-batch process<sup>32</sup>. For the LCA, the pH-stat fed-batch process is the only biological production system considered.

Residual minerals can be separated from the product by (re-)crystallization from methanol<sup>7</sup>. This option and the impact on the overall system dynamics was however not taken into account.

## Calculations

**Bioreactor System.** In the small-scale pH-stat fed-batch process a molar production yield (mol *cis, cis*-muconic acid/mol benzoic acid) of 96% was achieved with *P. putida* KT2440-JD1<sup>20</sup>. This is further assumed for all four different feedstocks, as they are all similar aromatic compounds that can be converted to *cis, cis*-muconic acid.

**Energy and Emission.** Aspen<sup>+</sup> lists the resulting energy duties of the internal bioprocessing in terms of flows, i.e. GJ/h. Consequently, the bioprocessing demands in CED, CExD and CO<sub>2</sub>eq emission values per ton pure adipic acid can be calculated for both final broth concentrations of *cis, cis*-muconic acid and are presented in Table 1. The feed-level demands for growth, maintenance, and pH regulation are listed in Table 2 for the bioreactor at both final broth concentrations of *cis, cis*-muconic acid per ton pure adipic acid, which provide the basis for calculating the associated CED, CExD and CO<sub>2</sub>eq emission values. Hereby it is assumed that for option 2 the duration and

medium consumption is similar, independent of the different specific productivity and final concentration of *cis*, *cis*-muconic acid. Furthermore, for each of the four feedstocks based on the stoichiometric conversion rate and respective feed level per final product, the associated CED, CExD and CO<sub>2</sub>eq emission per ton pure adipic acid were calculated (Table 3). Figure 3 illustrates the resulting potential CED, CExD and CO<sub>2</sub>eq emissions induced for option 1 and 2 compared to the traditional petrochemical production route of adipic acid. As described, the greenhouse gas emissions are combined and expressed as the total CO<sub>2</sub>eq emission, but special consideration should be paid to the major reduction potential N<sub>2</sub>O.

**Table 1.** Bioprocessing demands.

Option 1	Aspen Symbol	System Demand and Emissions			
		CED*	CExD**	CO <sub>2</sub>	N <sub>2</sub> O
		GJ/ton	kg/ton		
Bioreactor	FERMENT	0.56	1.05	0.03	0.00
Hydrogenation reactor	HYDROGEN	35.06	45.07	2.14	0.00
Evaporator Duty	EVAPORATE-CONDENSE	4.03	7.61	0.25	0.00
Crystallizer	CRYSTAL	0.74	1.64	0.04	0.00
<b>Total</b>	-	<b>40.38</b>	<b>55.37</b>	<b>2.47</b>	<b>0.00</b>
Option 2	Aspen Symbol	System Demand and Emissions			
		CED*	CExD**	CO <sub>2</sub>	N <sub>2</sub> O
		GJ/ton	kg/ton		
Bioreactor	FERMENT	0.24	0.45	0.01	0.00
Hydrogenation reactor	HYDROGEN	15.14	19.47	0.93	0.00
Evaporator Duty	EVAPORATE-CONDENSE	1.74	3.29	0.11	0.00
Crystallizer	CRYSTAL	0.32	0.71	0.02	0.00
<b>Total</b>	-	<b>17.44</b>	<b>23.92</b>	<b>1.07</b>	<b>0.00</b>

cumulative energy demand (CED)\*; cumulative exergy demand (CExD)\*\*

**Table 2.** Feed-level demands for bacterial growth during production of *cis*, *cis*-muconic acid.

Option 1	Symbol	Feed Levels	System Demand and Emissions			
			CED*	CExD**	CO <sub>2</sub>	N <sub>2</sub> O
		ton/ton	GJ/ton	kg/ton		
Magnesium Chloride	MgCl <sub>2</sub> ·6H <sub>2</sub> O	0.01	0.00	0.00	0.03	0.00
Ammonium Sulphate	(NH <sub>4</sub> ) <sub>2</sub> SO <sub>4</sub>	0.16	0.60	0.67	36.72	33.50
Potassium Phosphate	K <sub>2</sub> HPO <sub>4</sub>	0.21	0.37	0.55	24.67	0.00
Sodium Phosphate	NaH <sub>2</sub> PO <sub>4</sub> ·2H <sub>2</sub> O	0.12	0.06	0.11	3.82	0.00
Glucose	C <sub>6</sub> H <sub>12</sub> O <sub>6</sub>	1.01	8.39	8.74	512.26	23.48
Sodium Hydroxide	NaOH	0.56	13.93	18.07	598.70	0.02
Hydrochloric Acid	HCl	0.58	2.41	2.62	137.64	3.95
<b>Total</b>	-	-	<b>25.76</b>	<b>30.77</b>	<b>1313.84</b>	<b>60.95</b>
Option 2	Symbol	Feed Levels	System Demand and Emissions			
			CED*	CExD**	CO <sub>2</sub>	N <sub>2</sub> O
		ton/ton	GJ/ton	kg/ton		
Magnesium Chloride	MgCl <sub>2</sub> ·6H <sub>2</sub> O	0.00	0.00	0.00	0.01	0.00
Ammonium Sulphate	(NH <sub>4</sub> ) <sub>2</sub> SO <sub>4</sub>	0.07	0.26	0.29	15.86	14.47
Potassium Phosphate	K <sub>2</sub> HPO <sub>4</sub>	0.09	0.16	0.24	10.66	0.00
Sodium Phosphate	NaH <sub>2</sub> PO <sub>4</sub> ·2H <sub>2</sub> O	0.05	0.03	0.05	1.65	0.00
Glucose	C <sub>6</sub> H <sub>12</sub> O <sub>6</sub>	0.44	3.62	3.78	221.26	10.14
Sodium Hydroxide	NaOH	0.56	13.93	18.07	598.70	0.02
Hydrochloric Acid	HCl	0.54	2.24	2.44	127.98	3.68
<b>Total</b>	-	-	<b>20.24</b>	<b>24.87</b>	<b>976.12</b>	<b>28.30</b>

cumulative energy demand (CED)\*; cumulative exergy demand (CExD)\*\*

**Table 3.** Bioreactor-feedstock demands.

	Symbol	Conversion Rates	Feed Levels	System Demand and Emissions			
				CED*	CExD**	CO <sub>2</sub>	N <sub>2</sub> O
		%	ton/ton	GJ/ton	kg/ton		
Benzoic acid	C <sub>7</sub> H <sub>6</sub> O <sub>2</sub>	96	0.90	55.86	58.65	3343.35	0.00
Impure aromatics	C <sub>7</sub> H <sub>6</sub> O <sub>2</sub>	96	0.90	22.70	24.51	0.00	0.00
Toluene	C <sub>7</sub> H <sub>8</sub>	96	0.68	38.09	40.00	2829.87	0.00
Lignin (phenol)	C <sub>6</sub> H <sub>5</sub> OH	96	0.69	7.71	9.55	470.61	2.66

cumulative energy demand (CED)\*; cumulative exergy demand (CExD)\*\*

## Results and Discussion

**Reduction of Fossil Fuel and Related Greenhouse Gas Emission.** The production of *cis, cis*-muconic acid from benzoic acid by *P. putida* KT2440-JD1 in a pH-stat fed-batch process<sup>20</sup> was used as a model system for the limited LCA of a combined biological and chemical process for the production of adipic acid. The data in Table 2 and 3 reveal that glucose, sodium hydroxide and the feedstock for the carbon backbone of *cis, cis*-muconic acid play important roles in the total fossil fuel energy demand and greenhouse gas emission of the system. For the low final product concentration of option 1, use of the chemical pure laboratory benzoic acid feedstock did not contribute to an environmental impact decrease (Fig. 3). Compared to benzoic acid, impure aromatics led to an increase in the overall fossil fuel reduction potential: for option 1 from -17.8GJ/ton and -35.3GJ/ton to 15.4GJ/ton and -1.2GJ/ton CED and CExD, respectively and for option 2 from 10.7GJ/ton and 2.0GJ/ton to 43.9GJ/ton and 36.2GJ/ton CED and CExD, respectively. This reveals the huge potential of employing impure aromatics over benzoic acid as a feedstock. The robustness and productivity of *P. putida* KT2440-JD1 with impure aromatics however remains to be determined. The other pure petrochemical feedstock toluene has a neutral fossil fuel reduction potential for option 1 at 0.0GJ/ton CED and -16.7GJ/ton CExD. The most sustainable option would be using the biobased material lignin for phenols: for option 1 and 2 the highest calculated reduction potential of CED (30.4 and 58.9 GJ/ton respectively) and CExD (13.8 and 51.1 GJ/ton respectively) are achievable. When phenol from lignin is used as a carbon source the CED would decrease 29% (30.4 GJ/ton) for option 1 and 57% (58.4 GJ/ton) for option 2 compared to the traditional petroleum-based production route. As the biological delignification and isolation techniques improve, a switch to a lignin-based feedstock is foreseeable<sup>33</sup>.

For both product concentrations the CO<sub>2</sub>eq emissions are reduced for all of the different carbon backbone feedstocks (petrochemical and biomass-based). For option 2 the reduction is higher, which relates to a lower consumption of glucose and ammonium sulphate per ton product. A reduction in CO<sub>2</sub>eq emission can especially be achieved when the N<sub>2</sub>O emission is also restricted in the combined biological and chemical process for the production of adipic acid (Fig. 3). As a first option, it might be advantageous to use the protein rich co-product slurry of the glucose production to offset ammonium sulphate of the feed-level demands. This would reduce the N<sub>2</sub>O emissions of the feed-level demands for ammonium sulphate to practically zero, achieving a decrease of an average of 47% or 38% of the CO<sub>2</sub>eq emissions for option 1 and 2, respectively. Therefore, in Figure 3 the optimized CO<sub>2</sub>eq extinction is added representing these calculations. For option 1 and 2, the optimized CO<sub>2</sub>eq emissions concern a reduction in the magnitude ranging from 9.8 to 13.1 and 14.0 to 17.4 ton CO<sub>2</sub>eq/ton adipic acid, respectively.

Increasing the final product concentration of *cis*, *cis*-muonic acid in the bioreactor will result in a reduction of glucose and NPK per ton product reducing the environmental impact, assuming that the requirements of *P. putida* KT2440-JD1 for growth and production are constant. By increasing the final concentration less water is present, which directly results in less bioprocessing energy per ton adipic acid. The required energy is directly proportional to the concentration of *cis*, *cis*-muonic acid in the broth. It is imperative that any future biotechnological work should aim for the highest solid loading possible. The bulk of the bioprocessing energy is attributed to the hydrogenation reactor, therefore this effect is greater for this process step than any other unit. As shown in option 2 with 4.26% *cis*, *cis*-muonic acid, the energy required for the hydrogenation was 15.1GJ/ton whereas in option 1 with only 1.85% 35.1GJ/ton was required (Table 1). In option 2 together with the lower feed-level demands this reduced the bioprocessing energy by more than 50%, which even facilitated an energy mitigation potential for benzoic acid. A further doubling of the final product concentration to beyond 8% would result in a highly competitive system, which might be feasible since *P. putida* KT2440-JD1 can grow in mineral medium up to 8.7% *cis*, *cis*-muonic acid<sup>19</sup>. Alternatively, the high energy intensity of the hydrogenation-evaporation process of the *cis*, *cis*-muonic acid-containing fermentation broth could be reduced by extracting *cis*, *cis*-muonic acid from the acidified broth with e.g. cold diethyl ether<sup>8</sup>. This will result in a much higher concentration of *cis*, *cis*-muonic acid in cold diethyl ether, and the evaporation will require much less energy since the boiling temperature of cold diethyl ether (34.6°C) is much lower than water. Furthermore, the solvent used for extraction purifies the product from salts and should have a high extraction efficiency, since this has a large influence on the environmental impact.

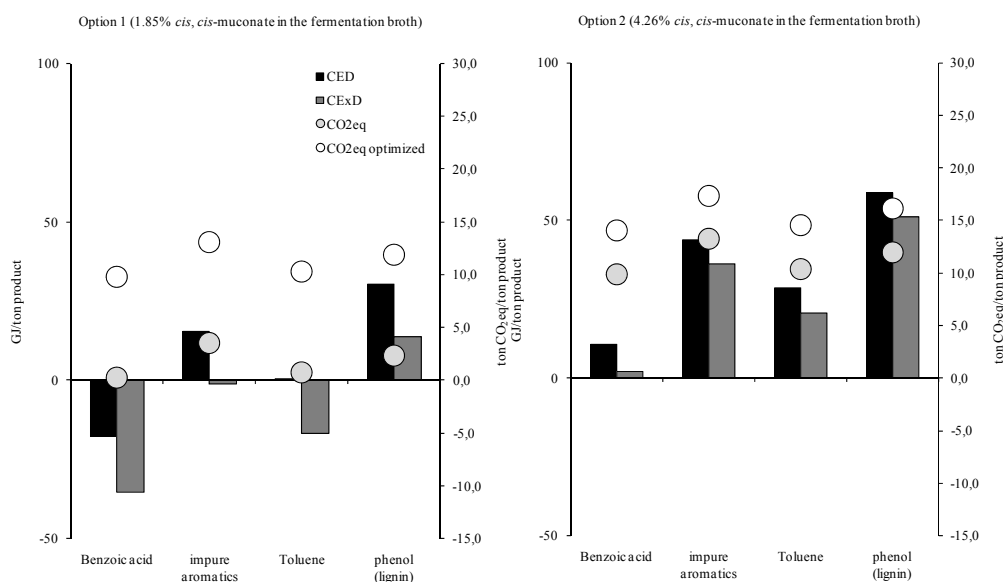


**Figure 3.** Cumulative energy demand (CED), cumulative exergy demand (CExD) and the CO<sub>2</sub> equivalent (optimized) (CO<sub>2</sub>eq) emissions per ton pure adipic acid induced for option 1 and 2 using various feedstocks for a combined biological and chemical process compared to the traditional petrochemical process of adipic acid.

**Biological Process.** Compared to existing small-scale biological production systems<sup>6,7,8</sup>, the small-scale pH-stat fed-batch process with *P. putida* KT2440-JD1 has allowed for a further optimization of the biological production of *cis, cis*-muconic acid<sup>20</sup>. The volumetric productivity (g/L) of the process could be further improved by applying a cell-recycle system, since this will increase the cell density. Choi et al. were the first who addressed the cell-recycling issue for *cis, cis*-muconic acid production, and reached a volumetric productivity of 5.5 g/(L·h)<sup>34</sup>. Unfortunately, they were unable to maintain a continuous recycle system for more than 2 days due to membrane fouling. By combining the pH-stat fed-batch bioprocess with a cell retention system, the volumetric productivity of a cell-recycle bioreactor is expected to increase significantly, assuming that the pH-control still is accurate at high cell densities. While this only has a minor impact on the energy consumption (Table 1 (bioreactor)), it does have a major impact on the economic parameters of an industrial scale bio-reactor. Another positive effect is that recycling of biomass would reduce the consumption of glucose and NPK, which lowers the environmental impact of the bioprocess. To retain the cells, new process technology in the form of membrane separation must first be resolved with cell fouling stipulating the main hurdle.

## Conclusions of the Limited LCA

The environmental impact concerning the CED, CExD and CO<sub>2</sub>eq emission of the manufacturing of the nylon-6,6 precursor adipic acid can be reduced by replacing the current petroleum-based chemical process with a combined biological and chemical process that is based on a small-scale pH-stat fed-batch bioprocess to produce *cis, cis*-muconic acid using *P. putida* KT2440-JD1<sup>20</sup>. The usage of different carbon backbone feedstocks (both petrochemical and biomass-based), the final product concentration in the fermentation broth, and the level of N<sub>2</sub>O emission have a large influence on the environmental impact. At a final concentration of 1.85% *cis, cis*-muconic acid in the fermentation broth, the CED is only improved when using impure aromatics or phenol derived from lignin. Should the bioprocess be further optimized to increase the final concentration of *cis, cis*-muconic acid to 4.26%, the CED and CExD are reduced for all the assessed feedstocks (benzoic acid, impure aromatics, toluene, and phenol). Additionally, the CO<sub>2</sub>eq emissions for option 2 are reduced more as for option 1. In order to further reduce the CO<sub>2</sub>eq emission compared to the petrochemical process, it is assumed that the N<sub>2</sub>O emission can be actively decreased in the combined biological and chemical process by using the protein rich co-product slurry of the glucose production to offset ammonium sulphate of the feed-level demands. The highest reductions were achieved with impure aromatics and phenol.

Several possibilities exist to improve the environmental and economical impact of the bioprocess, like i) improvements of *P. putida* KT2440-JD1 by enhancing the catechol 1,2-dioxygenase activity, reducing the sensitivity of the enzyme to putative product inhibition by *cis, cis*-muconic acid in the cell, increasing the possibly limiting transport of *cis, cis*-muconic acid through the cell membrane, and extension of the range of aromatic feedstocks that can be co-metabolized to *cis, cis*-muconic acid; ii) enhancement of the volumetric productivity of the bioprocess and reduction of the demand for nutrients by recycling the biomass; iii) reduction of the energy demand of the hydrogenation-

evaporation process by extraction of *cis*, *cis*-muconic acid from the fermentation broth with e.g. diethyl ether.

A huge potential for employing impure aromatics has been revealed as well as for phenol derived from the biological delignification and isolation techniques. Yet, the robustness and productivity of *P. putida* KT2440-JD1 with impure aromatics remains to be determined, while the biological delignification and isolation techniques have to be improved considerably before a switch to a lignin-based feedstock is foreseeable.

### **Acknowledgements**

This research was carried out within the research programme of the Kluyver Centre for Genomics of Industrial Fermentation, which is part of the Netherlands Genomics Initiative.

## References

1. ICIS Pricing and ICIS News, [http://www.icispricing.com/il\\_shared/Samples/SubPage121.asp](http://www.icispricing.com/il_shared/Samples/SubPage121.asp), accessed 2008.
2. Shimizu A, Tanaka K, Fujimori M. 2000. Abatement technologies for N<sub>2</sub>O emissions in the adipic acid industry. *Chemosphere-global change science* 2:425-434
3. Patel M. 2003. Cumulative energy demand (CED) and cumulative CO<sub>2</sub> emissions for products of the organic chemical industry. *Energy* 28:721-740.
4. EcoInvent Databank V2.1, <http://www.ecoinvent.org>, accessed 2008.
5. Draths KM, Frost JW. 1993. Environmentally Compatible Synthesis of Adipic Acid from & Glucose. *J Am Chem Soc* 116:399-400.
6. Bang SG, Choi CY. 1995. Do-stat fed-batch production of *cis*, *cis*-muconic acid from benzoic-acid by *Pseudomonas putida* Bm014. *J Ferment Bioeng* 79:381-383.
7. Mizuno S, Yoshikawa N, Schi M, Mikawa T, Imada Y. 1988. Microbial-production of *cis*, *cis*-muconic acid from benzoic-acid. *Appl Microbiol Biotechnol* 28:20-25.
8. Schmidt E, Knackmuss HJ. 1984. Production of *cis*, *cis*-Muconate from benzoate and 2-fluoro-*cis*, *cis*-muconate from 3-fluorobenzoate by 3-chlorobenzoate degrading bacteria. *Appl Microbiol Biotechnol* 20:351-355.
9. vanDuuren(1) JBJH, Wijte D, Leprince A, Puchalka J, Wery J, dos Santos VAP, Eggink G, Mars AE. Generation of a *catR* deficient mutant of *P. putida* KT2440 that produces *cis*, *cis*-muconate from benzoate at high rate and yield. *Submitted*.
10. Jiménez JI, Miñambres B, García JL, Díaz E. 2002. Genomic analysis of the aromatic catabolic pathways from *Pseudomonas putida* KT2440. *Environ Microbiol* 4:824-841.
11. Federal register. Certified host-vector systems 1982:17197.
12. Nelson KE, Weinel C, Paulsen IT, Dodson RJ, Hilbert H, Martins dos Santos VAP, Fouts DE, Gill SR, Pop M, Holmes M, Brinkac L, Beanan M, DeBoy RT, Daugherty S, Kolonay J, Madupu R, Nelson W, White O, Peterson J, Khouri H, Hance I, Chris Lee P, Holtzapple E, Scanlan D, Tran K, Moazzez A, Utterback T, Rizzo M, Lee K, Kosack D, Moestl D, Wedler H, Lauber J, Stjepandic D, Hoheisel J, Straetz M, Heim S, Kiewitz C, Eisen JA, Timmis KN, Dusterhöft A, Tümmeler B, Fraser CM. 2002. Complete genome sequence and comparative analysis of the metabolically versatile *Pseudomonas putida* KT2440. *Environ Microbiol* 4:799-808.
13. Ramos JL, Wasserfallen A, Rose K, Timmis KN. 1987. Redesigning metabolic routes: manipulation of TOL plasmid pathway for catabolism of alkylbenzoates. *Science* 235:593-596.
14. Wackett LP. 2003. *P. putida* - a versatile biocatalyst. *Nat. Biotechnol.* 21:136-138.
15. Hatti-Kaul R, Törnqvall U, Gustafsson L, Börjesson P. 2007. Industrial biotechnology for the production of bio-based chemicals--a cradle-to-grave perspective. *Trends Biotechnol.* 25:119-124.
16. Feist CF, Hegeman GD. 1969. Phenol and benzoate metabolism by *Pseudomonas putida*: regulation of tangential pathways. *J Bacteriol* 100:869-877.
17. Panke S, Sánchez-Romero JM, de Lorenzo V. 1998. Engineering of quasi-natural *Pseudomonas putida* strains for toluene metabolism through an *ortho*-cleavage degradation pathway. *Appl Environ Microbiol* 64:748-751.
18. Tao Y, Fishman A, Bentley WE, Wood TK. 2004. Oxidation of benzene to phenol, catechol, and 1,2,3-trihydroxybenzene by toluene 4-monooxygenase of *Pseudomonas mendocina* KR1 and toluene 3-monooxygenase of *Ralstonia pickettii* PKO1. *Appl Environ Microbiol* 70:3814-3820.
19. Haigler BE, Pettigrew CA, Spain JC. 1992. Biodegradation of mixtures of substituted benzenes by *Pseudomonas* sp. strain JS150. *Appl Environ Microbiol.* 58:2237-2244.
20. vanDuuren(2) JBJH, Yang Y, Wijte D, Martins dos Santos VAP, Mars AE, Eggink G. pH-stat fed-batch process to enhance the production of *cis*, *cis*-muconate from benzoate by *Pseudomonas putida* KT2440-JD1. *Submitted*.
21. International Organization for Standardization. 2006. Life cycle assessment. ISO 14040:2006
22. PE International, GaBi 4, <http://www.pe-international.com/gabi/>.
23. Szargut J, Morris DR, Steward FR. 1988. Exergy Analysis of Thermal, Chemical, and Metallurgical Processes. Springer-Verlag 332.
24. Brehmer B, Struik PC, Sanders J. 2008. Using an energetic and exergetic life cycle analysis to assess the best applications of legumes within a biobased economy. *Biomass Bioenerg* 32:1175-1186.

25. International Fertilizer Association (IFA). 1998. The Fertilizer Industry's Manufacturing Processes and Environmental Issues; Paris 73.
26. Brehmer(1) B. 2008. Chemical biorefinery perspectives Chapter 5: Primary Energy Input.
27. U.S. Department of Energy (DOE). 2002. Mining Industry of the Future: Energy and Environmental Profile of the U.S. Mining Industry. In Energy Efficiency and Renewable Energy (EERE).
28. Brehmer B, Sanders J. 2007. Energetic and Exergetic life cycle analysis to explain the hidden costs and effects of current sulphur utilisation. *Int J Exergy* 4:117-133.
29. Brehmer(2) B. 2008. Chemical biorefinery perspectives Chapter 6: Secondary Energy Input. <http://www.vpp.wur.nl/UK/Research/Publications/>.
30. Ministry of Agriculture Nature and Food Quality (LNV). 2006. Online Crop Statistics
31. Ramos JL, Duque E, Gallegos MT, Godoy P, Ramos-Gonzalez MI, Rojas A, Teran W, Segura A. 2002. Mechanisms of solvent tolerance in gram-negative bacteria. *Annu Rev Microbiol* 56:743-768.
32. Schmid A, Dordick JS, Hauer B, Kiener A, Wubbolts M, Witholt B. 2001. Industrial biocatalysis today and tomorrow. *Nature* 409:258-268.
33. Chakar FS, Ragauskas AJ. 2004. Review of current and future softwood kraft lignin process chemistry. *Ind Crop Prod* 20:131-141.
34. Choi WJ, Lee EY, Cho MH, Choi CY. 1997. Enhanced production of *cis*, *cis*-muconate in a cell-recycle bioreactor. *J Ferment Bioeng* 84:70-76.

# Chapter 6

## Discussion and outlook

## Towards a biotechnological production of aromatic intermediates

One of the major advantages of biotechnological processes is that new biomass-based resources and waste streams can be used as substrates for the production of chemicals and fuels, thereby reducing the demand for fossil fuel and possibly also the emission of greenhouse gas. However, the competition in terms of economic cost with existing products obtained from petrochemicals is challenging at the moment<sup>1</sup>. Given that oil is a limited resource, it is expected that its availability will decrease and consequently its price will significantly increase, which would make biomass-based products more competitive in the future. Currently, the production of pharmaceutical compounds are especially suitable and interesting for biotechnological processes, because of their high values and complex synthetic steps due to their special chemical structures and often the requirement of enantiomeric purity. In order to convert the petrochemical industry to a biotechnological and biobased industry, it is important to realize that the development of bioprocesses requires the involvement of different scientific disciplines. Technological advances in molecular techniques, enzyme engineering, omics techniques, and metabolic engineering have provided new alternative approaches for the optimization of enzymes and microorganisms. These tools can help to speed up development of biotechnological processes, thereby decreasing the investment costs.

A biotechnological process involves a bioconversion or a biosynthesis step after which the product has to be recovered and purified. Depending on the type of reaction, enzymes or whole cell biocatalysts are being used for the conversion of a substrate into a product<sup>2</sup>. For chiral resolution and enantio- and regio selective polymerisation sole enzymes are used, which can be used in aqueous medium or in the presence of solvents and/or supercritical fluids in the absence of added water. The use of enzymes in non aqueous medium might lead to higher final concentrations, new specificity of enzymes and reversal of hydrolytic conversions. Whole cells are being applied in processes where the conversion becomes more complex as a consequence of the involvement of a co-factor requiring reaction, and/or a cascade of enzymatic steps. Oxgenases can be cofactor dependent and have a relatively short half-life outside the cell. Therefore this important class of enzymes is not very suitable for application in *in vitro* conditions<sup>3</sup>. Some important features of whole cell biocatalysts are the requirement of transport of substrate and/or product over the cell membrane, and the ability to regenerate cofactors during the process. The kinetic parameters of rate-limiting enzymes and stability of the process are important factors that determine the economic feasibility of a whole cell biocatalytic process. By applying the above described tools the production rate, final concentration, and product yield can be influenced positively. Besides biocatalysis, product recovery and purification are also crucial parts of the bioprocess. For example, membrane engineering for separation of biomass and media is an important and still developing downstream processing technology.

Biotechnology can be applied for the production of end products as well as intermediates. An example of a biotechnologically produced intermediate is *cis, cis*-muconate, which can be converted to adipic acid, a building block for nylon-6,6<sup>4</sup>. *cis, cis*-Muconate can be accumulated from benzoate at a production yield of up to 100% and can easily be acidified and hydrogenated to adipic acid. For this conversion, whole cells were used instead of sole enzymes, given the involvement of two dioxygenase reactions, a co-factor and a cascade of enzymatic steps. *Pseudomonas putida* KT2440

is an attractive biocatalyst for this process since it is able to metabolize aromatic compounds and its metabolic capability is very versatile<sup>5,6,7</sup>. Consequently, other aromatic compounds such as toluene, phenol, or waste products from aromatics production, which have a lower energetic value, can also be used as substrates. Other examples of processes concerning a co-metabolized substrate to a product with *Pseudomonas sp.* are the production of 2-quinoxalinecarboxylic acid, and 5-methylpyrazine-2-carboxylic acid by *P. putida* ATCC 33015<sup>8,9</sup>, and the conversion of styrene to the enantiopure (S)-styrene oxide by *Pseudomonas sp.* strain VLB120ΔC<sup>10</sup>. For *P. putida* S12, other processes have been described whereby metabolic routes were redesigned concerning several interesting examples of co-metabolism: the conversion of 5-(hydroxymethyl)furfural to 2,5-furandicarboxylic acid, the conversion of toluene to 3-methylcatechol, and testosterone 15β-hydroxylation<sup>11,12,13</sup>.

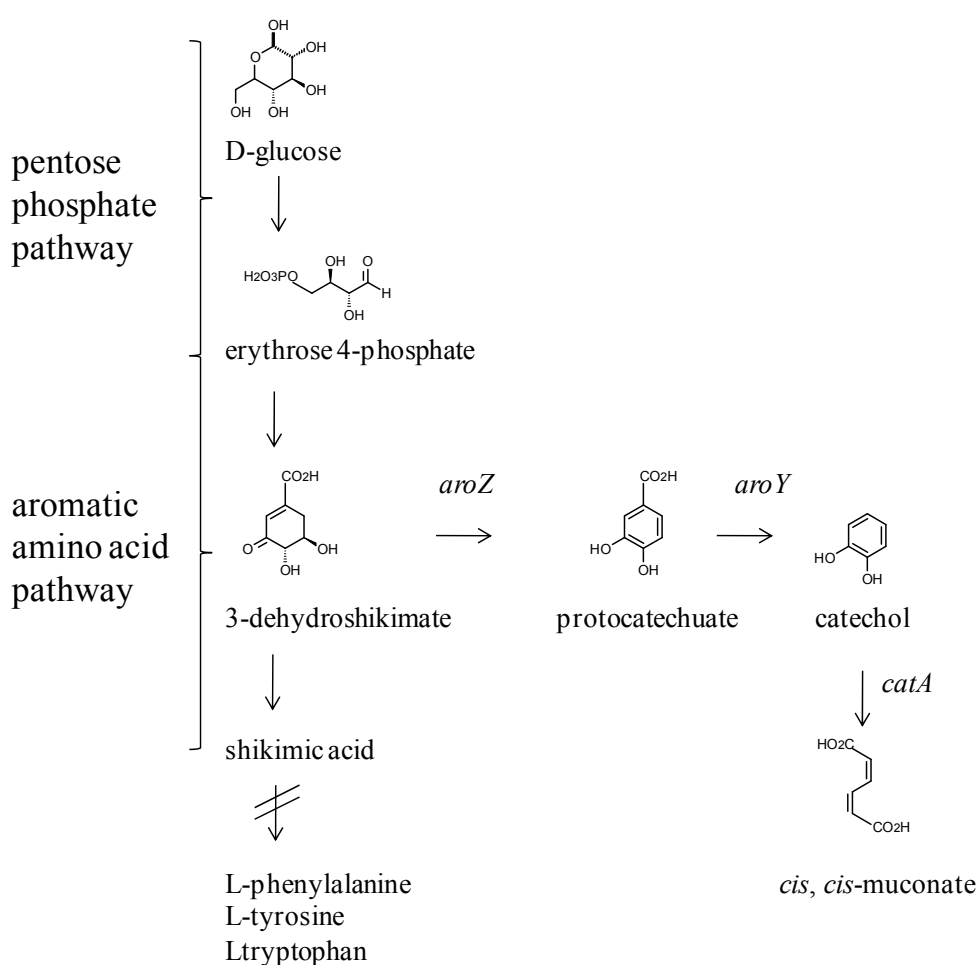


**Figure 1.** Biosynthetic pathway from D-glucose to *cis, cis*-muconate created in *E. coli* WN1/pWN2.248 via the pentose phosphate pathway, aromatic amino acid pathway, and DHS dehydratase (*aroZ*), protocatechuate decarboxylase (*aroY*), and catechol 1,2-dioxygenase (*catA*)<sup>4</sup>.

To shift from the petrochemical-based to a biotechnological-based production of *cis, cis*-muconate, not only phenol from lignin but also D-glucose can also be used as a substrate. To accomplish the

conversion of D-glucose to *cis, cis*-muconate, a biosynthetic pathway was created in *E. coli* WN1/pWN2.248, which is not naturally present in *E. coli*<sup>4,14</sup> (Fig. 1). This pathway was generated by introducing 3 heterologous genes: *aroZ* of *Klebsiella pneumonia*, which was two times integrated in the genome; and *aroY* and *catA* of *Klebsiella pneumonia* and *Acinetobacter calcoaceticus*, respectively, which were expressed from a plasmid. These genes encode the last three conversion steps of 3-dehydroshikimate, which is naturally produced in *E. coli*, to *cis, cis*-muconate. The product yield of glucose is 22%, because the feedstock glucose is also used for growth and maintenance. Other examples of whole cell biocatalytic conversion of glucose via the central metabolism to aromatic compounds are the production of cinnamic acid<sup>15</sup>, *p*-coumarate<sup>16</sup>, *p*-hydroxybenzoate<sup>17</sup>, phenol<sup>18</sup>, and *p*-hydroxy-styrene<sup>19</sup> with *P. putida* S12.

In this research project, firstly the biocatalyst *P. putida* KT2440-JD1 was developed for the conversion of benzoate to *cis, cis*-muconate. Secondly, a pH-stat fed-batch process was developed. Thirdly, a genome-scale metabolic model of *P. putida* (iJP815) was constrained to predict more accurately the physiology of the cell when grown on glucose. Furthermore, a life cycle assessment (LCA) was made in which the production process is modeled based on energy and exergy demand and green house gas emission.

### The biocatalyst *P. putida* KT2440-JD1

A mutant *P. putida* KT2440-JD1 was obtained from the wild type by NTG-mutagenesis<sup>20</sup> and selection for growth in the presence of 3-fluorobenzoate (Chapter 2). This compound is a substrate analogue for benzoate that becomes toxic when converted<sup>21,22</sup>. In contrast to the wild type strain, *P. putida* KT2440-JD1 cannot utilize benzoate as sole source of carbon and energy. Instead, benzoate is co-metabolized to *cis, cis*-muconate while the strain grows on glucose. The conversion of catechol to *cis, cis*-muconate is the rate-limiting step in the benzoate degradation pathway<sup>21,22,23</sup>. Possibly, this conversion is relatively slow, because of the cleavage of the benzene ring<sup>21</sup>. Catechol 1,2-dioxygenase catalyzes the conversion of catechol to *cis, cis*-muconate. According to this research and as earlier postulated by Jiménez *et al.* gene *catA2* (*PP\_3166*) functions besides *catA* as catechol 1,2-dioxygenase in *P. putida* KT2440<sup>5</sup>. These genes are situated on the *ben* and *cat* operon, respectively. Apart from their overall amino acid sequence similarity of 76%, the active binding sites of both enzymes are 100% similar (Chapter 2). When grown in the presence of benzoate, the genes *catA2* and *catA* are both expressed in *P. putida* KT2440, whereas only gene *catA2* is expressed in *P. putida* KT2440-JD1. The whole *cat* operon, on which *catA* is situated, cannot be expressed anymore in the mutant as a consequence of a point mutation in the regulator gene *catR*. Catechol is therefore only converted by the dioxygenase encoded by *catA2*. Presumably this limits the conversion capacity for catechol of *P. putida* KT2440-JD1 compared to the wild type.

We observed the accumulation of catechol during a pH-stat fed batch process (Chapter 3), which indicates that the conversion of catechol to *cis, cis*-muconate is indeed rate-limiting. Catechol functions as central metabolite, and is also known as a stressor since it forms reactive oxygen species and spontaneously coloured polymers<sup>7,22,24-27</sup>.

## Process development for the accumulation of *cis, cis*-muconate

The specific uptake rate of benzoate during batch cultures of *P. putida* KT2440-JD1 was higher than the specific production rate of *cis, cis*-muconate at increasing concentrations of benzoate (Chapter 3). This suggested the accumulation of a metabolic intermediate, which was confirmed by the accumulation of catechol in the medium after a pulse of 20 mM benzoate during the pH-stat fed-batch process. Catechol is known to be toxic, and probably inhibits growth of *P. putida* KT2440-JD1. The accumulation of catechol may thus explain why benzoate is more toxic than *cis, cis*-muconate. To avoid the simultaneous accumulation of catechol and *cis, cis*-muconate, benzoate was fed under a pH-regulated limited condition during the laboratorial pH-stat fed-batch process with *P. putida* KT2440-JD1. The medium acidifies when benzoate is converted to *cis, cis*-muconate. Therefore, the addition of benzoate was coupled to its own conversion by linking its inflow with regulation of the pH. Although the specific production rate of *cis, cis*-muconate in the pH-stat fed-batch culture was not as high as the rate observed during batch cultivations, it was higher than those described in other laboratorial processes<sup>21,28-32</sup> (Table 1). At increasing concentrations of *cis, cis*-muconate, the specific production rate of *cis, cis*-muconate decreased, which may be due to feedback inhibition. *P. putida* KT2440-JD1 still grew after reaching the final concentration *cis, cis*-muconate of 1.85%. As the pH no longer decreased, the automated addition of benzoate ceased. After manually adding extra benzoate, catechol was formed and the growth stopped. The presence of catechol is also expected to reduce the conversion of benzoate to *cis, cis*-muconate, because it causes the down regulation of the *ben* operon (Chapter 3). According to the proteome of *P. putida* KT2440-JD1 during the process, the strain minimised costs in terms of energy and motility during the production of *cis, cis*-muconate. Such a response was also found in *P. putida* KT2440 in a hostile environment caused by the presence of aromatics<sup>33</sup>, indicating that *P. putida* KT2440-JD1 senses the presence of *cis, cis*-muconate and/or some catechol as stressors. Besides feedback inhibition active transport of *cis, cis*-muconate out of the cell could also limit the production rate of *cis, cis*-muconate<sup>34</sup>. Additionally, the protein OprH was up-regulated, which is involved in the maintenance of the cell envelope integrity as was shown for OprL<sup>35,36</sup>. The membrane stabilization may be increased by *P. putida* KT2440-JD1 to limit the inflow of benzoate and *cis, cis*-muconate to limit the toxicity of these compounds.

**Table 1.** Maximum specific productivities, maximum volumetric productivities and final concentrations of *cis, cis*-muconate of various production processes from benzoate with different strains, or from glucose with *E. coli* WN1/pWN2.248.

Process	Strain	Maximum specific productivity (g g dcw <sup>-1</sup> h <sup>-1</sup> )	Maximum volumetric productivity (g L <sup>-1</sup> h <sup>-1</sup> )	Final concentration (g L <sup>-1</sup> )
pH-stat fed-batch	<i>P. putida</i> KT2440-JD1 (this research)	0.60	0.8	18.5
fed-batch	<i>Spingobacterium</i> sp. GCG <sup>28</sup>	>0.1	>0.1	>0.1
cell-recycle system	<i>P. putida</i> BM014 <sup>29</sup>	0.14**	5.5**	12**
DO-stat fed-batch	<i>P. putida</i> BM014 <sup>30</sup>	0.21	2.2	32
fed-batch	<i>Arthrobacter</i> sp. <sup>31</sup>	n.d.*	1.1	44
fed-batch	<i>Pseudomonas</i> sp. B13 <sup>21</sup>	0.24	0.8	7
Fed batch	<i>E. coli</i> WN1/pWN2.248 <sup>32</sup>	0.06	1.7	36.8

\* not determined; \*\* steady values

The biotechnological conversion of benzoate to *cis, cis*-muconate is an aqueous process. The product is a polar compound at pH 7 and acts as a solvent after acidification to pH 2.5. Consequently, it is not possible to apply a two-phase system during the process to extract the product with a solvent from the polar medium, because the strain cannot grow at such a low pH. In order to reduce the production time and the energy costs for growth a continuous process instead of a batch mode has to be developed. Cell recycle processes are known to increase the biomass concentrations in the process, which would increase the volumetric production rate. To retain the cells, membrane separation of the biomass and the medium is the best approach as it is gentle and does not damage or kill the cells. A volumetric productivity of  $5.5 \text{ g l}^{-1} \text{ h}^{-1}$  for 7 days is described for the production of *cis, cis*-muconate during a cell recycle process with *P. putida* BM014<sup>29</sup>. However, regulated feeding strategy can also be applied during cell recycling processes, which is expected to further increase the high volumetric productivity of this regime.

### Systems biology as a tool for analyzing *P. putida* KT2440

To analyze *P. putida* KT2440 from a system biology perspective a constraint-based metabolic model (iJP815) of this strain was developed<sup>37</sup>. To improve this model, the model-relevant parameters – growth associated maintenance (GAM), non-growth associated maintenance (NGAM), and biomass composition were determined from the experimentally measured growth-related factors of the strain, such as molecular composition (proteins, carbohydrates, lipids, RNA and DNA)<sup>38,39,40</sup>, maximal growth yield, and maintenance. To this end, the strain was grown on glucose in a continuous culture at a number of dilution rates, ranging from 0.05 to  $0.49 \text{ h}^{-1}$  (Chapter 4). The experiments revealed that energetic expenses of *P. putida* KT2440 during growth are higher than that of *E. coli* K12, whereas the macro-molecular composition of both bacteria is similar<sup>41</sup>. Interestingly, no overflow metabolism was detected in any of the continuous fermentations. This is in contrast to *Escherichia coli* K-12, which accumulates by-products at a *D* exceeding  $0.4 \text{ h}^{-1}$ <sup>42</sup>. The lack of overflow metabolism highlights the suitability of *P. putida* KT2440 as a biocatalyst. Overflow metabolism occurs due to restrictions in the TCA cycle or in the respiratory NADH turnover. The generation of energy and the sufficient availability of NADH and NAD<sup>+</sup> are of importance when a strain is used as biocatalyst for a cofactor dependent conversion and the primary export of the product out of the cell. These results confirm the data presented earlier showing that *P. putida* can compensate for high energy demands<sup>43</sup>.

The energetic expenses (GAM and NGAM) as well as the biomass composition influence for a large part flux variability analysis (FVA) simulations, which provide a basis for numerous applications of metabolic reconstructions including rational strain design for biotechnological applications. The newly obtained values of GAM and NGAM caused larger changes to the outcome of the FVA simulations than the new biomass composition (Chapter 4). All these changes contributed to the increased accuracy of predictions of the iJP815 model. Further restriction of enzymatic conversions with already published <sup>13</sup>C measurements only decreased the maximum FVA distances excluding flux distributions that are far from the experimental phenotype<sup>44</sup>. The best agreement possible was reached within the limitations of constraint-based modeling. The model predictions were also compared (indirectly) with transcriptomic data. The flux balance analysis

(FBA)-predicted fluxes and the levels of respective mRNA transcripts were consistent with each other.

To unravel the metabolic wiring of the cell during its growth on glucose and other carbon and energy sources, the availability of an accurate model is essential. To quantify the change between two steady states a dynamic model can be generated with various time-related “omic” data from one condition to another. For example while the dilution rate is increased and decreased from one steady state to another, five measurements can be taken, of which three between the two steady states<sup>45,46</sup>. Next, by implementing the regulation network in the metabolic model (iJP815) the FBA and FVA predictions can possibly be made even more accurate. Mutants can be engineered and tested experimentally to generate more knowledge and/or to test hypotheses. Besides, to further constrain the solution space of the model, experimental data, including growth related parameters, <sup>13</sup>C-flux measurements, and transcriptomic data, from other conditions, such as continuous cultures under the limitation of e.g. nitrogen or phosphate, can be obtained.

### **Life cycle assessment**

Innovative sustainable process technologies are needed for a shift from the petrochemical based industry to the combined biotechnological and biobased industry. To support business and R&D strategies LCA can compare manufacture process designs or use and disposal of products. The limited LCA study described in this thesis concerns the energy and exergy demand and green house gas emission for the combined biological and chemical production of adipic acid compared to the current petrochemical production process (Chapter 5). Data concerning the biocatalytic conversion are based on the performed pH-stat fed-batch process. The use of different feedstocks has a large impact on the environmental benefits of bio-based production processes<sup>1</sup>. The energy demand is negatively influenced when substrates with a lower energetic value, such as benzoic acid (62.4 GJ/ton), are used. Other substrates that were incorporated are impure benzoic acid (25.4 GJ/ton), toluene (56.4 GJ/ton), and phenol (11.2 GJ/ton) obtained from lignin. For benzoic acid and toluene the oil production was taken into account as well as the stoichiometric carbon content for the CO<sub>2</sub> emission. Because impure benzoate is considered a waste product the energy demand was directly linked to its formation and no CO<sub>2</sub> emissions are considered. Phenol received its own theoretical energy process burden based on its chemical formation and agricultural system. It was shown that the process energy demand for the product treatment and extraction per ton adipic acid depends on the concentration *cis*, *cis*-muconate in the medium. Through LCA, it was predicted that the energy and exergy demand and green house gas emission were reduced as compared to the petrochemical process of adipic acid at 4.26% *cis*, *cis*-muconate with benzoate as substrate. However, product concentrations of biotechnological processes are generally low compared to chemical processes<sup>2</sup>. As a result, biotechnological processes per ton product have higher energy costs for the production process and product crystallization from water.

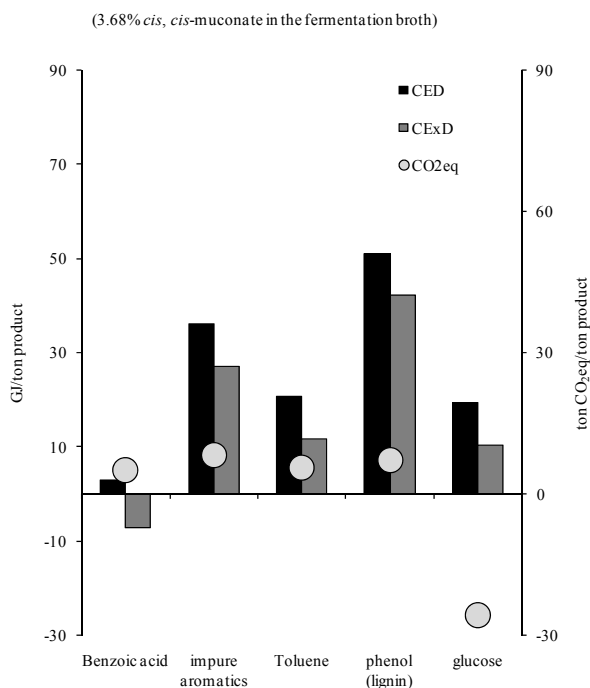


**Figure 2.** Cumulative energy demand, cumulative exergy demand, and the CO<sub>2</sub> equivalent emissions per ton pure adipic acid using various feedstocks for a combined biological and chemical process compared to the traditional petrochemical process of adipic acid.

As described before, besides aromatic compounds also D-glucose (8.3 GJ/ton) can be used as substrate for the production of *cis, cis*-muconate by *E. coli* WN1/pWN2.248 (Fig. 1). The distinctive feature of this process is that glucose, besides being used for growth and maintenance, is also used as substrate for the production of *cis, cis*-muconate. As a consequence, a low production yield of 22% (mol/mol) was obtained. To compare the energy and exergy demand and green house gas emission for the production of adipic acid for all substrates a LCA was made of the 4 described aromatic compounds and glucose (Fig. 2). The concentration *cis, cis*-muconate was set at 3.68%. This concentration was reached by *E. coli* WN1/pWN2.248 and can theoretically be reached by *P. putida* KT2440-JD1. The medium, product treatment and extraction were considered to be the same. The product yield on glucose is low but the low energetic value of glucose makes it a competitive substrate considering the decrease of energy and exergy demand for the production of adipic acid. The production of glucose, however, does cause a reasonable amount of green house gas emission especially in the form of N<sub>2</sub>O, see chapter 5, which is 286 times more severe as greenhouse gas than CO<sub>2</sub>. Therefore the CO<sub>2</sub>eq emission for the production of adipic acid from glucose is negatively influenced. Through advanced systems and synthetic biology methods, the yield on glucose can possibly be improved to reduce further the environmental impact. However, only a yield of 60% (mol/mol) compensates the amount of green house gas emission as caused by the petrochemical production of adipic acid. The use of phenol as substrate would yield the best result to produce adipic acid considering the savings in energy and exergy demand and green house gas emission compared to the petrochemical process for adipic acid. However, to use phenol as substrate delignification techniques have to be significantly improved.

To optimize the production process of adipic acid energetically a solvent such as cold diethyl ether can be applied to extract the product, after product and biomass separation and acidification to pH 2.5. In this procedure the salts are removed and the final product concentration is increased. This higher final product concentration together with a lower boiling temperature for the solvent (34.6°C) leads to a decrease of process energy per ton product for the hydrogenation and evaporation steps. In addition, methanol can be used to extract and crystallize the product<sup>21</sup>. Alternatively, acidified precipitated *cis, cis*-muconate can also be solved and (re)crystallized in methanol to purify it from salts by applying activated carbon in combination of filtration<sup>31,47,48</sup>.

Possibly a higher final concentration *cis, cis*-muconate could be reached by expressing an extra *catA* in *P. putida* KT2440-JD1 e.g. of *Arthrobacter sp.*<sup>31</sup> and/or by expressing genes related to the export of *cis, cis*-muconate out of the cell. With the Gram-positive bacterium *Arthrobacter sp.* the highest published final concentration of 4.4% *cis, cis*-muconate was reached (Table 1). To test if catechol 1,2-dioxygenase of *P. putida* KT2440 is indeed limiting compared to *Arthrobacter sp.*, the kinetics of the *catA* genes of both strains can be characterized by expressing these genes on a plasmid<sup>49,50</sup>. The up-regulation of OprH during the pH-stat could indicate its relevance in limiting the export of *cis, cis*-muconate out of the cell. However, a possible lower expression of OprH could destabilize the cell membrane. Because OprH was shown to be regulated by the magnesium concentration in *P. aeruginosa*, it might be interesting to repeat the pH-stat with increased and decreased magnesium concentrations in the medium<sup>51</sup>.

Other approaches to reach a higher final concentration could be based on evolutionary engineering or the synthesis of a synthetic operon for the conversion of benzoate to *cis, cis*-muconate. The cells that have a higher ability to convert catechol are supposed to increase their fitness, because catechol causes oxidative stress and its conversion is rate limiting. Adaptive evolution by continuously exposing cells to increased concentrations of *cis, cis*-muconate and catechol is expected to improve the ability to convert catechol. This experiment could best be performed in sequence-batch reactors at starting concentrations of 100 mM *cis, cis*-muconate and 20-40 mM benzoate<sup>52</sup>. Benzoate should be fed in pulses to reduce the selection advantage for mutants that can partially convert the benzoate to CO<sub>2</sub> and H<sub>2</sub>O and thereby diminish the stress for benzoate. In order to obtain a holistic impression of how the biocatalyst adapts during these experiments and to apply systems metabolic engineering, it is of interest to take samples for transcriptomics and proteomics after a fixed number of generations<sup>53,54</sup>. Additionally, upregulated genes, e.g. for catechol 1,2-dioxygenase and/or membrane proteins can be sequenced to search for mutations. Alterations in sequences can function as leads to improve enzymes with protein engineering or random recombination<sup>55</sup>.

Furthermore, to understand the networks underlying cell behaviour we need to take into account various levels of regulation to analyse the metabolic and stress response to catechol. This can be done by obtaining the transcriptomic, proteomic, and metabolic profiles of the wild type and *P. putida* KT2440-JD1 in the presence of catechol. In order to obtain these profiles, the wild type and mutant can be pulsed by 5 mM catechol while grown in continuous cultures on glucose in the presence or absence of benzoate. Of the two genes encoding for catechol 1,2-dioxygenase only *catA*, which is expressed in the wild type, will be indirectly induced by the presence of catechol. The compound is converted to *cis, cis*-muconate, which functions as inducer of the *cat* operon<sup>56,57</sup>. It is expected that gene *catA2* only can be induced in the presence of benzoate. By taking samples

before and after a pulse of catechol the global physiology of the cell with respect to various cellular regulations based on a metabolic profile can be analyzed, for example transcriptional and translational regulation. Possibly also specific *cis*, *cis*-muconate transporter functions over the cell membrane can be determined, because the mutant converts catechol to *cis*, *cis*-muconate in the presence of benzoate. Since the responses are presumed to be different, variations in expression patterns of genes, proteins and metabolites are expected. The results obtained will lead to more insight concerning the degradation of catechol.

Compared to other strains, *P. putida* KT2440 has already a unique *ben* operon, because of the inclusion of gene *catA2* that likely encodes catechol 1,2-dioxygenase for the conversion of catechol to *cis*, *cis*-muconate<sup>5</sup>. Possibly, that the conversion is regulated by one promoter is also the reason why such a high specific production rate was measured as compared to other results from literature. By synthesizing a new operon with an extra (improved) gene encoding catechol 1,2-dioxygenase and/or genes involved in the export of *cis*, *cis*-muconate out of the cell, the biocatalyst might become more applicable for the industrial production of *cis*, *cis*-muconate<sup>58</sup>.

## Conclusion

According to the developed LCA for the combined biological and chemical process for adipic acid production compared to the petrochemical process, a concentration of 4.26% *cis*, *cis*-muconate in the fermentation broth with benzoate as substrate is sufficient to save energy, exergy and green house gas emission. A final product concentration higher than 4.26% would result in an economically competitive system. As described, testing new feedstocks with a lower energetic value, optimizing the biocatalyst, and process developments as e.g. the use of solvents and a cell-recycle process are interesting possibilities to further optimize the process. Lack of detailed knowledge is the major bottleneck for the development of processes that enable to come closer to the theoretical maximum reachable final concentration of *cis*, *cis*-muconate from catechol. Detail studies of the various known structures of catechol 1,2-dioxygenase, as well as of the global regulatory machinery and exporter genes are warranted. Given that *P. putida* KT2440-JD1 is able to grow in the presence of a concentration of 8.7% *cis*, *cis*-muconate, it can theoretically be benchmarked as the maximum reachable concentration<sup>59</sup>. To provide more accurate predictions with the model iJP815 for e.g. knockout targets of the strain for application in a biotechnological process, the solution space of the model was constrained when grown on glucose. The further development of the versatile and energetically robust *P. putida* KT2440 as biocatalyst is promising and supported by state of art techniques; however its ability of reaching a high final concentration should still be improved.

## References

1. Hatti-Kaul R, Törnvall U, Gustafsson L, Börjesson P. 2007. Industrial biotechnology for the production of bio-based chemicals--a cradle-to-grave perspective. *Trends Biotechnol* 25:119-124.
2. Schmid A, Dordick JS, Hauer B, Kiener A, Wubbolts M, Witholt B. 2001. Industrial biocatalysis today and tomorrow. *Nature* 409:258-268.
3. Duetz WA, van Beilen JB, Witholt B. 2001. Using proteins in their natural environment: potential and limitations of microbial whole-cell hydroxylations in applied biocatalysis. *Curr Opin Biotechnol* 12:419-425.
4. Draths KM, Frost JW. 1993. Environmentally Compatible Synthesis of Adipic Acid from & Glucose. *J Am Chem Soc* 116:399-400.
5. Jiménez JI, Miñambres B, García E, Díaz JL. 2002. Genomic analysis of the aromatic catabolic pathways from *Pseudomonas putida* KT2440. *Environ Microbiol* 4:824-841.
6. Nelson KE, Weinl C, Paulsen IT, Dodson RJ, Hilbert H, Martins dos Santos VAP, Fouts DE, Gill SR, Pop M, Holmes M, Brinkac L, Beanan M, DeBoy RT, Daugherty S, Kolonay J, Madupu R, Nelson W, White O, Peterson J, Khouri H, Hance I, Chris Lee P, Holtzapple E, Scanlan D, Tran K, Moazzez A, Utterback T, Rizzo M, Lee K, Kosack D, Moestl D, Wedler H, Lauber J, Stjepandic D, Hoheisel J, Straetz M, Heim S, Kiewitz C, Eisen JA, Timmis KN, Dusterhöft A, Tümmler B, Fraser CM. 2002. Complete genome sequence and comparative analysis of the metabolically versatile *Pseudomonas putida* KT2440. *Environ Microbiol* 4:799-808.
7. Wackett LP. 2003. *P. putida* - a versatile biocatalyst. *Nat Biotechnol* 21:136-138.
8. Wong JW, Watson Jr. HA, Bouressa JF, Burns MP, Cawley JJ, Doro AE, Guzek DB, Hintz MA, McCormick EL, Scully DA, Siderewicz JM, Taylor WJ, Truesdell SJ, Wax RG. 2002. Biocatalytic Oxidation of 2-Methylquinoxaline to 2-Quinoxalinecarboxylic Acid. *Org Proc Res Dev* 6:477-481.
9. Kiener A. 1992. Enzymatic Oxidation of Methyl Groups on Aromatic Heterocycles: A Versatile Method for the Preparation of Heteroaromatic Carboxylic Acids. *Angew Chem Int Ed* 6:774-775.
10. Park JB, Bühler B, Panke S, Witholt B, Schmid A. 2007. Carbon metabolism and product inhibition determine the epoxidation efficiency of solvent-tolerant *Pseudomonas* sp. strain VLB120ΔC. *Biotechnol Bioeng* 98:1219-1229.
11. Koopman F, Wierckx N, de Winde JH, Ruijsenaars HJ. 2010. Efficient whole-cell biotransformation of 5-(hydroxymethyl)furfural into FDCA, 2,5-furandicarboxylic acid. *Bioresour Technol* 101:6291-6296.
12. Wery J, Mendes da Silva DI, de Bont JA. 2000. A genetically modified solvent-tolerant bacterium for optimized production of a toxic fine chemical. *Appl Microbiol Biotechnol* 54:180-185.
13. Ruijsenaars HJ, Sperling EM, Wiegerinck PH, Brands FT, Wery J, de Bont JA. 2007. Testosterone 15β-hydroxylation by solvent tolerant *Pseudomonas putida* S12. *J Biotechnol* 131:205-208.
14. Niu W, Draths KM, Frost JW. 2002. Benzene-free synthesis of adipic acid. *Biotechnol Prog* 18:201-211.
15. Nijkamp K, van Luijk N, de Bont JA, Wery J. 2005. The solvent-tolerant *Pseudomonas putida* S12 as host for the production of cinnamic acid from glucose. *Appl Microbiol Biotechnol* 69:170-177.
16. Nijkamp K, Westerhof RG, Ballerstedt H, de Bont JA, Wery J. 2007. Optimization of the solvent-tolerant *Pseudomonas putida* S12 as host for the production of *p*-coumarate from glucose. *Appl Microbiol Biotechnol* 74:617-624.
17. Verhoef S, Ruijsenaars HJ, de Bont JA, Wery J. 2007. Bioproduction of *p*-hydroxybenzoate from renewable feedstock by solvent-tolerant *Pseudomonas putida* S12. *J Biotechnol* 132:49-56.
18. Wierckx NJ, Ballerstedt H, de Bont JA, Wery J. 2005. Engineering of solvent-tolerant *Pseudomonas putida* S12 for bioproduction of phenol from glucose. *Appl Environ Microbiol* 71:8221-8227.
19. Verhoef S, Wierckx N, Westerhof RG, de Winde JH, Ruijsenaars HJ. 2009. Bioproduction of *p*-hydroxystyrene from glucose by the solvent-tolerant bacterium *Pseudomonas putida* S12 in a two-phase water-decanol fermentation. *Appl Environ Microbiol* 75:931-936.
20. Adelberg EA, Mandel M, Chen GCC. 1965. Optimal conditions for mutagenesis by *N*-Methyl-*N'*-Nitro-*N*-Nitrosoguanidine in *Escherichia Coli* K12. *Biochem Biophys Res Commun* 18:788-795.
21. Schmidt E, Knackmuss HJ. 1984. Production of *cis*, *cis*-Muconate from benzoate and 2-fluoro-*cis*, *cis*-muconate from 3-fluorobenzoate by 3-chlorobenzoate degrading bacteria. *Appl Microbiol Biotechnol* 20:351-355.
22. Schreiber A, Hellwig M, Dorn E, Reineke W, Knackmuss HJ. 1980. Critical reactions in fluorobenzoic acid degradation by *Pseudomonas* sp. B13. *Appl Environ Microbiol* 39:58-67.
23. Kim BJ, Choi WJ, Lee EY, Choi CY. 1988. Enhancement of *cis*, *cis*-muconate productivity by overexpressing of catechol 1,2-dioxygenase in *Pseudomonas putida* BCM114. *Biotechnol Bioprocess Eng* 3:112-114.

24. Feist CF, Hegeman GD. 1969. Phenol and benzoate metabolism by *Pseudomonas putida*: regulation of tangential pathways. *J Bacteriol* 100:869-877.
25. Benndorf D, Loffhagen N, Babel W. 2001. Protein synthesis patterns in *Acinetobacter calcoaceticus* induced by phenol and catechol show specificities of responses to chemostress. *FEMS Microbiol Lett* 200:247-252.
26. Smith JT, Vinjamoori DV. 1995. Rapid determination of logarithmic partition coefficients between n-octanol and water using micellar electrokinetic capillary chromatography. *J Chromatogr B Biomed Appl* 669:59-66.
27. Benndorf D, Thiersch M, Loffhagen N, Kunath C, Harms H. 2006. *Pseudomonas putida* KT2440 responds specifically to chlorophenoxy herbicides and their initial metabolites. *Proteomics* 6:3319-3329.
28. Wu CM, Lee TH, Lee SN, Lee YA, Wu JY. 2006. Microbial synthesis of *cis, cis*-muconic acid from benzoate by *Sphingobacterium* sp GCG generated from effluent of a styrene monomer (SM) production plant. *Biochem Eng J* 29:35-40.
29. Choi WJ, Lee EY, Cho MH, Choi CY. 1997. Enhanced production of *cis, cis*-muconate in a cell-recycle bioreactor. *J Ferment Bioeng* 84:70-76.
30. Bang SG, Choi CY. 1995. Do-stat fed-batch production of *cis, cis*-muconic acid from benzoic-acid by *Pseudomonas putida* Bm014. *J Ferment Bioeng* 79:381-383.
31. Mizuno S, Yoshikawa N, Schi M, Mikawa T, Imada Y. 1988. Microbial-production of *cis, cis*-muconic acid from benzoic-acid. *Appl Microbiol Biotechnol* 28:20-25.
32. Niu W, Draths KM, Frost JW. 2002. Benzene-free synthesis of adipic acid. *Biotechnol Prog* 18:201-211.
33. Domínguez-Cuevas P, González-Pastor JE, Marqués S, Ramos JL, de Lorenzo V. 2006. Transcriptional tradeoff between metabolic and stress-response programs in *Pseudomonas putida* KT2440 cells exposed to toluene. *J Biol Chem* 281:11981-11991.
34. van Maris AJ, Konings WN, van Dijken JP, Pronk JT. 2004. Microbial export of lactic and 3-hydroxypropanoic acid: implications for industrial fermentation processes. *Metab Eng* 6:245-255.
35. Ramos JL, Duque E, Rodríguez-Herva JJ, Godoy P, Haïdour A, Reyes F, Fernández-Barrero A. 1997. Mechanisms for solvent tolerance in bacteria. *J Biol Chem* 272:3887-3890.
36. Volkens RJ, de Jong AL, Hulst AG, van Baar BL, de Bont JA, Wery J. 2006. Chemostat-based proteomic analysis of toluene-affected *Pseudomonas putida* S12. *Environ Microbiol* 8:1674-1679.
37. Puchalka J, Oberhardt MA, Godinho M, Bielecka A, Regenhardt D, Timmis KN, Papin JA, Martins dos Santos VA. 2008. Genome-scale reconstruction and analysis of the *Pseudomonas putida* KT2440 metabolic network facilitates applications in biotechnology. *PLoS Comput Biol* 4(10).
38. Hanegraaf PP, Muller EB. 2001. The dynamics of the macromolecular composition of biomass. *J Theor Biol* 212:237-251
39. Lange HC, Heijnen JJ. 2001. Statistical reconciliation of the elemental and molecular biomass composition of *Saccharomyces cerevisiae*. *Biotechnol Bioeng* 75:334-344.
40. Reed JL, Palsson BØ. 2003. Thirteen years of building constraint-based *in silico* models of *Escherichia coli*. *J Bacteriol* 185: 2692-2699.
41. Reed JL, Vo TD, Schilling CH, Palsson BO. 2003. An expanded genome-scale model of *Escherichia coli* K-12. *Genome Biol* 4:R54.
42. Kayser A, Weber J, Hecht V, Rinas U. 2005. Metabolic flux analysis of *Escherichia coli* in glucose-limited continuous culture. I. Growth-rate-dependent metabolic efficiency at steady state. *Microbiology* 151:693-706.
43. Blank LM, Ionidis G, Ebert BE, Bühler B, Schmid A. 2008. Metabolic response of *Pseudomonas putida* during redox biocatalysis in the presence of a second octanol phase. *FEBS J* 27:5173-5190.
44. Fuhrer T, Fischer E, Sauer U. 2005. Experimental identification and quantification of glucose metabolism in seven bacterial species. *J Bacteriol* 187:1581-1590.
45. Bonneau R. 2008. Learning biological networks: from modules to dynamics. *Nat Chem Biol* 4:658-664.
46. Reed JL, Famili I, Thiele I, Palsson BØ. 2006. Towards multidimensional genome annotation. *Nat Rev Genet* 7:130-141.
47. Liese A, Seelback K, Wandrey C. 2006. Industrial biotransformations. Wiley-VCH.
48. Yoshikawa N, Mizuno S, Ohta K, Suzuki M. 1990. Microbial production of *cis, cis*-muconic acid. *J Biotechnol* 14:203-210.
49. de Lorenzo V, Eltis L, Kessler B, Timmis KN. 1993. Analysis of *Pseudomonas* gene products using *lacI<sup>P</sup>/Ptrp-lac* plasmids and transposons that confer conditional phenotypes. *Gene* 123:17-24.

50. Matera I, Ferraroni M, Kolomytseva M, Golovleva L, Scozzafava A, Briganti F. 2010. Catechol 1,2-dioxygenase from the Gram-positive *Rhodococcus opacus* 1CP: Quantitative structure/activity relationship and the crystal structures of native enzyme and catechols adducts. *J Struct Biol* 170:548-564.
51. Macfarlane EL, Kwasnicka A, Ochs MM, Hancock RE. 1999. PhoP-PhoQ homologues in *Pseudomonas aeruginosa* regulate expression of the outer-membrane protein OprH and polymyxin B resistance. *Mol Microbiol* 34:305-316.
52. Kuyper M, Toirkens MJ, Diderich JA, Winkler AA, van Dijken JP, Pronk JT. 2005. Evolutionary engineering of mixed-sugar utilization by a xylose-fermenting *Saccharomyces cerevisiae* strain. *FEMS Yeast Res* 5:925-934.
53. Cooper TF, Rozen DE, Lenski RE. 2003. Parallel changes in gene expression after 20,000 generations of evolution in *Escherichia coli*. *Proc Natl Acad Sci U.S.A.* 100:1072-1077.
54. Park JH, Lee SY, Kim TY, Kim HU. 2008. Application of systems biology for bioprocess development. *Trends Biotechnol* 26:404-412.
55. Kaper T, Brouns SJ, Geerling AC, De Vos WM, Van der Oost J. 2002. DNA family shuffling of hyperthermostable  $\beta$ -glycosidases. *Biochem J* 368:461-470.
56. Houghton JE, Brown TM, Appel AJ, Hughes EJ, Ornston LN. 1995. Discontinuities in the evolution of *Pseudomonas putida cat* genes. *J Bacteriol* 177:401-412.
57. Parsek MR, Shinabarger DL, Rothmel RK, Chakrabarty AM. 1992. Roles of CatR and *cis*, *cis*-muconate in activation of the *catBC* operon, which is involved in benzoate degradation in *Pseudomonas putida*. *J Bacteriol* 174:7798-7806.
58. Zhang K, Sawaya MR, Eisenberg DS, Liao JC. 2008. Expanding metabolism for biosynthesis of nonnatural alcohols. *Proc Natl Acad Sci U S A.* 105:20653-20658.
59. Ibarra RU, Edwards JS, Palsson BO. 2002. *Escherichia coli* K-12 undergoes adaptive evolution to achieve *in silico* predicted optimal growth. *Nature* 420:186-189.



## Summary

### Optimization of *Pseudomonas putida* KT2440 as host for the production of *cis, cis*-muconate from benzoate

*P. putida* KT2440 was used as biocatalyst given its versatile and energetically robust metabolism. Therefore, a mutant was generated and a process developed based on which a life cycle assessment (LCA) was performed. Additionally, the growth related parameters were experimentally obtained to constrain the metabolic model iJP815 further.

The mutant *Pseudomonas putida* KT2440-JD1 was derived from *P. putida* KT2440 after NTG-mutagenesis and exposure to 3-fluorobenzoate. The strain was no longer able to grow with benzoate as a single source of carbon and energy. Instead, benzoate was co-metabolized to *cis, cis*-muconate that accumulated in the culture medium while the strain grew on glucose. In batch cultures, a maximal production rate per gram biomass of 2.0 g *cis, cis*-muconate g<sub>DCW</sub><sup>-1</sup> h<sup>-1</sup> was obtained. This is 8-fold higher than thus far reported. The *cat* operon was no longer expressed in *P. putida* KT2440-JD1 due to a point mutation in the regulator gene *catR*. This operon contains the genes for the conversion of catechol to metabolites of the central metabolism, including *catA*, which encodes a catechol 1,2-dioxygenase. Consequently, benzoate is converted in the mutant by enzymes that are encoded on the *ben* operon. This operon includes a gene (*catA2*; *PP\_3166*) that encodes an additional catechol 1,2-dioxygenase, thus allowing the conversion of benzoate to *cis, cis*-muconate.

In batch cultures the maximal growth rate of *P. putida* KT2440-JD1 in mineral medium with glucose decreased linearly in the presence of increasing concentrations of benzoate and/or *cis, cis*-muconate and finally stopped at 6 g L<sup>-1</sup> benzoate or 85 g L<sup>-1</sup> *cis, cis*-muconate. The inhibitory effects of both compounds were cumulative and no synergistic effects were observed. The maximal uptake rate of benzoate was higher than the production rate of *cis, cis*-muconate per gram biomass during growth on glucose in the presence of benzoate, indicating that a benzoate derivative accumulated in the cells, which is likely to be catechol, as accumulation of this intermediate was observed. Catechol is known to cause oxidative stress, and the accumulation of catechol and benzoate should be prevented during the production of *cis, cis*-muconate. This is feasible by coupling the addition of benzoate to the decrease of the pH of the culture medium in a so-called pH-stat process, as the cultivation medium acidifies only when benzoate has been converted to *cis, cis*-muconate. Such a pH-stat fed-batch process resulted in the production of 18.5 g L<sup>-1</sup> *cis, cis*-muconate from benzoate with a molar yield of 96%.

The phenotype of *P. putida* KT2440 can be assessed by the constraint-based metabolic model iJP815. The solution space of the model based on flux variability analysis was further constrained by growth associated maintenance, non-growth associated maintenance, and biomass composition determined from the experimentally measured growth-related factors of the strain that were generated during continuous cultivations at various dilution rates (*D*) (0.05-0.49) h<sup>-1</sup>. Transcriptomic profiles obtained at a *D* of 0.2 h<sup>-1</sup> were consistent with model predictions of

expressed genes based on flux balance analysis. The growth-related macro molecular composition of the biomass was similar as measured with *E. coli* K-12. However, growth parameters like the maximum biomass yield and maintenance coefficient were different. The energy required for assembly of *P. putida* KT2440 is higher compared to *E. coli* W3110, which will result in higher costs of glucose in biotechnological processes. On the other hand, the metabolism is robust as even at a  $D$  of  $0.49\text{ h}^{-1}$  no overflow metabolism was observed. The lack of overflow metabolism is of great importance as it underscores the capacity of *P. putida* KT2440 as biocatalyst e.g. for conversions involving cofactor dependent oxygenase reactions. Further restriction of enzymatic conversions with already published  $^{13}\text{C}$  measurements only decreased the maximum solution space excluding solutions that are far from the experimental phenotype. Possibly, the best agreement was reached within limitations of constraint-based modeling.

A LCA was performed on a combined biological and chemical process for the production of adipic acid. The outcome was compared with the traditional chemical process. The LCA focused on the cumulative energy demand, cumulative exergy demand and the  $\text{CO}_2$  equivalent emissions, with  $\text{CO}_2$  and  $\text{N}_2\text{O}$  separate. Acidified *cis, cis*-muconate can be easily hydrogenated to adipic acid a resource for nylon-6,6 used in carpets and the auto industry, because of its long lasting and strong features. Feedstocks have a large effect on the overall environmental impact. The soil bacterium *P. putida* KT2440 has a versatile metabolism and is able to convert various feedstocks to *cis, cis*-muconate. Consequently, the use of feedstocks with a lower energy demand were taken into account besides benzoate, including: the petrochemical based feedstocks impure aromatics and toluene, and the biomass based feedstock phenol (from lignin). The effect of an increase of the final concentration *cis, cis*-muconate in the fermentor broth from 1.85% to 4.26% was modeled as *P. putida* KT2440-JD1 was able to consume benzoate up to 4.26% *cis, cis*-muconate. At a final concentration of 1.85% *cis, cis*-muconate, the use of impure aromatics and lignin instead of benzoate reduced the energy demand compared to the chemical production of adipic acid. The applicability of these feedstocks depends on the metabolic robustness of *P. putida* KT2440-JD1 with impure aromatics, and/or the development of an efficient process for the production of phenol from lignin. At a final concentration of 4.26% *cis, cis*-muconate the process energy and  $\text{CO}_{2\text{eq}}$  emissions were reduced for all feedstocks.

The pH-stat fed-batch process had a higher production rate per gram biomass compared to other processes although the speed was significantly lower as measured during the batch cultures. By generating a high cell density in combination of a pH-regulated inflow of benzoate, the volumetric productivity will increase as has been described for a cell-recycle process. While this only has a minor impact on the energy consumption, it does have a major impact on the economic parameters of an industrial scale bio-reactor. Recycling biomass with a membrane and using a solvent, as e.g. cold diethyl ether, after the acidification of the medium (pH 2.5) for the extraction of *cis, cis*-muconate, could further reduce the environmental impact. The use of solvents will result in a higher product concentration and/or the evaporation will require less energy since the boiling temperature of solvents is most often lower than water.

## Samenvatting

### Optimalisatie van *Pseudomonas putida* KT2440 als gastheer voor de productie van *cis, cis*-muconaat met benzoaat als substraat

*P. putida* KT2440 is gebruikt als biokatalysator, omdat het een uitgebreid metabool systeem heeft, waarmee een groot aantal uiteenlopende verbindingen efficiënt kunnen worden omgezet. Daarom werd een mutant en proces ontwikkeld, waarvan een levenscyclusanalyse (LCA=life cycle assessment) werd uitgevoerd. Daarnaast werden de groei afhankelijke parameters bepaald om de oplossingsruimte van het metabool model iJP815 verder te verkleinen.

De mutant *Pseudomonas putida* KT2440-JD1 werd verkregen vanuit *P. putida* KT2440 na het toepassen van NTG-mutagenese en het blootstellen aan 3-fluorobenzoaat. Benzoaat werd door de mutant niet langer gebruikt als groeisubstraat, maar werd cometabolisch omgezet naar *cis, cis*-muconaat, dat in het medium accumuleerde terwijl de stam groeide op glucose. De maximale productiviteit van *cis, cis*-muconaat per gram biomassa was acht keer hoger in batch cultures dan eerder beschreven, en bedroeg  $2,0 \text{ g } cis, cis\text{-muconaat } g_{DCW}^{-1} \text{ h}^{-1}$ . De mutant heeft een punt mutatie in het regulatie gen *catR*, waardoor het *cat* operon niet meer tot expressie komt. Dit operon bevat de genetische informatie voor de omzetting van catechol naar intermediären van het centrale metabolisme, waaronder een gen voor een catechol 1,2-dioxygenase. Als gevolg, in *P. putida* KT2440-JD1 kan benzoaat alleen nog wordt omgezet door enzymen die gecodeerd worden door genen op het *ben* operon. Het *ben* operon bevat ook een gen (*cata2*; *PP\_3166*) dat zeer waarschijnlijk codeert voor een alternatief catechol 1,2-dioxygenase, waardoor de omzetting naar *cis, cis*-muconaat mogelijk is.

De maximale groeisnelheid van *P. putida* KT2440 op glucose in mineraal medium nam lineair af in de aanwezigheid van toenemende concentraties benzoaat en/of *cis, cis*-muconaat en stopte uiteindelijk bij een concentratie van  $6 \text{ g L}^{-1}$  benzoaat of  $85 \text{ g L}^{-1}$  *cis, cis*-muconaat. De remmende effecten van beide componenten waren cumulatief en er werden geen synergetische effecten gevonden. De maximale opname snelheid van benzoaat was hoger dan de maximale productie snelheid van *cis, cis*-muconaat per gram biomassa tijdens de groei op glucose in aanwezigheid van benzoaat, wat duidt op de accumulatie van een benzoaat derivaat. Deze derivaat is waarschijnlijk catechol, aangezien de accumulatie van catechol is waargenomen tijdens de omzetting van benzoaat naar *cis, cis*-muconaat. Catechol veroorzaakt oxidatieve stres, en de accumulatie van benzoaat en catechol moet worden voorkomen tijdens de productie van *cis, cis*-muconaat. Dit is mogelijk door de toevoeging van benzoaat te koppelen aan de daling van de pH in het medium met behulp van een zogenaamd pH-stat proces, aangezien het medium pas verzuurd wanneer *cis, cis*-muconaat is gevormd uit benzoaat. Tijdens een dergelijk pH-stat fed-batch proces werd een eindconcentratie van  $18,5 \text{ g L}^{-1}$  *cis, cis*-muconaat bereikt met een molaire product opbrengst van 96%.

Het fenotype van *P. putida* KT2440 als biokatalysator kan worden voorspeld door middel van het gelimiteerde metabool model iJP815. De oplossingsruimte gebaseerd op flux variatie analyse werd

verder gelimiteerd. Deze limitering was verkregen door groei afhankelijk onderhoud, groei onafhankelijk onderhoud en de biomassa samenstelling te bepalen van experimenteel gemeten groei afhankelijke factoren van de stam, die werden verkregen door middel van continu fermentaties met verschillende verdunningssnelheden ( $D$ ) (0,05-0,49)  $\text{h}^{-1}$ . Transcriptomics verkregen met een  $D$  van 0,2  $\text{h}^{-1}$  hadden een hoge overeenkomst met de op flux balans analyse gebaseerde modelvoorspelling van genen die tot expressie komen. De groei gerelateerde macro moleculaire samenstelling van de biomassa was in overeenkomst met die van *E. coli* K-12. Echter, groei parameters zoals biomassa opbrengst en onderhoudscoëfficiënt waren verschillend. De energie die nodig is voor het produceren van biomassa was hoger bij *P. putida* KT2440, hetgeen zal resulteren in hogere kosten voor glucose in biotechnologische processen. Aan de andere kant bleek het metabool systeem zeer robuust, aangezien zelfs tijdens een verdunningssnelheid van 0,49  $\text{h}^{-1}$  geen ophoping van metabolieten werd waargenomen. De afwezigheid van metaboliet accumulatie is van groot belang omdat het de geschiktheid van *P. putida* KT2440 als biokatalysator aantoont bv. voor de omzetting van cofactor afhankelijke oxygenase reacties. Verdere beperkingen van enzymatische omzettingen gebaseerd op al eerdere gepubliceerde  $^{13}\text{C}$  label experimenten verminderden enkel de uiterste waarden van de model voorspellingen. Daarbij werden oplossingen uitgesloten die erg verschillend zijn van het experimenteel bepaalde fenotype. Waarschijnlijk is het beste resultaat verkregen binnen de beperkingen van gelimiteerd metabool modelleren.

Een beperkte analyse van een LCA werd uitgevoerd voor het gecombineerde biologische en chemische proces voor de productie van adipinezuur. Het resultaat werd vergeleken met het traditioneel chemische proces. De LCA richtte zich op de cumulatieve energie vraag, de cumulatieve exergie vraag en de  $\text{CO}_2$  equivalent uitstoot, met  $\text{CO}_2$  and  $\text{N}_2\text{O}$  apart. Aangezuurd *cis, cis*-muconaat kan gemakkelijk worden gehydrogeneerd in adipinezuur een grondstof voor nylon-6,6 wat wordt toegepast in vloerbedekkingen en de auto industrie, omdat het product duurzaam en sterk is. Grondstoffen hebben een groot effect op de algehele milieu impact. De grondbacterie *P. putida* KT2440 heeft een flexibel metabolisme en is in staat om meerdere grondstoffen om te zetten in *cis, cis*-muconaat. Daarom zijn ook grondstoffen met een lagere energie vraag meegenomen in de LCA, zoals: onzuivere aromatische verbindingen en toluen, welke beide van petrochemisch aard zijn, en fenol (van lignine) hetgeen uit biomassa wordt gevormd. Het effect van een toename van de eindconcentratie van *cis, cis*-muconaat in het fermentatie medium van 1,85% naar 4,26% werd eveneens gemodelleerd. Aangezien *P. putida* KT2440-JD1 benzoaat kan consumeren tot 4,26%. Bij een eindconcentratie van 1,85% *cis, cis*-muconaat werd de energievraag van het productie proces van adipinezuur verminderd ten opzichte van chemische geproduceerde adipinezuur indien onzuivere aromatische verbindingen en fenol uit lignine werden gebruikt als grondstof. De toepasbaarheid van deze grondstoffen hangt echter af van de robuustheid van het metabolisme van *P. putida* KT2440-JD1 betreffende de omzetting van onzuivere aromatische verbindingen en/of de verbetering van de efficiëntie van het productieproces van fenol uit lignine. Bij een eindconcentratie van 4,26% *cis, cis*-muconaat is de energievraag van het productie proces en de  $\text{CO}_{2\text{eq}}$  uitstoot voor alle grondstoffen verminderd.

Het pH-stat fed-batch proces heeft een hogere productie snelheid per gram biomassa ten opzichte van andere processen ondanks dat de snelheid significant lager was dan gemeten tijdens de batch cultures. Door het genereren van een hoge cel dichtheid in combinatie met pH-gereguleerde

toevoeging van benzoaat zal de volumetrische productiviteit toenemen zoals eerder beschreven voor een “cell-recycle” proces. Ondanks dat dit slechts een geringe invloed heeft op het energieverbruik heeft het een grote invloed op de winstgevendheid van een industrieel proces. Het hergebruiken van cellulaire biomassa door gebruik te maken van membraan scheiding, en het gebruik van een oplossingsmiddel zoals bv. koude diethylether voor de extractie van *cis*, *cis*-muconaat na aanzuren (pH 2.5), zouden de milieu impact verder kunnen verminderen. Het gebruik van oplossingsmiddelen resulteert in een hogere product concentratie en/of de verdamping vereist minder energie, gezien de kooktemperatuur van oplossingsmiddelen meestal lager is dan van water.



## Zusammenfassung

### Optimierung des *Pseudomonas putida* KT2440 als Wirt für die Produktion von *cis, cis*-Mukonat aus Benzoat

*P. putida* KT2440 wurde wegen seines vielfältigen und energetisch stabilen Stoffwechsels als Biokatalyst benutzt. Dafür wurde eine Mutante generiert und ein Prozess entwickelt, auf dessen Grundlage eine Ökobilanz (LCA=life cycle assessment) durchgespielt wurde. Ergänzend wurden die Wachstumsparameter experimentell ermittelt, um das Stoffwechselmodell iJP815 zu belegen.

Die Mutante *Pseudomonas putida* KT2440-JD1 stammt von *P. putida* KT2440 ab, wozu dieser Stamm einer NTG-Mutagenese unterzogen und 3-Fluorbenzoat ausgesetzt wurde. Der Stamm war mit Benzoat als einziger Kohlenstoff- und Energiequelle nicht mehr in der Lage zu wachsen. Stattdessen wurde Benzoat co-umgewandelt in *cis, cis*-Mukonat, welches sich im Kulturmedium vermehrte, wenn der Stamm auf Glukose angezogen wurde. In Batchkulturen wurde eine 8 mal höhere Produktionsrate pro Gramm Biomasse erreicht als vorher mit 2,0 g *cis, cis*-Mukonat  $\text{g}_{\text{DCW}}^{-1} \text{h}^{-1}$  beschrieben. Durch die Punktmutation im Regulator-Gen *catR* wurde das *cat*-operon nicht mehr in *P. putida* KT2440-JD1 induziert. Dieses Operon beinhaltet die Gene für die Umwandlung von Catechinsäure zu Stoffwechselprodukten des Hauptstoffwechsels inklusive *catA*, welches die 1,2 Catechol-dioxygenase codiert. Als Konsequenz daraus wird Benzoat nur durch die Gene in *cis, cis*-Mukonat umgewandelt, die auf dem *ben* operon exprimiert werden. Dieses Operon beinhaltet ein Gen (*catA2*; *PP\_3166*), das sehr wahrscheinlich die 1,2 Catechol-dioxygenase codiert, die die Umwandlung von Benzoat zu *cis, cis*-Mukonat erlaubt.

In Batchkulturen nahm die maximale Wachstumsrate von *P. putida* KT2440-JD1 in einem mineralischen Medium mit Glukose linear ab, wenn die Konzentration von Benzoat und/oder *cis, cis*-Mukonat zunahm und endete bei 6 g  $\text{L}^{-1}$  Benzoat oder 85 g  $\text{L}^{-1}$  *cis, cis*-Mukonat. Die hemmenden Wirkungen beider Komponenten verstärkten sich; Synergieeffekte wurden nicht beobachtet. Die maximale Benzoat-Aufnahmerate pro Gramm Biomasse war höher als die Produktion von *cis, cis*-Mukonat während der Kultur auf Glukose in der Anwesenheit von Benzoat, was darauf hinweist, dass sich ein Benzoat-Derivat in den Zellen akkumuliert hatte, welches wahrscheinlich Catechinsäure ist, weil die Akkumulation dieses Zwischenproduktes beobachtet wurde. Catechinsäure ist bekannt als Verursacher von oxidativem Stress und deshalb sollte die Akkumulation von Catechinsäure und Benzoat während der Produktion von *cis, cis*-Mukonat verhindert werden. Dies ist möglich, weil durch die Zugabe von Benzoat der pH-Wert des Kulturmediums in einem sogenannten pH-stat-Prozess absinkt. Das Kulturmedium säuert nur an, wenn Benzoat in *cis, cis*-Mukonat umgesetzt ist. Aus einem solchen pH-stat fed-batch-Prozess resultierte eine Produktion von 18,5 g  $\text{L}^{-1}$  *cis, cis*-Mukonat von Benzoat mit einem molaren Produktertrag von fast 100%.

Der Phänotyp von *P. putida* KT2440 als Biokatalyst kann vorausgesehen werden mit dem Stoffwechselmodell von iJP815. Der Lösungsspielraum des Modells, das auf Flussvarianzanalyse

basiert ist wurde verkleinert. Diese Verkleinerung wurde erzielt durch wachstumsbezogene Versorgung, nicht wachstumsbezogene Versorgung und Biomassezusammenstellung, welche von experimentell gemessenen wachstumsbezogenen Faktoren des Stammes bestimmt wurden, die während kontinuierlichen Kultivierungen mit unterschiedlichen Verdünnungsraten ( $D$ ) (0.05-0.49)  $\text{h}^{-1}$  ermittelt wurden. Transcriptomics-Daten, die bei einer  $D$  von 0,2  $\text{h}^{-1}$  gemessen wurden, zeigten eine große Übereinstimmung mit den auf Flussbilanzanalyse basierenden Modellrechnungen von exprimierten Genen. Die wachstumsbezogenen makromolekularen Kompositionen von der Biomasse waren so wie die mit *E. coli* K-12 gemessenen Daten, obwohl die Wachstumsparameter von maximalem Biomasseertrag und Versorgungskoeffizienten unterschiedlich festgelegt wurden. Die ausgemessene Energie, die für das Wachstum von *P. putida* KT2440 benötigt wird, war höher als die im Vergleich zu *E. coli* W3110, welches aus den höheren Kosten für Glucose in biotechnologischen Prozessen resultiert. Andererseits ist der Stoffwechsel robust, weil selbst bei einer  $D$  von 0,49  $\text{h}^{-1}$  keine Nebenmetaboliten akkumuliert wurden. Die Abwesenheit von Nebenmetaboliten ist von großer Bedeutung, weil das etwas über die Kapazität von *P. putida* KT2440 als Biokatalyst aussagt, z.B. für die Umsetzung involvierter Kofaktoren abhängig von Sauerstoffreaktionen. Weitere Einschränkungen enzymatischer Umwandlungen mit schon publizierten Ergebnissen von  $^{13}\text{C}$ -Messungen, verkleinern den maximalen Lösungsraum. Ergebnisse, die weit vom experimentellen Phänotyp lagen wurden ausgeschlossen. Möglicherweise wurden die besten Zusammenstellungen von Einschränkungen für Stoffwechselmodellierungen erreicht.

Eine LCA wurde auf der Grundlage eines kombinierten biologischen und chemischen Prozesses für die Produktion von Adipinsäure erstellt. Das Ergebnis wurde mit traditionellen chemischen Prozessen verglichen. Die LCA war auf den kumulativen Energieverbrauch, den kumulativen Exergie-Verbrauch, und die  $\text{CO}_2$ -äquivalenten Emissionen fokussiert, wobei  $\text{CO}_2$  und  $\text{N}_2\text{O}$  einzeln betrachtet wurden. Angesäuertes *cis, cis*-Mukonat kann einfach zu Adipinsäure umgewandelt werden, welche eine Quelle für Nylon-6,6 ist, das wegen seiner elastischen und stabilen Eigenschaften in Teppichböden und in der Autoindustrie benutzt wird. Die Rohstoffe haben einen großen Effekt auf die gesamten ökologischen Belastungen. Das Bodenbakterium *P. putida* KT2440 hat einen vielfältigen Stoffwechsel und ist in der Lage unterschiedliche Rohstoffe in *cis, cis*-Mukonat umzuwandeln. Konsequenterweise waren neben Benzoat noch Rohstoffe mit niedrigerem Energiebedarf berücksichtigt, wie die in der Petrochemie produzierten Rohstoffe wie unreine aromatische Verbindungen und Toluol und die aus Biomasse produzierten Rohstoffe wie Phenol (aus Lignin). Auch wurde eine Steigerung der Endkonzentration von *cis, cis*-Mukonat in der Fermentierbrühe von 1,85% zu 4,26% errechnet. *P. putida* KT2440-JD1 war in der Lage Benzoat zu konsumieren bis zu 4,26% *cis, cis*-Mukonat. Ab einer Endkonzentration von 1,85% *cis, cis*-Mukonat reduziert die Verwendung von unreinen Aromaten und Lignin anstelle von Benzoat den Energiebedarf im Vergleich zur chemischen Produktion von Adipinsäure. Der Einsatz dieser Rohstoffe hängt von der Robustheit des Stoffwechsels von *P. putida* KT2440-JD1 für unreine aromatische Verbindungen und/oder der Entwicklung von effizienteren Prozessen für die Produktion von Phenol aus Lignin ab. Bei einer finalen Konzentration von 4,26% *cis, cis*-Mukonat wurden die Prozessenergie und  $\text{CO}_{2\text{eq}}$ -Emissionen für alle Rohstoffe reduziert.

Der pH-stat fed-batch-Prozess hatte eine höhere Produktionsrate pro Gramm Biomasse verglichen mit anderen Prozessen, aber die Geschwindigkeit war signifikant niedriger als in Batchkulturen gemessen. Bei Erreichen einer hohen Zelldichte in Kombination mit einer pH-regulierten Benzoat-Zugabe wird erwartet, dass die Volumetrische Produktion im Vergleich zu Ergebnissen von Zell-Recycle-Prozessen erhöht wird. Weil dies nur einen kleinen Einfluss auf den Energieverbrauch hat, ist es von großer Bedeutung für die Wirtschaftlichkeit von großen industriellen Bioreaktoren. Die Wiederverwendung von Biomasse durch eine Membran und der Nutzung eines Lösungsmittels, wie z.B. kaltes Diethylether, nach der Ansäuerung des Mediums (pH 2.5) für die Extraktion von *cis, cis*-Mukonat, könnte noch zusätzlich die Umweltbelastung reduzieren. Die Verwendung von Lösungsmittel wird resultieren in einer erhöhten Produkt-Endkonzentration und/oder das Ausdampfen wird weniger Energie benötigen, weil die Kochtemperatur von Lösungsmitteln meistens niedriger ist als die von Wasser.



## Acknowledgements

During my PhD I got acquainted to many people, from whom I received a lot of support. Without having a supporting group of people around me, this would not have been possible. Besides work, I also experienced a lot of joy and happiness. All together, in the 7 years of research I gained much knowledge and excitement. I hope in my career I will keep meeting many people with whom I can work together to gain more knowledge and achieve new goals.

First of all I would like to thank Astrid Mars and Gerrit Eggink, who have hired me at the beginning of this project as a PhD and thereby offered me the possibility to develop myself as a scientist. I am and will be always grateful with this opportunity. Especially I would like to thank Astrid very much for her valuable contribution during the writing of the publications.

Apart from the nice cooperation with the colleagues in Wageningen, I am happy that I met Ben Brehmer, Mathieu Streefland, Gino Baart, and Ronald Maas. We had many fruitful discussions, whereby I could mirror myself and put matters into perspective. Furthermore, the cooperation with Ben certainly did enlarge the scope of my research, which also resulted in a publication. In Wageningen I also worked together with the MSc. student Yu Yang, which was a pleasant experience.

In Apeldoorn/ Delft I met Jan Wery, Jan de Bont, Hendrik Ballerstedt, Nick Wierckx, Rita Volkers, and Harald Ruijsenaars from TNO. By working together, we obtained the biocatalyst, which was pretty cool. Also Dorien Wijte was visiting the lab and we also carried out experiments together. This atmosphere that all people are working together on *P. putida* was really inspiring and productive.

The third and last place that I worked during my PhD was HZI in Braunschweig. As a scientist, I have the feeling that I developed here the most. The environment was quite challenging. I would like to thank Prof. Vitor dos Santos for giving me the opportunity. Many thanks to Bianka Karge for the nice work together and for her support in general. It is a pity we probably cannot continue our cooperation. Furthermore I would like to mention Ignacio Poblete, Jacek Puchałka, Audrey Leprince, Gurudutta Panda, Blair Prochnow, Carolyn Lam, Piotr Bielecki, Agatha Bielecki, Danielle Janus, Christoph Ulmer, and of course all other people at HZI who had helped me. Jacek was part of the Kluyver Center from the beginning and we were able to write an article together. Also I want to mention the nice cooperation with Rui Marinho, and Brendan Ryback who were BSc. students at HZI.

Besides colleagues I also had contact with other people during my PhD. First of all I think of my “jaarclub” Gerben de Vries, Hugo Lamers, Kristof van Assche, Maarten van Vuurde, Ruud van Gorp and Stijn Koole. But I met also other people as Santiago López Ridoura, Pablo Tiltonell, Noor van der Hoeven, Kate Collins, Tanja Weigel, and Bastiaan Brak with whom I was living together at the Costerweg in Wageningen. I know Tjebbe van der Meer from Wageningen and later Göttingen. We formed a nice group of people. And of course my friends Patrick Okanya and Rudi Alberts whom I met in Braunschweig. Thank you guys for the nice conversation and drinks.

At last I would like to thank my family pa, ma (Jos en Lea van Duuren) and of course my brother (Robert van Duuren) and his girlfriend (Ruth Post). Especially when the PhD did not work out as I wanted, they always supported me.

Cheers,  
Joost

## Curriculum Vitae

Jozef B.J.H. (Joost) van Duuren was born in Vlaardingen (The Netherlands) on the 9<sup>th</sup> of May 1977. He went to the primary school in his home town Vlaardingen and continued his secondary education at the Scholen Gemeenschap Spieringshoek in Schiedam. After receiving the VWO diploma in 1996 he started to study biology at Wageningen University. His MSc. thesis was conducted at the laboratory of microbiology at Wageningen university. It focused on characterization of micro organisms in contaminated soil. His internship was conducted at the entomology department of University California Riverside. It focused on studying the virulence of the Gram negative bacterium *Xylella fastidiosa* by using the phylogenetic software program RRTree.



In 2002 he started working at Witteveen and Bos at the department environment to classify soil contaminations in the Netherlands. In 2004, he started his doctoral research at the institute Food and Biobased Research in collaboration with the Bioprocess Engineering group of Wageningen University under the supervision of Prof. Dr. Gerrit Eggink and Dr. Astrid Mars. In 2007 he moved to the Helmholtz Centre for Infection Research at the Synthetic and Systems Biology Research Group of Prof. dr. ir. Vitor dos Santos.



## Publications

**van Duuren JBJH**, Wijte D, Leprince A, Karge B, Puchalka J, Wery J, Martins dos Santos VAP, Eggink G, Mars AE. 2011. Generation of a *catR* deficient mutant of *P. putida* KT2440 that produces *cis*, *cis*-muconate from benzoate at high rate and yield. J Biotechnol. in press.

**van Duuren JBJH**, Wijte D, Karge B, Yang Y, Martins dos Santos VAP, Mars AE, Eggink G. pH-stat fed-batch process to enhance the production of *cis*, *cis*-muconate from benzoate by *Pseudomonas putida* KT2440-JD1. Biotechnol Progr. In press.

**van Duuren JBJH**, Brehmer B, Mars AE, Eggink G, Dos Santos VAP, Sanders JPM. 2011. A limited LCA of bio-adipic acid: Manufacturing the nylon-6,6 precursor adipic acid using the benzoic acid degradation pathway from different feedstocks. Biotechnol Bioeng. 108:1298-1306.

Ballerstedt H, Volkers RJM, Mars AE, Hallsworth JE, dos Santos VA, Puchalka J, **van Duuren J**, Eggink G, Timmis KN, de Bont JAM, Wery J. 2007. Genomotyping of *Pseudomonas putida* strains using *P. putida* KT2440-based high-density DNA microarrays: implications for transcriptomics studies. Appl Microbiol Biotechnol. 75:1133-1142.

### Submitted:

**van Duuren JBJH**, Puchalka J, Mars AE, Eggink G, Martins dos Santos VAP. Modeling growth on glucose of *Pseudomonas putida* KT2440 under carbon limited conditions



## Overview of completed training activities



### Discipline specific activities

#### *Courses*

Practical training to work with genomics and *P. putida* (Apeldoorn, The Netherlands, 2005)  
EPS systems biology course: Principles of ~omics data analysis (2nd edition) (Wageningen, The Netherlands, 2005)  
BSDL advanced course on applied genomics of industrial fermentation (Wageningen, The Netherlands, 2006)  
MFCS/ win 3.0 user training (Braunschweig, Germany, 2009)

#### *Conferences and symposia*

First till the Fifth Symposium Kluiver Centre for Genomics of Industrial Fermentation (Noordwijkerhout, The Netherlands, 2004-2008)  
10<sup>th</sup> en 11<sup>th</sup> Dutch Biotechnology Congress (Ede, The Netherlands, 2004 and 2006)  
International PhD Symposium of the Helmholtz International Research School for Infection Biology (Braunschweig, Germany, 2008)  
Pseudomonas 12<sup>th</sup> International Conference (Hannover, Germany, 2009)  
Progress Seminar HZI-Structural Biology, Chemical Biology and Biochemistry (Braunschweig, Germany, 2010)

### General courses

VLAG PhD week (Bilthoven, The Netherlands, 2006)  
Centa scientific writing (Wageningen, The Netherlands, 2006)

### Optionals

Process Engineering PhD study tour (Canada, 2004)  
Brainstorm week Process Engineering (Margraten and 2x Wageningen, The Netherlands, 2005, 2007 and 2009)  
Process Engineering PhD study tour (Denmark and Sweden, 2006)  
Synthetic and Systems Biology retreat (Braunschweig and Goslar, Germany, 2008 and 2009)

The research described in this thesis was financially supported by the Kluyver Centre for Genomics of Industrial Fermentation, which is part of the Netherlands Genomics Initiative.

Financially support from Wageningen University for printing this thesis is gratefully acknowledged.